Founded 1905

MODELING AND CONTROL OF FLEXIBLE LINK ROBOTS

BY

TIAN ZHILING

(B. Eng., Zhejiang Univ.)

A THESIS SUBMITTED

FOR THE DEGREE OF MASTER OF ENGINEERING

DEPARTMENT OF ELECTRICAL & COMPUTER ENGINEERING

NATIONAL UNIVERSITY OF SINGAPORE

2004

Acknowledgements

First of all, I would like to express my deepest gratitude to my supervisor, Associate Professor Shuzhi Sam Ge, not only for his technical direction in my research work, but also for his philosophical inspiration that would be helpful throughout my life. Many of the original ideas in my research come from his inspirational suggestions.

I would also like to express my appreciation to my co-supervisor Professor Tong Heng Lee for his kind and beneficial suggestions.

I am also grateful to Dr. Zhuping Wang, Mr. Pey Yuen Tao, Dr. Fan Hong, Dr. Mingxuan Sun, Dr. Yuanqing Xia, Dr. Yunong Zhang, Dr. Kok Zuea Tang, Mr. Xuecheng Lai and Mr. Keng Peng Tee for their helpful discussions on the work of this thesis. I would also like to thank all of my friends at National University of Singapore (NUS) for creating a friendly and happy environment for my research.

My deepest gratitude goes to my wife Yajuan and my parents for their love, understanding and sacrifice. Their support is an indispensable source of my strength and confidence to overcome any barrier.

Extended appreciation goes to NUS for supporting me financially and providing me the opportunity with the research facilities.

Summary

In this thesis, dynamic modeling of rotational/translational flexible link robots are studied. Subsequently, controller design and experimental evaluations of the model are investigated.

For the simulations and controller design, both the Assumed Modes Method (AMM) and the Finite Element Method (FEM) are investigated for completeness. For both the methods, it is shown that different dynamic models (linear or nonlinear) can be obtained through different representations of the position of the flexible link. By generalizing the modeling of single link robot, the modeling of a n-link robot is presented. From the simulation results of the proposed controller utilizing the single link models and the multi-link model, it is shown that all the derived models are able to provide reasonably good approximations to the original flexible robot system.

In this thesis, The main contributions lie in:

- New property of the system is found. In a flexible link robot, by assuming that payload mass and payload inertia is sufficiently small, the inertia matrix has negative off-diagonal components in its first column. In controller design, the

new property leads to a prior knowledge of the sign of the items that control input is affine to. It is essential in solving the adaptive control problem for unknown parameter system.

- Based on the simple model derived in the modeling part, an adaptive control using neural networks is proposed. The main idea is to regroup the system into two reduced order system based on singular perturbation theory. However, for an unknown parameter system, the equilibrium trajectory of the fast system is unavailable for controller design. By using the essential properties of the system, the adaptive law is constructed by regarding it as a constant in the fast time scale. Simulations are carried out to evaluate the effectiveness of the controller.

- To cater for interaction with the environment, a constrained robot control is proposed. Based on singular perturbation theory, a composite strategy is carried out by using a slow control design for the rigid part and a fast control for stabilizing the flexible part. Simulations are conducted for a planar two link flexible robot in contact with a compliant surface. It is shown that the proposed controller can guarantee the regulation of contact force and tracking of end-point to the desired trajectories.

Contents

List of Figures

Chapter 1

Introduction

1.1 Background and Motivation

Conventional rigid-link robots have been widely used in industrial automations. However, to obtain high accuracy in the end-point position control of these robots, the weight to payload ratio of the robots must be high, and the operation speed is normally quite slow. At the same time, large power supply and thus considerable energy consumption is inevitable to operate these heavy-weight robots. These drawbacks greatly limit the applications of these robots in the fields where high speed, high accuracy and low energy consumption are required.

Flexible link robots with a number of potential advantages, such as faster operation, low energy consumption, and higher load-carrying capacity for the amount

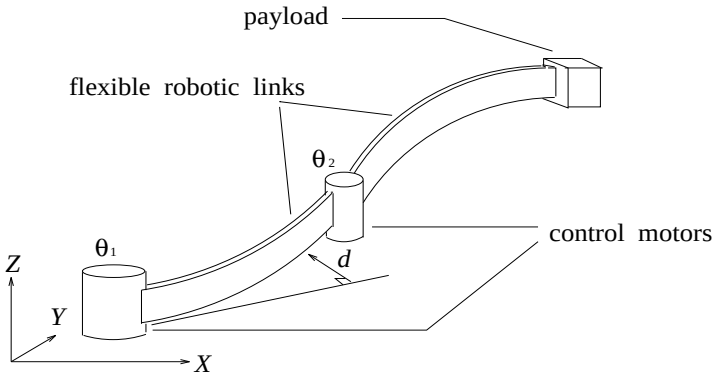

Figure 1.1: A two-flexible-link robot

of energy expended stemming from the use of light-weight flexible link manipulators, have received much attention. However, compared to rigid robot, structural flexibility causes many difficulties in modeling the manipulator dynamics and guaranteeing stable and efficient motion of the end-effector. For a rigid link robot, the position of the payload, i.e., the variable to be controlled, is determined by the joint angles which are defined in certain coordinate systems. The joint angles can be directly controlled by motors, and thus the number of the variables to be controlled is equal to the number of the control inputs. For flexible link robots, the flexible links will undergo deformation in motion due to the flexibility of the link. Taking the first link as an example (Figure 1.1), one can see that a point on this link has a deviation d from the undeformed position, and therefore the motion of the point, related to d, is not completely determined by the joint angle θ_1. A further conclusion can be made that one needs an infinite number of d's to describe the motion of the whole link. In other words, the control objective becomes more challenging since the number of the variables to be controlled is much more than that of the

control inputs [1].

On the other hand, a number of conventional linear as well as nonlinear techniques have been developed in recent years to address the problem of controlling single link manipulators. However, a frequently encountered problem in industrial applications, such as polishing, inserting, fastening, etc., is to control a robot in contact with a surface. This typical constrained motion task often requires a multi-link flexible robot, due to the reduction in degrees of freedom in the system. More importantly, unlike the free motion robot, the control of constrained robot has an additional and more difficult objective, i.e., the regulation of the contact force to the desired set-point.

1.2 Previous Work

Lightweight manipulators offer many challenges in comparison to rigid manipulators. Energy consumption is smaller, so the payload to arm weight ration can be increased and fast movements can be achieved. Due to these characteristics, this class of manipulators is specially suitable for a number of nonconventional robotic applications. Thus, the importance of having an accurate model that can adequately describe the dynamics of the manipulator is obvious.

The original dynamics of a flexible link robot is governed by coupled Partial Differential Equations (PDEs) and Ordinary Differential Equations (ODEs), and thus is

a distributed-parameter system possessing an infinite dimensionality [2–4]. Since the infinite dimensionality is the most difficult thing to handle in controller design, the original dynamics is, reduced to finite dimensional models using either the Assumed Modes Method (AMM) or the Finite Element Method (FEM) by making some acceptable assumptions.

In AMM, the elastic deflection of a flexible link is represented by an infinite number of separable modes [5, 6]. Only the first few low frequency modes are dominant in the robot system, thus, the modes are truncated to a finite dimension models. There are two types in AMM: constrained modes and unconstrained modes

- In the constrained mode method, it is generally obtained by assuming that there is no joint acceleration and solving the Euler-Bernoulli beam equation under certain types of boundary conditions. Different types of boundary conditions may result in different type of modes shape functions. Two frequently used ones are the clamped-free and pinned-free boundary condition. In [7, 8], the models with these two type of boundary conditions are used in controller design. It is found that the pinned-free is more accurate than clamped free with a relative small hub inertia [9, 10].

- In the unconstrained mode method, the models are decouped for each mode [6]. The mode-shape functions are rigorously formulated and dependent on the control input, thus, the analytic form of the model may be difficult to

obtain.

In AMM, the concept of natural frequencies are explicit. However, the assumed harmonic modes do not have any physical meanings.

The FEM modeling of flexible link robots (and associated controller design) can be found in [11–16]. In this method, the flexible link is divided into a finite number of elements. The link's elastic deformation is represented in the form of a linear combination of admissible functions and generalized coordinates. There are many kinds of admissible function which meets certain nodes boundary conditions [17]. Most commonly used admissible functions is the B-spline function that is introduced in [18, 19]. The alternative choice is to use the solutions of the differential equation which governs the static bending of the considered beam [17]. In FEM, all the generalized coordinates are physically meaningful, however, the concepts of natural frequencies are not explicit.

Although the explicit models have been derived for the case of a one link flexible arm, its simplicity prevents thorough understanding of the full nonlinear interactions between rigid and flexible components of arm dynamics. Thus, various formalism have been proposed for dynamic modeling of multi-link arms [20, 21]. In [22], a dynamic model of multi-link flexible robot arms, limiting to the case of planar manipulators with no torsional effects is derived. The model is derived by the Lagrangian technique in conjunction with the AMM. Links are modeled as

Euler-bernoulli beams satisfying proper clamped-mass boundary conditions. Some models of constrained flexible robots are developed in [23, 24], and a solution algorithm is presented for the closed loop inverse kinematics (CLIK) problem [25, 26]. It is formulated in differential terms by deriving a suitable Jacobian that relates the joint and deflection rates to the tip rate [27, 28].

From a modeling standpoint, the scenario is complicated by the presence of additional deflection variables, compared to the case of rigid manipulators, where the joint variables are sufficient to describe the system configuration. On the other hand, from a control standpoint, it is desired to reduce link deflections, but the trouble is that there are more control variables than control inputs.

In view of the above difficulties, the most effective control strategies for flexible link arms have been developed at the joint level, such as linear control [29], optimal control [30], sliding mode control [31], direct strain feedback control [3], inverse dynamics methods, and energy-based control [32, 33], have been studied based on a truncated model obtained from either the FEM or AMM [1]. An effective control method for flexible link robots is the singular perturbation method [34–36]. Based on singular perturbation theory, the rigid motion (joints motion) and the vibration of the flexible links are decoupled and generate a composite control law [34]. This method is attractive because it make used of the two time-scale nature of the system dynamics. In particular, by selecting the fast states to be the elastic forces and their time derivatives, and slow states to be that of the equivalent rigid manipulator,

a linear stabilizer (fast control) is designed to stabilize the fast subsystem around the equilibrium trajectory defined by the slow subsystem under the effect of the slow control [35, 36] , and a nonlinear controller is used to make the slow dynamics track the desired trajectories. In [35], a singular perturbation model for the case of multi-link manipulators is introduced which follows a similar approach in terms of modeling as that introduced in [37] for the case of flexible joint manipulators. The singular perturbation approach is also considered in [38, 39]. A comparison is made experimentally between some of these methods in [36]. On the other hand, several researchers use the integral manifold approach introduced in [40] to control the flexible link manipulator [41, 42]. In [41], a linear model of the single flexible link manipulator is considered. A nonlinear model of a two link flexible manipulators is used in [42]. In this approach, new fast and slow outputs are defined and the original tracking problem is reduced to track the slow output and stabilized the fast dynamics.

However, all of these works are based on the exact knowledge about the nonlinear functions or the bounds of uncertainties. Such a priori knowledge may be difficult to obtain in practice. To overcome the limitation, the approximation capabilities of neural networks have been utilized to approximate the nonlinear characteristics of the systems. The introduction of neural networks can remove the need for the tedious dynamic modeling and the error prone process in obtaining the regression matrix. In recent literature, there have been many neural network controls

proposed for robot arm [43–45]. On the other hand, in a series of work [46–48], the control of the slow subsystem is designed and analyzed based on fuzzy logic algorithm to handle uncertainties.

In fact, the tasks of industrial robots may be divided into two categories. The first category is the so-called free motion task, and the second category, involves interactions between the robot end-effector and the environment. Many robot applications in manufacturing encounter some kind of contact between the end-effector and the environment, as the robot moves along a prescribed trajectory. Therefore, constrained robots have become a useful mathematical method to model the physical and dynamic effects of a robot when it is engaged in contact tasks. Unlike free motion control, where the only control objective is trajectory tracking or set-point regulation, the control of a constrained robot has an additional difficulty in controlling the constrained force.

During interaction with the environment, it is required to consider both force control and position control. While several control methods exist for the rigid robot manipulators, only few works addressed the control problem of flexible link robots. A hybrid position and force control approach is proposed in [18, 19, 49, 50]. A non-linear decoupling method was considered in [51], and the application of computed-torque controller for constrained robots was carried out in [52]. All the existing methods are dependent on the exact cancellation of the robot dynamics to achieve the desired results.

1.3 Work in the Thesis

In this thesis, dynamic modeling and control are investigated for flexible link robots. It is organized as follows.

Chapter 2 reviews the two existing modeling methods: AMM and FEM. Although some of the proposed control strategies in this thesis require no knowledge or only a partial knowledge about the system dynamics, the analytical model of the system is still needed for the purpose of simulation and controller design. In single link cases, it is shown that different dynamic models (linear or nonlinear) can be obtained through different representations of the position of the flexible link. In addition, some properties are discovered in this chapter, which is essential in solving an open control problem in the following control design.

In Chapter 3, the problem of control design based on singular perturbation theory is considered. Under the assumption of large link stiffness, the original system is regrouped into two subsystems: fast system for flexible dynamics and slow system for rigid dynamics. Then, both the Proportional Integral and Differential (PID) control for the known system and the adaptive neural control for the unknown system are explored. The main difficulty comes from the fast controller design for the unknown system, which requires a priori knowledge of the equilibrium $\bar{\zeta}$. By investigating the dynamic model, some critical properties of inertia matrix $\mathbf{M}$ are found. Using these properties, a fast subcontroller is designed based on

$\boldsymbol{\eta}_2$. In addition, $\bar{\zeta}$ is considered as a constant in the boundary layer [53]. Model based and neural network based adaptive subcontrollers are proposed for the fast unknown dynamics by updating the estimation of $\bar{\zeta}$ in the fast feedback loop. The controllers ensure that the system asymptotically converge to a bounded invariant set. Furthermore, due to the existence of internal structural damping in a flexible link in practice, the flexible robot tends to stop vibrating and finally stop at the under-formed position. Consequently, the controller approaches cannot hold at a nonzero constant, which implies that tip regulation is achieved.

Chapter 4 discusses modeling methodology and force control scheme of constrained flexible manipulators. A two time scale manipulators is proposed, based on the arguments developed for rigid robots in contact with compliant environments. In contrast with unconstrained manipulator, the hybrid control scheme, in which force and position are considered separately, controls both force and position in the full space. In order to cancel out the effects of the static torques acting on the rigid part of the manipulator dynamics, a new control input u is introduced. Then, by using similar arguments in [24], a singular perturbation control is designed to guarantee the force regulation and position tracking. The fast stabilizer is constructed to control the dynamics related to link flexibility. The control laws are tested in simulation on a two-link planar constrained manipulator.

Finally, Chapter 5 gives the conclusion of the thesis and makes suggestions for future work.

Chapter 2

Modeling of Flexible Structures

2.1 Introduction

Several of the control strategies for flexible link robots described in the remainder of this thesis rely on an accurate dynamic model of the system. For the purpose of controller design and simulations, the modeling methods AMM and FEM are reviewed in this chapter. Creating a dynamic model that accounts for link flexibility adds additional challenges beyond the standard rigid link robot dynamics. The most apparent complexity arises due to the additional degree-of-freedom (DOF) associated with link deformations. Although in theory this adds an infinite number of DOF, in practice only a finite number are used to generate a model that is sufficiently accurate for predictive simulation and control design. For multilink flexible robots, the models based on AMM can be found in [22], and the multilink

model based on FEM is proposed in this chapter.

2.2 Modeling of a Single-Link Flexible Robot

In this section, we discuss several dynamic modeling approaches for a single-link flexible robot. The Assumed Modes Method (AMM) and the Finite Element Method (FEM) are introduced in detail.

In the AMM modeling, the elastic deflection of the beam is represented by, theoretically an infinite number of separable modes, but practically only finite number of modes with comparatively low frequencies are considered as they are generally dominant in the system's dynamic behaviour. The method of arc approximation is used to represent the position of the flexible link, which leads to a linear time invariant model.

In the FEM modeling, the flexible link is divided into a finite number of elements. The generalized coordinates of the system are the displacements and rotations of the dividing nodes [17] with respect to a reference local frame. The position of the flexible beam is represented by a Cartesian vector, and the resulting model is nonlinear. The arc approximation of the position in this case is also briefly discussed.

For convenience, we make following assumption [1]:

Assumption 2.1: *The flexible link of the robot, with uniform density and flexural rigidity, is an Euler-Bernoulli beam.*

Assumption 2.2: *The deflection of the flexible link is small compared to the length of the link.*

Assumption 2.3: *The payload attached to the free tip of the flexible robot is a concentrated mass.*

Assumption 2.4: *The base end of the robot is clamped to the rotor of a motor.*

Assumption 2.5: *The effects of any kinds of damping are neglected.*

Assumption 2.6: *The flexible robot only operates in the horizontal plane.*

Some basic notations are listed below:

L: the length of the flexible beam;

EI: the uniform flexural rigidity of the flexible beam;

ρ: the uniform mass per unit length of the flexible beam;

M_t: the concentrated mass tip payload;

I_h: the hub inertia;

$\tau(t)$: the torque applied by the motor at the base;

$\theta(t)$: the joint rotation angle;

$y(x,t)$: the elastic deflection measured from the undeformed beam;

$p(x,t)$: arc approximation of the position of a point on the beam;

$\vec{r}$: the position vector of a point on the beam in the fixed frame XOY; and

$\vec{r}^*$: the position vector $\vec{r}$ represented in the local frame xOy.

2.2.1 AMM modeling

In this section, we review the dynamic model of a single-link flexible robot as shown in Figure 2.1 by using the AMM. The method used is the constrained modes method. The modes shape functions are obtained by solving the Euler-Bernoulli's beam equation. The boundary conditions of the Euler-Bernoulli's beam equation are of clamped-free type by selecting the local reference frame in such a way, i.e., the horizontal axis is always tangent to the flexible beam at the base. Such a selection of reference frame also means that its horizontal axis is actually the position of the undeformed beam, and represents the rigid (joint) motion of the flexible robot. The position of the flexible beam is represented in the ways of arc approximation, which lead to a linear time-invariant model.

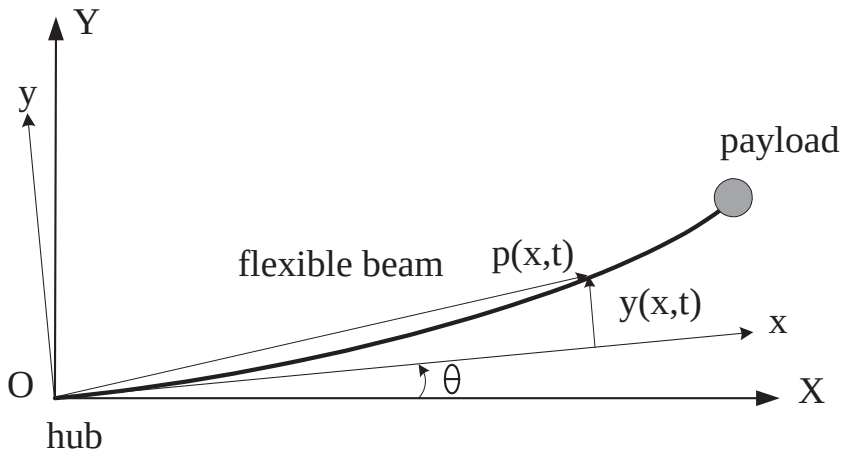

Figure 2.1: AMM modeling of a flexible robot

Arc Approximation

In the AMM modeling with constrained modes, the elastic vibration of the flexible beam is generally assumed to be of the form

$$y(x,t) = \sum_{i=1}^{\infty} \phi_i(x) q_i(t)$$

where $\phi_i(x)$ are, the modes shape functions or the eigen-functions and will be defined later, and $q_i(t)$ are the generalized coordinates. Each $q_i(t)$ corresponds to a DOF of the system.

It is well known that the first several modes (corresponding to lower frequencies) are dominant in describing the system dynamics. The infinite series can be truncated into a finite one, i.e.,

$$y(x,t) = \sum_{i=1}^{N} \phi_i(x) q_i(t), \quad 0 \leq x \leq L \tag{2.1}$$

where N is the number of the modes which are taken into consideration.

In order to use the Euler-Lagrange's equations to obtain the dynamic equations of the system, we need to calculate the kinetic energy and the potential energy of the system. Since the elastic deflection $y(x,t)$ is assumed to be small, the arc $p(x,t)$ as shown in Figure 2.1 is used to approximate the position of a point on the flexible beam.

Solution of the Euler-Bernoulli's Beam Equation

Under the assumption of small deflection, $y(x,t)$ is considered small and the position of a point on the flexible beam can be approximated by

$$p(x,t) = x\theta(t) + y(x,t) \tag{2.2}$$

which is frequently used in the literature, e.g. in [8, 9], and others. From now on, the space variable $0 \leq x \leq L$ holds for all the time unless otherwise stated.

The total kinetic energy E_k can be calculated by

$$\begin{aligned} E_k &= E_{km} + E_{kb} + E_{kp} \\ &= \frac{1}{2} I_h \dot{\theta}^2 + \frac{\rho}{2} \int_0^L \dot{p}^2(x,t) dx + \frac{1}{2} M_t \dot{p}^2(L,t) \end{aligned} \tag{2.3}$$

where

$$E_{km} = \frac{1}{2} I_h \dot{\theta}^2, \;\; E_{kb} = \frac{\rho}{2} \int_0^L \dot{p}^2(x,t) dx, \;\; E_{kp} = \frac{1}{2} M_t \dot{p}^2(L,t)$$

are the kinetic energies of the motor, the flexible beam and the tip payload, respectively. From the assumptions stated at the beginning of this chapter, the potential

energy of the system only comes from the bending strain energy of the flexible beam, i.e.,

$$\begin{aligned} E_p &= \frac{1}{2}EI\int_0^L \left[\frac{\partial^2 p(x,t)}{\partial x^2}\right]^2 dx \\ &= \frac{1}{2}EI\int_0^L \left[\frac{\partial^2 y(x,t)}{\partial x^2}\right]^2 dx \\ &= \frac{EI}{2}\int_0^L [y''(x,t)]^2 dx \end{aligned} \tag{2.4}$$

where the primes denote the derivatives with respect to time and space, respectively. Let $W = \tau(t)\theta(t)$. According to the extended Hamilton's Principle:

$$\int_{t_o}^{t_f} \delta(E_k - E_p + W)dt = 0 \tag{2.5}$$

where $t_o < t < t_f$ is the operating interval and δ is the variational derivative [54], and substituting (2.3) and (2.4) into (2.5), we obtain the following system dynamics:

$$(I_h + \frac{1}{3}\rho L^3)\ddot{\theta}(t) + \rho\int_0^L x\ddot{y}(x,t)dx + M_t L[L\ddot{\theta}(t) + \ddot{y}(L,t)] = \tau \tag{2.6}$$

$$\rho[x\ddot{\theta}(t) + \ddot{y}(x,t)] = -EIy''''(x,t) \tag{2.7}$$

(2.6) is an ordinary differential equation (ODE) representing the moment balance at the base end of the robot, and (2.7) is the partial differential equation (PDE) describing the vibration of the flexible link. The corresponding boundary conditions are given by the following set of equations:

$$y(0,t) = 0 \tag{2.8}$$

$$y'(0,t) = 0 \tag{2.9}$$

$$y''(L,t) = 0 \tag{2.10}$$

$$EIy^{'''}(L,t) = M_t[L\ddot{\theta}(t) + \ddot{y}(L,t)] \tag{2.11}$$

(2.8) and (2.9) hold because the reference frame xOy is selected such that the axis Ox is tangent to the beam at the base. The third boundary condition, (2.10) comes directly from the zero value of the bending moment at the tip (note the tip payload is a concentrated mass), and the fourth one, (2.11) is actually the motion equation of the tip payload M_t.

In the constrained modes method, $\ddot{\theta} = 0$ is assumed, and the dynamic equation (2.7) reduces to the Euler-Bernoulli's beam equation:

$$\rho\ddot{y}(x,t) = -EIy^{''''}(x,t) \tag{2.12}$$

and the corresponding boundary conditions (2.8)-(2.11) becomes

$$y(0,t) = 0 \tag{2.13}$$

$$y^{'}(0,t) = 0 \tag{2.14}$$

$$y^{''}(L,t) = 0 \tag{2.15}$$

$$EIy^{'''}(L,t) = M_t\ddot{y}(L,t) \tag{2.16}$$

From the method of separating variables [55], we assume that the solution of (2.12) is of the form

$$y(x,t) = \Phi(x)Q(t)$$

Substituting this solution into (2.12) yields

$$\frac{\Phi^{''''}}{\Phi} \cdot \frac{EI}{\rho} = -\frac{\ddot{Q}}{Q} \tag{2.17}$$

Since the left hand side of (2.17) is only dependent on x and the right hand side is a purely time-varying function, it is obvious that both sides must be constant. If we denote the constant by k, we can obtain two ordinary differential equations, namely,

$$\ddot{Q}(t) + kQ(t) = 0 \tag{2.18}$$

$$\Phi^{''''}(x) = \frac{\rho}{EI} k\Phi(x) \tag{2.19}$$

and the boundary conditions (2.13)-(2.16) are reduced to

$$\Phi(0) = 0 \tag{2.20}$$

$$\Phi^{'}(0) = 0 \tag{2.21}$$

$$\Phi^{''}(L) = 0 \tag{2.22}$$

$$\Phi^{'''}(L) = -\frac{M_t}{EI} k\Phi(L) \tag{2.23}$$

Thus, the associated boundary value problem is to find the solutions of (2.19) under (2.20)-(2.23). The solutions are generally called the eigen-functions/modes shape functions of the system. Clearly, $Q(t)$ and $\Phi(x)$ of (2.18) and (2.19) should be such that $y(x,t) = \Phi(x)Q(t)$ satisfies the boundary conditions in (2.13)-(2.16). In [9], the time dependent function $Q(t)$ is assumed to be harmonic with frequency ω and thus $k = \omega^2$. However, this assumption is not necessary, as it is shown that the solution of (2.19) is trivial when $k \leq 0$ [1].

Finally, let k be a positive number given by $k = \omega^2$, equation (2.19) can be re-written as

$$\Phi''''(x) = (\frac{\beta}{L})^4 \Phi(x) \tag{2.24}$$

Considering (2.30), the general solution of (2.24) is of the form

$$\Phi(x) = C_1 \cos\frac{\beta x}{L} + C_2 \cosh\frac{\beta x}{L} + C_3 \sin\frac{\beta x}{L} + C_4 \sinh\frac{\beta x}{L} \tag{2.25}$$

From the boundary conditions (2.20)-(2.23), we have the set of equations

$$\begin{cases} C_1 + C_2 = 0 \\ C_3 + C_4 = 0 \\ -C_1 \cos\beta + C_2 \cosh\beta - C_3 \sin\beta + C_4 \sinh\beta = 0 \\ C_1(\sin\beta + \frac{M_t\beta}{\rho L}\cos\beta) + C_2(\sinh\beta + \frac{M_t\beta}{\rho L}\cosh\beta) \\ \quad + C_3(\frac{M_t\beta}{\rho L}\sin\beta - \cos\beta) + C_4(\cosh\beta + \frac{M_t\beta}{\rho L}\sinh\beta) = 0 \end{cases} \tag{2.26}$$

To obtain nontrivial solutions, the determinant of the coefficient matrix of (2.26) must be zero, i.e.,

$$1 + \cosh\beta\cos\beta + \frac{M_t\beta}{\rho L}(\sinh\beta\cos\beta - \cosh\beta\sin\beta) = 0 \tag{2.27}$$

which may be satisfied by an infinite number of β. Note that only positive values of β are used.

The boundary value problem in this case is proposed in [1]. For completeness, it is re-written as

$$\Phi''''(x) = (\frac{\beta}{L})^4 \Phi(x) \tag{2.28}$$

$$\begin{cases} \Phi(0) = 0 \\ \Phi'(0) = 0 \\ \Phi''(L) = 0 \\ \Phi'''(L) + \frac{M_t}{EI}\omega^2\Phi(L) = 0 \end{cases} \tag{2.29}$$

where β/L is given by

$$\left(\frac{\beta}{L}\right)^4 = \frac{\rho}{EI}\omega^2. \tag{2.30}$$

We have shown that the general solution of (2.28) is given by (2.25). Consider the first two equations in (2.26), we have

$$\Phi(x) = C_2\left[\cosh\frac{\beta x}{L} - \cos\frac{\beta x}{L}\right] + C_4\left[\sinh\frac{\beta x}{L} - \sin\frac{\beta x}{L}\right]$$

and from the third equation in (2.26), $\Phi(x)$ can be further written as

$$\Phi(x) = C_2\left[\cosh\frac{\beta x}{L} - \cos\frac{\beta x}{L} - \gamma\left(\sinh\frac{\beta x}{L} - \sin\frac{\beta x}{L}\right)\right] \tag{2.31}$$

where

$$\gamma = \frac{\cosh\beta + \cos\beta}{\sinh\beta + \sin\beta} \tag{2.32}$$

Thus, the solution of the boundary value problem (2.28)-(2.29) is given by (2.31), in which β should satisfy (2.27).

Since $\ddot{\theta} = 0$ is assumed (constrained modes), the Euler-Bernoulli's beam vibration system (2.12)-(2.16) is conservative, which can be solved if the initial conditions are specified. We hereby assumed that the initial moment is $t = 0$, and let the initial profiles of the system be given by

$$y(x, 0) \;=\; Y_0(x) \tag{2.33}$$

$$\dot{y}(x,0) = Y_{0d}(x) \tag{2.34}$$

Letting $0 < \beta_1 < \beta_2 < \cdots < \infty$ be the infinite number of positive solutions of (2.27), we can obtain an infinite number of solutions of the boundary value problem

$$\begin{aligned} \phi_i(x) &= A_i \bar{\phi}_i(x) \\ &= A_i \left[\cosh \frac{\beta_i x}{L} - \cos \frac{\beta_i x}{L} - \gamma_i \left(\sinh \frac{\beta_i x}{L} - \sin \frac{\beta_i x}{L} \right) \right] \\ & \quad i = 1, 2, \cdots \end{aligned} \tag{2.35}$$

where γ_i is calculated by (2.32) with corresponding β_i, and constants A_i's are to be determined later.

The time dependent function $Q(t)$, from (2.18), is now governed by the following equation

$$\ddot{Q}(t) + \omega^2 Q(t) = 0 \tag{2.36}$$

which indicates that $Q(t)$ is harmonic with frequency ω. For the infinite number of β_i's, we have, from (2.30), an infinite number of corresponding frequencies

$$\omega_i = \frac{\beta_i^2}{L^2} \sqrt{\frac{EI}{\rho}} \tag{2.37}$$

Generally ω_i is called the natural frequency of the mode $q_i(t)$. It follows that an infinite number of solutions of (2.36) exist

$$q_i(t) = B_i \cos \omega_i t + D_i \sin \omega_i t \tag{2.38}$$

where B_i and D_i are constants to be determined from the initial conditions later.

Note that (2.12) is linear and homogeneous, from the Superposition or Linearity Principle (i.e., Theorem 1 in [55]), a solution $y(x,t)$ can be given by

$$y(x,t) = \sum_{i=1}^{\infty} \phi_i(x) q_i(t) \tag{2.39}$$

By introducing the following orthogonal conditions [1]

$$\rho \int_0^L \phi_i \phi_j dx + M_t \phi_i(L) \phi_j(L) = \begin{cases} 0 & i \neq j \\ \rho & i = j \end{cases} \tag{2.40}$$

$$EI \int_0^L \phi_i'' \phi_j'' dx = \begin{cases} 0 & i \neq j \\ \omega_i^2 \rho & i = j \end{cases} \tag{2.41}$$

it can be easily to determine A_i, B_i and D_i [1].

$$A_i = \left[\frac{1}{\int_0^L \bar{\phi}_i^2(x) dx + \frac{M_t}{\rho} \bar{\phi}_i^2(L)} \right]^{\frac{1}{2}} \tag{2.42}$$

$$B_i = \int_0^L Y_0(x) \phi_i(x) dx + \frac{M_t}{\rho} Y_0(L) \phi_i(L) \tag{2.43}$$

$$D_i = \frac{1}{\omega_i} \left[\int_0^L Y_{0d}(x) \phi_i(x) dx + \frac{M_t}{\rho} Y_{0d}(L) \phi_i(L) \right] \tag{2.44}$$

Moreover, from $\int_0^L \bar{\phi}_i^2(x) dx = L$ ($\bar{\phi}_i(x)$ is given in (2.35)) when $M_t = 0$ [56] [8], A_i can be simplified to

$$A_i = \begin{cases} \sqrt{L}/L, & \text{when } M_t = 0 \\ 1/\left[L + \frac{\rho L^2}{M_t \beta_i^2} \left(\frac{1 + \cosh \beta_i \cos \beta_i}{\sinh \beta_i + \sin \beta_i} \right)^2 \right]^{\frac{1}{2}} & \text{when } M_t > 0 \end{cases} \tag{2.45}$$

It should be noted that the solution $y(x,t)$ obtained above is only valid for the conservative Euler-Bernoulli beam vibration system. For the original system (2.6)-(2.11) which is driven by the motor torque τ and thus nonconservative, the solution

(2.39) is invalid. However, in the AMM modeling with constrained modes, the flexible vibration of the nonconservative system is also assumed to be of the form (2.39), except that $q_i(t)$'s are not given by (2.38) but dependent on the control torque τ and are called the generalized coordinates of the system.

From (2.2), we have

$$\dot{p}(x,t) = x\dot{\theta}(t) + \dot{y}(x,t)$$

which leads to

$$\dot{p}^2(x,t) = x^2\dot{\theta}^2(t) + 2x\dot{\theta}(t)\dot{y}(x,t) + \dot{y}^2(x,t)$$

then considering (2.1) and the orthogonal condition in (2.40), we have the following equations

$$\begin{aligned}
&\textstyle\int_0^L x^2\dot{\theta}^2(t)dx = \frac{1}{3}L^3\dot{\theta}^2(t) \\
&\textstyle\int_0^L \dot{y}^2(x,t)dx = \sum_{i=1}^N \dot{q}_i^2(t)\left[1 - \frac{M_t}{\rho}\phi_i^2(L)\right] + 2\sum_{i,j=1\ i\neq j}^N \dot{q}_i\dot{q}_j\left[-\frac{M_t}{\rho}\phi_i(L)\phi_j(L)\right] \\
&\textstyle\int_0^L 2x\dot{\theta}\dot{y}dx = \sum_{i=1}^N 2\dot{\theta}\dot{q}_i\int_0^L x\phi_i(x)dx \\
&\dot{p}^2(L,t) = L^2\dot{\theta}^2 + 2L\textstyle\sum_{i=1}^N \dot{\theta}\dot{q}_i\phi_i(L) + \sum_{i=1}^N \dot{q}_i^2\phi_i^2(L) + 2\sum_{i,j=1\ i\neq j}^N \dot{q}_i\dot{q}_j\phi_i(L)\phi_i(L)
\end{aligned} \tag{2.46}$$

Substituting the equations in (2.46) into (2.3) and defining the generalized coordinates vector as

$$Q := [\theta\ q_1\ q_2\ \cdots\ q_N]^T \in R^{N+1} \tag{2.47}$$

we can re-write the kinetic energy E_k into the following compact form

$$E_k = \frac{1}{2}\dot{Q}^T M_A \dot{Q} \tag{2.48}$$

where $M_A \in R^{(N+1)\times(N+1)}$ is the symmetric and positive definite inertia matrix of the system which is given by

$$M_A = \begin{bmatrix} I_h + I_b + I_p & m_A^1 & m_A^2 & \cdots & m_A^N \\ m_A^1 & \sigma_A^1 & m_A^{12} & \cdots & m_A^{1N} \\ m_A^2 & m_A^{12} & \sigma_A^2 & \cdots & m_A^{2N} \\ \vdots & \vdots & \vdots & & \vdots \\ m_A^N & m_A^{1N} & m_A^{2N} & \cdots & \sigma_A^N \end{bmatrix} \tag{2.49}$$

The elements of M_A are defined as

$I_b = \frac{1}{3}\rho L^3$ (moment of inertia of the rigid motion w.r.t the base joint)

$I_p = M_t L^2$ (moment of inertia of the tip payload w.r.t. the base joint)

$\sigma_A^i = \rho\left[1 - \frac{M_t}{\rho}\phi_i^2(L)\right] + M_t\phi_i^2(L) = \rho$

$m_A^{ij} = \rho\left[-\frac{M_t}{\rho}\phi_i(L)\phi_j(L)\right] + M_t\phi_i(L)\phi_j(L) = 0$

$m_A^i = \rho\int_0^L x\phi_i(x)dx + M_t L\phi_i(L)$

$(i, j = 1, 2, \cdots, N, \quad i \neq j \text{ in } m_A^{ij})$

Property 2.1: *If $M_t = 0$, the definition of M_A can be modified here.*

$$M_A = \begin{bmatrix} I_h + I_b + I_p & m_1 & m_2 & \cdots & m_n \\ m_1 & \sigma_1 & 0 & \cdots & 0 \\ m_2 & 0 & \sigma_2 & \cdots & 0 \\ \vdots & \vdots & \vdots & & \vdots \\ m_n & 0 & 0 & \cdots & \sigma_n \end{bmatrix} \tag{2.50}$$

where $I_b = \frac{1}{3}\rho L^3$, $I_p = 0$ *(as* $M_t = 0$*),* $\sigma_i = \rho$, $m_i = \rho \int_0^L x\phi_i(x)dx$ *and* $(i, j = 1, 2, \cdots, N, \quad i \neq j$ *in* $m_{i,j})$. *The determinant of the coefficient matrix (2.27) can be rewritten as*

$$1 + \cosh\beta \cos\beta = 0 \tag{2.51}$$

With the help of the symbolic calculation software MAPLE, we obtain that

$$\begin{aligned} m_i &= \rho \int_0^L x\phi_i(x)dx \\ &= \rho L^2 \int_0^1 \frac{x}{L}\phi_i(\frac{x}{L})d(\frac{x}{L}) \end{aligned} \tag{2.52}$$

Noting the definition of ϕ_i *in (2.31), we have*

$$\begin{aligned} m_i &= \frac{\rho L^2}{2\beta_i \sinh\beta_i + 2\beta_i \sin\beta_i}\Big[4\cosh\beta_i + 4\cos\beta_i + e_i^{\beta}\sinh\beta_i \\ &\quad - \cosh\beta_i e^{-\beta_i} + e^{\beta_i}\sin\beta_i - 2 - 2\cosh\beta_i\cos\beta_i - e^{-\beta_i}\sinh\beta_i - \cos\beta_i e^{\beta_i} \\ &\quad - e^{-\beta_i}\sin\beta_i - \cos\beta_i e^{-\beta_i} - 2\sin\beta_i\sinh\beta_i - \cosh\beta_i e_i^{\beta}\Big] \\ &= \frac{\rho L^2}{2\beta_i \sinh\beta_i + 2\beta_i \sin\beta_i}\Big[4\cosh\beta_i + 4\cos\beta_i - \cosh\beta_i e^{-\beta_i} + e^{\beta_i}\sin\beta_i \\ &\quad - 3 - 2\cosh\beta_i\cos\beta_i - e^{-\beta_i}\sinh\beta_i - \cos\beta_i e^{\beta_i} - e^{-\beta_i}\sin\beta_i \end{aligned} \tag{2.53}$$

$$
\begin{aligned}
& -\cos\beta_i e^{-\beta_i} - 2\sin\beta_i \sinh\beta_i \Big] \\
= \; & \frac{\rho L^2}{2\beta_i \sinh\beta_i + 2\beta_i \sin\beta_i} \Big[4\cosh\beta_i + 4\cos\beta_i - \cosh\beta_i e^{-\beta_i} + e^{\beta_i}\sin\beta_i \\
& -1 - e^{-\beta_i}\sinh\beta_i - \cos\beta_i e^{\beta_i} - e^{-\beta_i}\sin\beta_i - \cos\beta_i e^{-\beta_i} \\
& -2\sin\beta_i \sinh\beta_i \Big] \\
= \; & \frac{\rho L^2 1}{2\beta_i \sinh\beta_i + 2\beta_i \sin\beta_i} \Big[4\cosh\beta_i + 4\cos\beta_i - \cosh\beta_i e^{-\beta_i} - 1 \\
& - \cos\beta_i e^{\beta_i} - e^{-\beta_i}\sinh\beta_i - \cos\beta_i e^{-\beta_i} \Big] \\
= \; & \frac{\rho L^2}{2\beta_i \sinh\beta_i + 2\beta_i \sin\beta_i} \Big[4\cosh\beta_i + 4\cos\beta_i - \cosh\beta_i e^{-\beta_i} \\
& +1 - e^{-\beta_i}\sinh\beta_i \Big] \\
= \; & \frac{\rho L^2}{2\beta_i \sinh\beta_i + 2\beta_i \sin\beta_i} \Big[4\cosh\beta_i + 4\cos\beta_i \Big] \\
= \; & \frac{2\rho L^2(\cosh\beta_i + \cos\beta_i)}{\beta_i(\sinh\beta_i + \sin\beta_i)} > 0
\end{aligned}
$$

This property is critical in the following discussion of controller design.

Substituting (2.1) into (2.4), the potential energy of the system can be calculated by

$$
\begin{aligned}
E_p &= \frac{1}{2} EI \int_0^L \left[\frac{\partial^2 y(x,t)}{\partial x^2} \right]^2 dx \\
&= \frac{1}{2} EI \left[\sum_{i=1}^{N} q_i^2 \int_0^L \phi_i''^2 dx + 2 \sum_{i,j=1 \; i \neq j}^{N} q_i q_j \int_0^L \phi_i'' \phi_j'' dx \right] \qquad (2.54)
\end{aligned}
$$

Recalling the orthogonal condition (2.41) and using (2.47), (2.54) can also be written into a compact form as

$$
\begin{aligned}
E_p &= \frac{1}{2} \sum_{i=1}^{N} q_i^2 \omega_i^2 \rho \\
&= \frac{1}{2} Q^T K_A Q \qquad (2.55)
\end{aligned}
$$

where K_A, the stiffness matrix of the system, is given by

$$K_A = \text{diag}[0\ \omega_1^2\rho\ \omega_2^2\rho\ \cdots\ \omega_N^2\rho] \in R^{(N+1)\times(N+1)} \tag{2.56}$$

By substituting equations (2.48) and (2.55) into the Euler-Lagrange's equations

$$\frac{d}{dt}\left(\frac{\partial(E_k - E_p)}{\partial\dot{Q}}\right) - \frac{\partial(E_k - E_p)}{\partial Q} = T = \begin{bmatrix} \tau(t) \\ 0 \\ \vdots \\ 0 \end{bmatrix} \tag{2.57}$$

we obtain the dynamic equation of the system as

$$M_A\ddot{Q} + K_A Q = T \tag{2.58}$$

where $T \in R^{N+1}$ denotes the generalized external force vector. From (2.48) and (2.55), one can see that both the inertia matrix M_A and the stiffness matrix K_A are constant matrices. It follows that the dynamic equation (2.58) is linear and time-invariant. This result actually comes from the arc approximation of the position of the beam by $p(x,t)$, which itself can be taken as a linearization process of the system dynamics. Such a linear model of the single-link flexible robot system is experimentally tested in [57], and it is shown there that the vibration frequencies obtained from the frequency response of the linear model is quite close to the experimental results.

Considering that a large amount of well-developed control theories concerned with a state-space model of the system, it is desirable to transform the dynamic equation

(2.58) into state-space form. Defining the following state vector

$$\begin{aligned} X &:= [Q^T \ \dot{Q}^T]^T \\ &= [\theta \ q_1 \ q_2 \ \cdots \ q_N \ \dot{\theta} \ \dot{q}_1 \ \dot{q}_2 \ \cdots \ \dot{q}_N]^T \in R^{2N+2} \end{aligned} \tag{2.59}$$

We have the corresponding linear state-space model,

$$\dot{X} = \begin{bmatrix} 0 & I \\ -M_A^{-1}K_A & 0 \end{bmatrix} X + \begin{bmatrix} 0 \\ M_A^{-1} \end{bmatrix} T \tag{2.60}$$

It should be pointed out that if the position of the beam is represented by the arc approximation, the linearity of the model will not be affected by the selection of different types of boundary conditions (which corresponds to different reference local frames in Figure 2.1). For example, in [9], a different linear model is obtained by using the pinned-free boundary conditions. Some research work has been carried out on the controller design based on these linear models, and the results, either numerical or experimental, are quite satisfactory [29], [9] and [58].

2.2.2 FEM modeling

In this section, we will introduce the FEM modeling of the single-link flexible robot system. In this method, the flexible beam is divided into a finite number of elements by some nodes, at which the characteristics (node variables) of the bending beam are assumed to be known, and the bending information at other points on the beam are then mathematically fitted by the node variables. The fitting functions

(or the admissible functions) here are selected to be the solutions of the differential equation which governs the static bending of the considered beam [17], though other choices, such as the B-spline functions [18], can also be used.

The parameters of the flexible beam, the motor and the tip payload are defined in the previous section. The system and the associated coordinates system are shown in Figure 2.2.

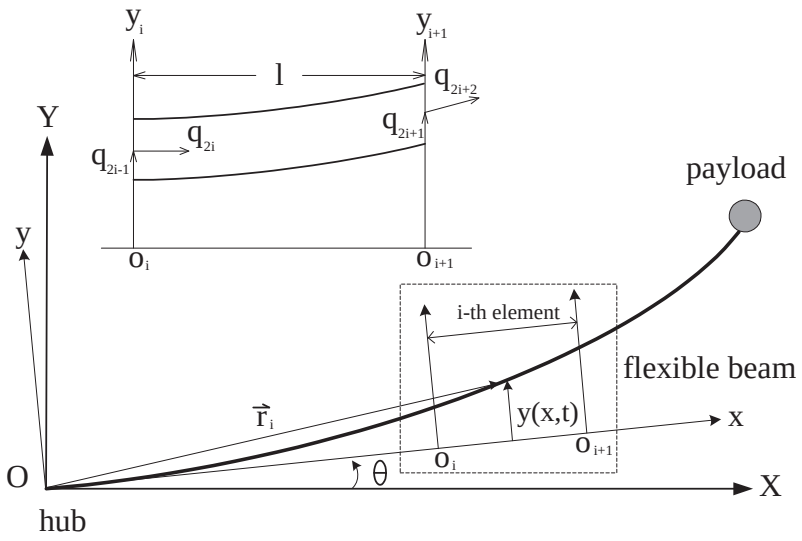

Figure 2.2: FEM modeling of a flexible robot.

For simplicity, the flexible beam is divided into a finite number, N, of elements with the same length $l = L/N$. The fixed base frame, as in Figure 2.1, is still denoted by XOY, however the local reference coordinate system is a little more complicated. There are totally N local reference frames, one for each of the N elements, i.e., frame $x_iO_iy_i$ is the reference frame for the ith element. All these N reference frames are in the same direction as frame $x_1O_1y_1$ (whose origin, O_1, coincides with the

base origin, O) which rotates with the hub. Obviously, the local frame $x_1O_1y_1$ is actually the reference frame xOy in Figure 2.1. The vector $\vec{O}_i$ in Figure 2.2 denote the position vector of the origin of frame $x_iO_iy_i$ with respect to the base frame XOY, and $\vec{r}_i$ is the position vector of the ith element with respect to the base frame XOY. From Figure 2.2, one may also note that the elastic deflection of the beam is represented with respect to the corresponding local frame, i.e., $y_i(x_i, t)$ is the elastic deflection of a point in the ith element measured in its own local frame $x_iO_iy_i$.

It should be pointed out that the beam's position here can also be expressed in either the arc approximation or the vector representation. However, only the latter is considered in this section. For the FEM modeling with arc approximation of beam's position, interested readers can refer to [13], in which it is shown that the arc approximation also leads to a linear time-invariant model. In the following section, we will show that the vector representation leads to a nonlinear model of the system.

Vector Representation

In this subsection, we would like to re-derive the dynamic model of the single-link flexible robot system with the position of a point on the beam being represented by the vector $\vec{r}$ as shown in Figure 2.1.

Noting that $\vec{r}$ denote the position vector of a point on the beam with respect to the fixed based frame XOY, and $\vec{r}^*$ with respect to the local frame xOy, using some basic knowledge of geometry, we have

$$\begin{aligned} \vec{r} &= T_r \vec{r}^* \\ &= T_r \begin{bmatrix} x \\ y(x,t) \end{bmatrix} \end{aligned} \tag{2.61}$$

where T_r is the orthogonal transformation function between the two considered frames given by

$$T_r = \begin{bmatrix} \cos\theta(t) & -\sin\theta(t) \\ \sin\theta(t) & \cos\theta(t) \end{bmatrix} \tag{2.62}$$

which satisfies

$$T_r^{-1} = T_r^T \tag{2.63}$$

From some basic geometry knowledge, we have

$$\vec{O}_i = \begin{bmatrix} (i-1)l\cos\theta(t) \\ (i-1)l\sin\theta(t) \end{bmatrix} \tag{2.64}$$

$$\begin{aligned} \vec{r}_i &= \vec{O}_i + T_r \begin{bmatrix} x_i \\ y_i(x_i,t) \end{bmatrix} \\ &(i = 1, 2, \cdots, N) \end{aligned} \tag{2.65}$$

where T_r in (2.62) is the orthogonal rotational transformation matrix between frames XOY and $x_iO_iy_i$. Combining equations (2.64) and (2.65) yields

$$\dot{\vec{r}}_i = \dot{\vec{O}}_i + \dot{T}_r \begin{bmatrix} x_i \\ y_i(x_i,t) \end{bmatrix} + T_r \begin{bmatrix} \dot{x}_i \\ \dot{y}_i(x_i,t) \end{bmatrix}$$

$$
\begin{aligned}
&= T_r \begin{bmatrix} 0 \\ (i-1)l\dot{\theta} \end{bmatrix} + T_r \begin{bmatrix} -y_i\dot{\theta} \\ x_i\dot{\theta} + \dot{y}_i \end{bmatrix} \\
&= T_r \begin{bmatrix} -y_i\dot{\theta} \\ [(i-1)l + x_i]\,\dot{\theta} + \dot{y}_i \end{bmatrix} \\
&= T_r \vec{W}_F
\end{aligned} \tag{2.66}
$$

where

$$
\vec{W}_F = \begin{bmatrix} -y_i\dot{\theta} \\ [(i-1)l + x_i]\,\dot{\theta} + \dot{y}_i \end{bmatrix}
$$

Solution of the Differential Equation Governing Static Bending of the Beam

Let us consider the ith element detailed in Figure 2.2. For the nodes through which we divide the beam into elements, each of them undergoes both translational and rotational displacements at the same time (axial displacement is neglected). Let q_{2i-1} and q_{2i+1} be the displacements of two nodes of the ith element and q_{2i} and q_{2i+2} be the two rotations, then q_{2i-1}, q_{2i+1}, q_{2i} and q_{2i+2} are the node variables through which the characteristics of other points in element i will be fitted.

Since there is a total of N elements, the number of node variable, q, is $2N + 2$, i.e., q_1, q_2, $\cdots$, q_{2N+2}. We can represent the elastic deflection in the ith element,

$y_i(x_i, t)$, by

$$y_i(x_i, t) = \sum_{j=1}^{4} \psi_j(x_i) q_{2(i-1)+j}(t) \qquad (2.67)$$
$$(i = 1,\ 2,\ \cdots,\ N \quad and \quad 0 < x_i < l)$$

where $\psi_j(x_i)$ are the admissible functions. Because each q_i corresponds to one DOF of the system, the variables q_1 to q_{2N+2} are actually the system's generalized coordinates. From Figure 2.2, we can obtain the boundary conditions with respect to the two nodes of the element [17]

$$\begin{cases} y_i(0,t) = q_{2i-1}(t) \\ \frac{\partial y_i(x_i,t)}{\partial x_i} \mid_{x_i=0} = q_{2i}(t) \\ y_i(l,t) = q_{2i+1}(t) \\ \frac{\partial y_i(x_i,t)}{\partial x_i} \mid_{x_i=l} = q_{2i+2}(t) \end{cases} \qquad (2.68)$$

Substituting (2.67) into (2.68) gives the boundary conditions of admissible functions $\psi_j(x_i)$, $\quad j = 1, 2, 3, 4$

$$\psi_j(0) = \begin{cases} 1 & j = 1 \\ 0 & \text{otherwise} \end{cases} \qquad (2.69)$$

$$\psi_j(l) = \begin{cases} 1 & j = 3 \\ 0 & \text{otherwise} \end{cases} \qquad (2.70)$$

$$\frac{d\psi_j(x)}{dx} \mid_{x=0} = \begin{cases} 1 & j = 2 \\ 0 & \text{otherwise} \end{cases} \qquad (2.71)$$

$$\frac{d\psi_j(x)}{dx} \mid_{x=l} = \begin{cases} 1 & j = 4 \\ 0 & \text{otherwise} \end{cases} \qquad (2.72)$$

We shall assume that the admissible functions $\psi_j(x)$, $j = 1, 2, 3, 4$, are given by the solution of the differential equation which governs the static bending of the beam subject to the above boundary conditions. That is, if we let $\psi(x)$ be the static elastic deflection, we have the differential equation of static bending of the beam [17]

$$\psi''''(x) = 0, \quad 0 < x < l$$

The general solution of this differential equation has the form

$$\psi(x) = c_1 x^3 + c_2 x^2 + c_3 x + c_4$$

Using boundary conditions (2.69)-(2.72), the four admissible functions can be obtained

$$\begin{cases} \psi_1(x) = 1 - 3\frac{x^2}{l^2} + 2\frac{x^3}{l^3} \\ \psi_2(x) = x - 2\frac{x^2}{l} + \frac{x^3}{l^2} \\ \psi_3(x) = 3\frac{x^2}{l^2} - 2\frac{x^3}{l^3} \\ \psi_4(x) = -\frac{x^2}{l} + \frac{x^3}{l^2} \end{cases}$$

In order to use the Euler-Lagrange's Equations, we need to obtain the total kinetic energy and the total potential energy of the system. Let E_{ki} and E_{pi} be the kinetic energy and the potential energy of the ith element, and E_{kp} and E_{km} be the kinetic energy of the point mass tip payload and the kinetic energy of the motor, and we have

$$\begin{aligned} E_{ki} &= \frac{1}{2}\rho \int_0^l \left\{\dot{\vec{r}}_i\right\}^T \left\{\dot{\vec{r}}_i\right\} dx_i \\ E_{pi} &= \frac{1}{2} EI \int_0^l \left[\frac{\partial^2 y_i}{\partial x_i^2}\right]^T \left[\frac{\partial^2 y_i}{\partial x_i^2}\right] dx_i \end{aligned}$$

$$
\begin{aligned}
E_{kp} &= \frac{1}{2} M_t \left\{ \dot{\vec{r}}_i \mid_{i=N,\, x_i=l} \right\}^T \left\{ \dot{\vec{r}}_i \mid_{i=N,\, x_i=l} \right\} \\
E_{km} &= \frac{1}{2} I_h \dot{\theta}^2
\end{aligned}
$$

From (2.66), E_{ki} can be calculated by

$$
\begin{aligned}
E_{ki} &= \frac{1}{2}\rho \int_0^l \left\{ \dot{\vec{r}}_i \right\}^T \left\{ \dot{\vec{r}}_i \right\} dx_i \\
&= \frac{1}{2}\rho \int_0^l \vec{W}_F^T T_r^T T_r \vec{W}_F dx_i \\
&= \frac{1}{2}\rho \int_0^l \vec{W}_F^T \vec{W}_F dx_i \\
&= \frac{1}{2}\rho \int_0^l \left\{ y_i^2 \dot{\theta}^2 + \left[(i-1)l + x_i \right]^2 \dot{\theta}^2 + \dot{y_i}^2 + 2\left[(i-1)l + x_i \right] \dot{\theta} \dot{y_i} \right\} dx_i \quad (2.73)
\end{aligned}
$$

Recalling (2.67), (2.73) can be reduced to a compact form

$$
E_{ki} = \frac{1}{2} \dot{Q}_i^T M_{Fi} \dot{Q}_i \quad (2.74)
$$

where, $Q_i = [\theta \;\; q_{2i-1} \;\; q_{2i} \;\; q_{2i+1} \;\; q_{2i+2}]^T$ is the generalized coordinates vector of the ith element, and $M_{Fi} \in R^{5\times 5}$ is the symmetric and positive definite mass matrix corresponding to the ith element. For clarity, we define the following quantities

$$
\begin{aligned}
& m_{Fi}^j = \rho \textstyle\int_0^l \left[(i-1)l + x_i \right] \psi_j(x_i) dx_i \quad j = 1,2,3,4 \\
& m_{Fi}^{jk} = \rho \textstyle\int_0^l \psi_j(x_i) \psi_k(x_i) dx_i \qquad\qquad j,k = 1,2,3,4, \quad j \neq k \\
& \sigma_{Fi}^j = \rho \textstyle\int_0^l \psi_j^2(x_i) dx_i \qquad\qquad j = 1,2,3,4
\end{aligned}
$$

and let d_i be the coefficient of the item associated with $\dot{\theta}^2$ in the E_{ki} expression, we have

$$
d_i = \rho \int_0^l \left[(i-1)l + x_i \right]^2 dx_i
$$

$$+\left[q_{2i-1}\ q_{2i}\ q_{2i+1}\ q_{2i+2}\right]\begin{bmatrix} \sigma_{Fi}^1 & m_{Fi}^{12} & m_{Fi}^{13} & m_{Fi}^{14} \\ m_{Fi}^{12} & \sigma_{Fi}^2 & m_{Fi}^{23} & m_{Fi}^{24} \\ m_{Fi}^{13} & m_{Fi}^{23} & \sigma_{Fi}^3 & m_{Fi}^{34} \\ m_{Fi}^{14} & m_{Fi}^{24} & m_{Fi}^{34} & \sigma_{Fi}^4 \end{bmatrix}\begin{bmatrix} q_{2i-1} \\ q_{2i} \\ q_{2i+1} \\ q_{2i+2} \end{bmatrix} > 0 \quad (2.75)$$

then the mass matrix M_{Fi} is given by

$$M_{Fi} = \begin{bmatrix} d_i & m_{Fi}^1 & m_{Fi}^2 & m_{Fi}^3 & m_{Fi}^4 \\ m_{Fi}^1 & \sigma_{Fi}^1 & m_{Fi}^{12} & m_{Fi}^{13} & m_{Fi}^{14} \\ m_{Fi}^2 & m_{Fi}^{12} & \sigma_{Fi}^2 & m_{Fi}^{23} & m_{Fi}^{24} \\ m_{Fi}^3 & m_{Fi}^{13} & m_{Fi}^{23} & \sigma_{Fi}^3 & m_{Fi}^{34} \\ m_{Fi}^4 & m_{Fi}^{14} & m_{Fi}^{24} & m_{Fi}^{34} & \sigma_{Fi}^4 \end{bmatrix} \quad (2.76)$$

It should be pointed out that (i) σ_{Fi}^j and m_{Fi}^{jk} are the same for all the elements because they are independent of i; (ii) $d_i > 0$ because M_{Fi} is positive definite. Similarly using (2.66) for E_{kp}, we have

$$\begin{aligned} E_{kp} &= \frac{1}{2} M_t \left\{ W_F^T W_F \right\} |_{i=N,\, x_i=l} \\ &= \frac{1}{2} \dot{Q_N}^T M_{Fp} \dot{Q_N} \end{aligned}$$

where $M_{Fp} \in R^{5\times 5}$ is the symmetric positive definite mass matrix of the tip payload,

which has the form

$$M_{Fp} = \begin{bmatrix} d_p & m_{Fp}^1 & m_{Fp}^2 & m_{Fp}^3 & m_{Fp}^4 \\ m_{Fp}^1 & \sigma_{Fp}^1 & m_{Fp}^{12} & m_{Fp}^{13} & m_{Fp}^{14} \\ m_{Fp}^2 & m_{Fp}^{12} & \sigma_{Fp}^2 & m_{Fp}^{23} & m_{Fp}^{24} \\ m_{Fp}^3 & m_{Fp}^{13} & m_{Fp}^{23} & \sigma_{Fp}^3 & m_{Fp}^{34} \\ m_{Fp}^4 & m_{Fp}^{14} & m_{Fp}^{24} & m_{Fp}^{34} & \sigma_{Fp}^4 \end{bmatrix}$$

with elements being defined by

$$m_{Fp}^j = LM_t\psi_j(x)\mid_{x=l} \quad j = 1,2,3,4$$

$$m_{Fp}^{jk} = M_t\psi_j(x)\psi_k(x)\mid_{x=l} \quad j,k = 1,2,3,4,\ j{\neq}k$$

$$\sigma_{Fp}^j = M_t\psi_j^2(x)\mid_{x=l} \quad j = 1,2,3,4$$

$$d_p = M_tL^2 + [q_{2N-1}\ q_{2N}\ q_{2N+1}\ q_{2N+2}] \begin{bmatrix} \sigma_{Fp}^1 & m_{Fp}^{12} & m_{Fp}^{13} & m_{Fp}^{14} \\ m_{Fp}^{12} & \sigma_{Fp}^2 & m_{Fp}^{23} & m_{Fp}^{24} \\ m_{Fp}^{13} & m_{Fp}^{23} & \sigma_{Fp}^3 & m_{Fp}^{34} \\ m_{Fp}^{14} & m_{Fp}^{24} & m_{Fp}^{34} & \sigma_{Fp}^4 \end{bmatrix} \begin{bmatrix} q_{2N-1} \\ q_{2N} \\ q_{2N+1} \\ q_{2N+2} \end{bmatrix}$$

Recalling the boundary conditions in (2.69)-(2.72), d_p and M_{Fp} can be further simplified as

$$d_p \;=\; M_tL^2 + M_tq_{2N+1}^2 > 0 \tag{2.77}$$

$$M_{Fp} = \begin{bmatrix} d_p & 0 & 0 & M_tL & 0 \\ 0 & 0 & 0 & 0 & 0 \\ 0 & 0 & 0 & 0 & 0 \\ M_tL & 0 & 0 & M_t & 0 \\ 0 & 0 & 0 & 0 & 0 \end{bmatrix}$$

Now, the total kinetic energy E_k is given by

$$\begin{aligned} E_k &= \sum_{i=1}^{N} E_{ki} + E_{kp} + E_{km} \\ &= \frac{1}{2}\sum_{i=1}^{N} \dot{Q}_i^T M_{Fi} \dot{Q}_i + \frac{1}{2}\dot{Q}_N^T M_{Fp} \dot{Q}_N + \frac{1}{2} I_h \dot{\theta}^2 \end{aligned} \tag{2.78}$$

The potential energy of the ith element E_{pi} is given by

$$\begin{aligned} E_{pi} &= \frac{1}{2} EI \int_0^l \left[\frac{\partial^2 r_i}{\partial x_i^2}\right]^T \left[\frac{\partial^2 r_i}{\partial x_i^2}\right] dx_i \\ &= \frac{1}{2} EI \int_0^l \left[\frac{\partial^2 y_i}{\partial x_i^2}\right]^2 dx_i \end{aligned} \tag{2.79}$$

which, by using (2.65), (2.67) and noting the orthogonality of the transfer matrix T_r, can be written into the following compact form

$$E_{pi} = \frac{1}{2} Q_i^T K_{Fi} Q_i \tag{2.80}$$

where $K_{Fi} \in R^{5\times 5}$ is the stiffness matrix of the ith element. For clarity, let us define the following notations

$$k_{Fi}^j = EI \int_0^l \psi_j''^2(x_i) dx_i \qquad j = 1,2,3,4$$

$$k_{Fi}^{jn} = EI \int_0^l \psi_j''(x_i)\psi_n''(x_i) dx_i \quad j,n = 1,2,3,4, \quad j \neq n$$

then K_{Fi} can be expressed as

$$K_{Fi} = \begin{bmatrix} 0 & 0 & 0 & 0 & 0 \\ 0 & k_{Fi}^{1} & k_{Fi}^{12} & k_{Fi}^{13} & k_{Fi}^{14} \\ 0 & k_{Fi}^{12} & k_{Fi}^{2} & k_{Fi}^{23} & k_{Fi}^{24} \\ 0 & k_{Fi}^{13} & k_{Fi}^{23} & k_{Fi}^{3} & k_{Fi}^{34} \\ 0 & k_{Fi}^{14} & k_{Fi}^{24} & k_{Fi}^{34} & k_{Fi}^{4} \end{bmatrix} \tag{2.81}$$

It should be noted that all K_{Fi} are the same because k_{Fi}^{j} and k_{Fi}^{jn} are actually independent of i. Thus the total potential energy of the system is

$$\begin{aligned} E_p &= \sum_{i=1}^{N} E_{pi} \\ &= \frac{1}{2} \sum_{i=1}^{N} Q_i^T K_{Fi} Q_i \end{aligned} \tag{2.82}$$

In the derivation above, we introduce $2N + 2$ generalized coordinates q_1, q_2, $\cdots$, q_{2N+2} and θ to calculate the kinetic energy and the potential energy of the system,however, we should note that the flexible beam is clamped onto the rotor of the motor at the base such that the base displacement and rotation are zeros for all time, i.e. $q_1 = q_2 = 0$. Thus the kinetic energy and the potential energy of the first element can be modified to

$$\begin{aligned} E_{k1} &= \frac{1}{2} \dot{Q_1^{'}}^T M_{F1}^{'} \dot{Q_1^{'}} \\ E_{p1} &= \frac{1}{2} {Q_1^{'}}^T K_{F1}^{'} Q_1^{'} \end{aligned}$$

where

$$Q_1^{'} = [\theta \; q_3 \; q_4]^T$$

$$M_{F1}^{'} = \begin{bmatrix} d_1 & m_{F1}^3 & m_{F1}^4 \\ m_{F1}^3 & \sigma_{F1}^3 & m_{F1}^{34} \\ m_{F1}^4 & m_{F1}^{34} & \sigma_{F1}^4 \end{bmatrix}$$

$$K_{F1}^{'} = \begin{bmatrix} 0 & 0 & 0 \\ 0 & k_{F1}^3 & k_{F1}^{34} \\ 0 & k_{F1}^{34} & k_{F1}^4 \end{bmatrix}$$

For simplicity, we shall drop the primes, i.e., $Q_1 = Q_1^{'}$, $M_{F1} = M_{F1}^{'}$ and $K_{F1} = K_{F1}^{'}$, here after.

Up till now, the kinetic energy and the potential energy of the system are respectively derived from the N local generalized coordinates vector Q_i. In order to obtain the dynamic model of the system, we need to transform the above results into a global generalized coordinate system. This is done as follows.

Introduce a vector $Q \in R^{2N+1}$ as

$$\begin{aligned} Q &= [\theta \; q_3 \; q_4 \; \cdots \; q_{2N+2}]^T \\ &= [\eta_1 \; \eta_2 \; \cdots \; \eta_{2N+1}]^T \end{aligned} \tag{2.83}$$

and a series of matrices H_i $(i = 1, 2, \cdots, N)$, with H_1 being defined as

$$H_1 = \begin{bmatrix} 1 & 0 & 0 & \cdots & 0 \\ 0 & 1 & 0 & \cdots & 0 \\ 0 & 0 & 1 & \cdots & 0 \end{bmatrix} \in R^{3\times(2N+1)}$$

and $H_i = [h_{j,k}] \in R^{5\times(2N+1)}$ $(i = 2, 3, \cdots, N)$, in which all the elements are zeros

except for $h_{1,1}$, $h_{2,2i-2}$, $h_{3,2i-1}$, $h_{4,2i}$ and $h_{5,2i+1}$ being equal to 1. It is easy to check that

$$Q_i = H_i Q \tag{2.84}$$

Defining two matrices

$$\begin{aligned} \tilde{M}_{Fi} &= H_i^T M_{Fi} H_i \in R^{(2N+1)\times(2N+1)} \\ \tilde{K}_{Fi} &= H_i^T K_{Fi} H_i \in R^{(2N+1)\times(2N+1)} \end{aligned}$$

and substituting (2.84) into (2.74) and (2.80) give

$$\begin{aligned} E_{ki} &= \frac{1}{2}\dot{Q}^T \tilde{M}_{Fi} \dot{Q} \\ E_{pi} &= \frac{1}{2} Q^T \tilde{K}_{Fi} Q \end{aligned}$$

The same generalization procedure can also be carried out on E_{kp} and E_{km} by introducing the following two matrices

$$\begin{aligned} \tilde{M}_{Fp} &= H_N^T M_{Fp} H_N \in R^{(2N+1)\times(2N+1)} \\ \tilde{M}_{Fm} &= \begin{bmatrix} I_h & 0 & \cdots & 0 \\ 0 & & & \\ \vdots & & 0 & \\ 0 & & & \end{bmatrix} \in R^{(2N+1)\times(2N+1)} \end{aligned} \tag{2.85}$$

then we have

$$\begin{aligned} E_{kp} &= \frac{1}{2}\dot{Q}^T \tilde{M}_{Fp} \dot{Q} \\ E_{km} &= \frac{1}{2}\dot{Q}^T \tilde{M}_{Fm} \dot{Q} \end{aligned}$$

Thus, the total kinetic energy and the potential energy of the system are given by

$$\begin{aligned} E_k &= \sum_{i=1}^{N} E_{ki} + E_{kp} + E_{km} \\ &= \frac{1}{2}\dot{Q}^T \left[\tilde{M}_{Fp} + \tilde{M}_{Fm} + \sum_{i=1}^{N} \tilde{M}_{Fi} \right] \dot{Q} \\ &= \frac{1}{2}\dot{Q}^T M_F \dot{Q} \end{aligned} \tag{2.86}$$

$$\begin{aligned} E_p &= \sum_{i=1}^{N} E_{pi} \\ &= \frac{1}{2} Q^T \left[\sum_{i=1}^{N} \tilde{K}_{Fi} \right] Q \\ &= \frac{1}{2} Q^T K_F Q \end{aligned} \tag{2.87}$$

where the symmetric positive definite mass matrix M_F and the stiffness matrix K_F are defined by

$$M_F = \tilde{M}_{Fp} + \tilde{M}_{Fm} + \sum_{i=1}^{N} \tilde{M}_{Fi} \tag{2.88}$$

$$K_F = \sum_{i=1}^{N} \tilde{K}_{Fi} \tag{2.89}$$

Since the first element of M_F is a function of generalized coordinates though other elements are all constants, it will be seen that the resulting model is nonlinear. Substituting (2.86) and (2.87) into the Euler-Lagrange's Equations (2.57), we arrive at the dynamic model

$$M_F(Q)\ddot{Q} + C_F(Q, \dot{Q})\dot{Q} + K_F Q = T \tag{2.90}$$

where the generalized external force vector $T = [\tau(t)\ 0\ \cdots\ 0]^T \in R^{(2N+1)\times 1}$ and the

matrix $C_F = [c_{kj}]$, $j, k = 1, 2, \cdots, 2N+1$ is calculated by

$$c_{kj} = \sum_{i=1}^{2N+1} \frac{1}{2} \left(\frac{\partial m_{F-kj}}{\partial \eta_i} + \frac{\partial m_{F-ki}}{\partial \eta_j} - \frac{\partial m_{F-ij}}{\partial \eta_k} \right) \dot{\eta}_i \tag{2.91}$$

in which m_{F-ij} denote the ijth element of M_F and η_i's are the system generalized coordinates defined in (2.83). Further defining the state vector $X = [Q^T \ \dot{Q}^T]^T$, we can obtain the state-space model of the system,

$$\dot{X} = \begin{bmatrix} 0 & I \\ -M_F^{-1}K_F & -M_F^{-1}C_F \end{bmatrix} X + \begin{bmatrix} 0 \\ M_F^{-1} \end{bmatrix} T \tag{2.92}$$

As we have stated above, only the first element of M_F is inconstant, which, from (2.88), is given by

$$m_{F-11} = d_p + I_h + \sum_{i=1}^{N} d_i \tag{2.93}$$

with $d_p > 0$ and $d_i > 0$ being defined in (2.77) and (2.75).

2.3 Modeling of Multi-link Flexible Robots

For a multi-link flexible robot, most existing models are based on AMM [22]. In this section, we derive the dynamic model of a multilink flexible robot based on FEM. The geometry of the robot is shown in Figure 2.3. In total, $2N$ frames are used to describe the system, i.e., $X_jO_jY_j$ and $x_jO_jy_j$, $j = 1, 2, \cdots, N$. Frame $X_1O_1Y_1$ is the fixed base frame. Other frames are all local reference frames attached to the corresponding motors, specifically axis O_jX_j $(j = 2, 3, \cdots, N)$ is defined as the tangent to the end tip of link $j-1$, and axis O_jx_j $(j = 1, 2, \cdots, N)$ is tangent to

link j at its base. The angular position of the jth link is denoted by θ_j measured in frame $X_jO_jY_j$. θ_j is actually the angular difference between frames $x_jO_jy_j$ and $X_jO_jY_j$.

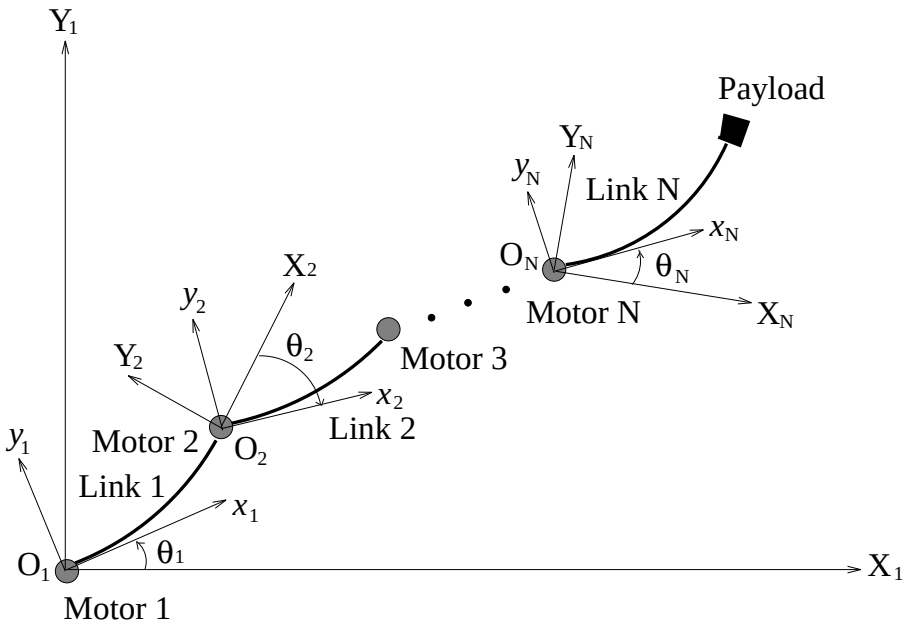

Figure 2.3: Geometry of the multi-link flexible robot

The multilink system geometry changes into the form shown in Figure 2.4, and those of the j-th link are detailed in Figure 2.5. The following notations are used throughout this section, unless otherwise stated.

(x_0, y_0): reference coordinates;

(x_j, y_j): local coordinates of frame $x_jO_jy_j$ that is attached to the j-th link;

$(x_{i,j}, y_{i,j})$: local coordinates of frame $x_{i,j}O_{i,j}y_{i,j}$that is attached to the i-th element of the j-th link;

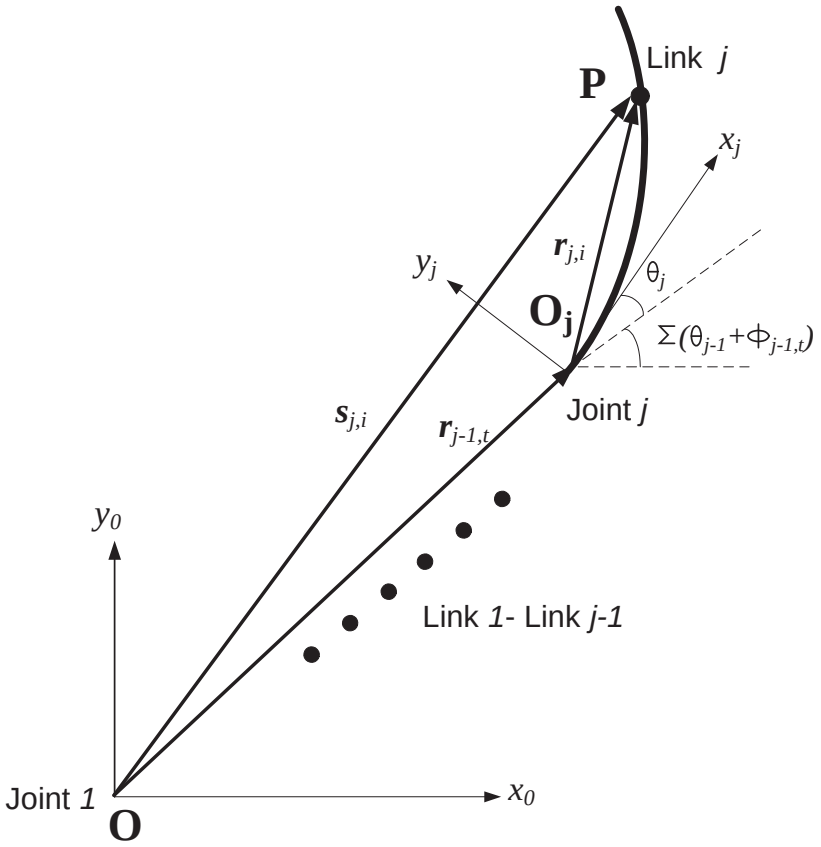

Figure 2.4: Structure of multilink flexible robot

θ_j: rigid angle at the j-th hub;

ϕ_{jt}: rotational displacement at the tip of the j-th link;

$q_{j,2i-1}$, $q_{j,2i+1}$: linear displacement at the two nodes of the element i of the j-th link;

$q_{j,2i}$, $q_{j,2i+2}$: rotational displacement at the two nodes of the element i of the j-th link;

$\mathbf{r}_{j,i}$: vector from O_j to point P in reference coordinates;

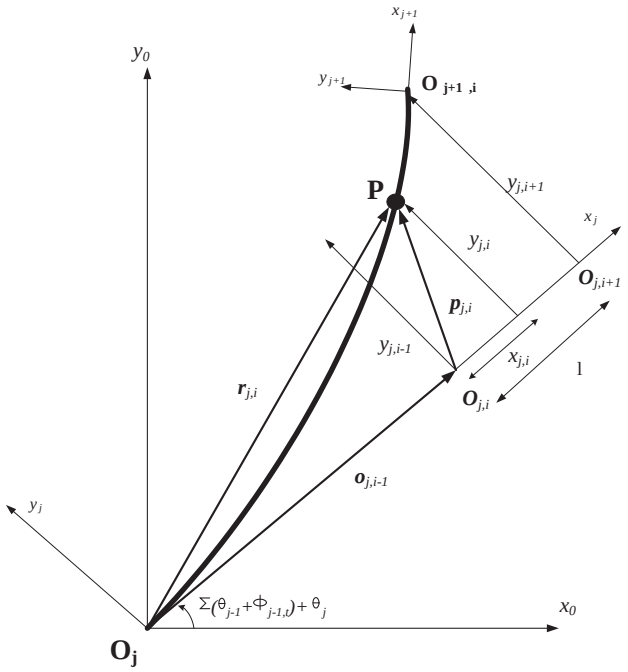

Figure 2.5: Structure of the j-th link

$\mathbf{r}_{j,t}$: position vector of O_j from O_{j-1} in reference coordinates;

$\mathbf{s}_{j,i}$: position vector of P from O;

$\mathbf{s}_j$: position vector of O_j from O;

$\mathbf{o}_{j,i}$: vector from O_j to $O_{j,i}$ in reference coordinates;

EI: the uniform flexural rigidity of the flexible beam;

ρ: the uniform mass per unit length of the flexible beam;

M_t: the concentrated mass tip payload;

I_{hj}: the hub inertia of the j-th link;

$\tau(t)_j$: the torque applied by the motor at the base;

$*_{j,i}$ be the i-th element of the j-th link, unless otherwise state.

According to the FEM, without loss of generality, we assume that the beam is divided into n parts of same length $l = L/n$. Recalling the structure of each element (Figure 2.2), let $q_{j,2i-1}$ and $q_{j,2i+1}$ be the displacements of two nodes, while $q_{j,2i}$ and $q_{j,2i+2}$ are the two rotations. Similarly, the elastic deflection in the j,i element $y_{j,i}$ can be represented by a weighted sum $q_{j,2i-1}$, $q_{j,2i}$, $q_{j,2i+1}$ and $q_{j,2i+2}$, and is given by

$$y_{j,i}(x_{j,i},t) = \sum_{k=1}^{4} \psi_k(x_{j,i}) q_{j,2(i-1)+k}(t) \tag{2.94}$$
$$(j = 1,\ 2,\ \cdots,\ N \quad i = 1,\ 2,\ \cdots,\ n \text{ and } \ 0 < x_{j,i} < l)$$

In accordance with the boundary conditions, say, $y_{j,i}(0,t) = q_{j,2i-1}(t)$, $\frac{\partial y_{j,i}(x_{j,i},t)}{\partial x_{j,i}} \mid_{x_{j,i}=0} = q_{j,2i}(t)$, $y_{j,i}(l,t) = q_{j,2i+1}(t)$, $\frac{\partial y_{j,i}(x_{j,i},t)}{\partial x_{j,i}} \mid_{x_{j,i}=l} = q_{j,2i+2}(t)$, the weights can be chosen as 3rd order polynomials, i.e.,

$$\mathbf{\Psi}(x_{j,i}) = \begin{bmatrix} 1 - \frac{3x_{j,i}^2}{l^2} + \frac{2x_{j,i}^3}{l^3} \\ x_{j,i} - \frac{2x_{j,i}^2}{l} + \frac{x_{j,i}^3}{l^2} \\ \frac{3x_{j,i}^2}{l^2} - \frac{2x_{j,i}^3}{l^3} \\ -\frac{x_{j,i}^2}{l} + \frac{x_{j,i}^3}{l^2} \end{bmatrix},$$

For the j-th link, the position of P on the i-th element is

$$\mathbf{s}_{j,i} = \mathbf{s}_j + \mathbf{r}_{j,i} \tag{2.95}$$

From Figure 2.5, we know

$$\mathbf{r}_{j,i} = \mathbf{o}_{j,i} + \mathbf{T}_j \begin{bmatrix} x_{j,i} \\ y_{j,i}(x_{j,i}, t) \\ 0 \end{bmatrix} \quad (i = 1, 2, \cdots, n) \tag{2.96}$$

It should be noted that the local coordinates (x_j, y_j) is now rotated by an angle of $(\alpha_{j-1} = \sum_{k=1}^{j-1}(\theta_k + \phi_{k,t}) + \theta_j)$ about the z-axis from the reference coordinates. This means that the transformation matrix which expressed the global coordinates in terms of the local coordinates of the j-th link is given by

$$\mathbf{T}_j(\alpha_{j-1}) = \begin{bmatrix} \cos\alpha_{j-1} & -\sin\alpha_{j-1} & 0 \\ \sin\alpha_{j-1} & \cos\alpha_{j-1} & 0 \\ 0 & 0 & 1 \end{bmatrix} \tag{2.97}$$

$$\mathbf{o}_{j,i} = \begin{bmatrix} (i-1)l\cos\alpha_{j-1} \\ (i-1)l\sin\alpha_{j-1} \\ 0 \end{bmatrix} \tag{2.98}$$

where $\mathbf{T}_j$ in (2.97) is the orthogonal rotational transformation matrix between frames $X_jO_jY_j$ and $x_{j,i}o_{j,i}y_{j,i}$. Combining equations (2.98), (2.96) yields

$$\dot{\mathbf{r}}_{j,i} = \dot{\mathbf{o}}_{j,i} + \dot{\mathbf{T}}_j \begin{bmatrix} x_{j,i} \\ y_{j,i}(x_{j,i}, t) \\ 0 \end{bmatrix} + \mathbf{T}_j \begin{bmatrix} \dot{x}_{j,i} \\ \dot{y}_{j,i}(x_{j,i}, t) \\ 0 \end{bmatrix}$$

$$
\begin{aligned}
&= \mathbf{T}_j \begin{bmatrix} 0 \\ (i-1)l\dot{\alpha}_{j-1} \\ 0 \end{bmatrix} + \mathbf{T}_j \begin{bmatrix} -y_{j,i}\dot{\alpha}_{j-1} \\ x_{j,i}\dot{\alpha_{j-1}} + \dot{y_{j,i}} \\ 0 \end{bmatrix} \\
&= \mathbf{T}_j \begin{bmatrix} -y_{j,i}\dot{\alpha}_{j-1} \\ \left[(i-1)l + x_{j,i}\right]\dot{\alpha}_{j-1} + \dot{y}_{j,i} \\ 0 \end{bmatrix} \\
&= \mathbf{T}_j \mathbf{T}_{j,i} \mathbf{q}_{j,i}
\end{aligned} \tag{2.99}
$$

where

$$
\mathbf{T}_{j,i} = \begin{bmatrix} -y_{j,i} & -y_{j,i} & -y_{j,i} & \mathbf{0} \\ \left[(i-1)l + x_{j,i}\right] & \left[(i-1)l + x_{j,i}\right] & \left[(i-1)l + x_{j,i}\right] & \mathbf{\Psi}(x_{j,i}) \\ 0 & 0 & 0 & \mathbf{0} \end{bmatrix}
$$

and

$$
\dot{\mathbf{q}}_{j,i} = [\dot{\theta}_1 \ \dot{\phi}_{1,t} \ \dot{\theta}_2 \ \dot{\phi}_{2,i} \ \cdots \ \theta_j \ \dot{q}_{j,1} \ \dot{q}_{j,2} \ \dot{q}_{j,3} \ \dot{q}_{j,4}]^T \tag{2.100}
$$

Now, let us reconsider equation (2.95). Recalling (2.99), its derivative can be given by

$$
\begin{aligned}
\dot{\mathbf{s}}_{j,i} &= \dot{\mathbf{s}}_j + \dot{\mathbf{r}}_{j,i} \\
&= \sum_{k=1}^{j-1} \dot{\mathbf{r}}_{k,t} + \dot{\mathbf{r}}_{j,i}
\end{aligned} \tag{2.101}
$$

We need to obtain the kinetic energy, potential energy and virtual work of each link, in order to apply Lagrange-Euler equations. Let $E_{k,j,i}$ and $E_{p,j,i}$ be the kinetic energy and the potential energy of the ith element of j-th link, and E_{kpj} and E_{kmj}

be the kinetic energy of the point mass tip payload and the kinetic energy of the motor, and we have

$$\begin{aligned} E_{k,j,i} &= \frac{1}{2}\rho \int_0^l \{\dot{\mathbf{s}}_{j,i}\}^T \{\dot{\mathbf{s}}_{j,i}\}\, dx_{j,i} \\ E_{p,j,i} &= \frac{1}{2} E_j I_j \int_0^l \left[\frac{\partial^2 y_{j,i}}{\partial x_{j,i}^2}\right]^T \left[\frac{\partial^2 y_{j,i}}{\partial x_{j,i}^2}\right] dx_{j,i} \\ E_{kp} &= \frac{1}{2} M_t \dot{\mathbf{s}}_N^T \dot{\mathbf{s}}_N \\ E_{kmj} &= \frac{1}{2} I_{hj} \dot{\theta}_j^{\,2} \end{aligned}$$

From (2.101), $E_{k,j,i}$ can be calculated by

$$\begin{aligned} E_{k,j,i} &= \frac{1}{2}\rho \int_0^l \{\dot{\mathbf{s}}_{j,i}\}^T \{\dot{\mathbf{s}}_{j,i}\}\, dx_{j,i} \\ &= \frac{1}{2}\rho \int_0^l \left[(\sum_{k=1}^{j-1} \dot{\mathbf{r}}_{k,t})^T (\sum_{k=1}^{j-1} \dot{\mathbf{r}}_{k,t}) + \dot{\mathbf{r}}_{j,i}^T \dot{\mathbf{r}}_{j,i} + \dot{\mathbf{r}}_{j,i}^T \sum_{k=1}^{j-1} \dot{\mathbf{r}}_{k,t} + (\sum_{k=1}^{j-1} \dot{\mathbf{r}}_{k,t})^T \dot{\mathbf{r}}_{j,i} \right] dx_{j,i} \\ &= \frac{1}{2} \dot{\mathbf{Q}}_{j,i}^T \dot{\mathbf{M}}_{j,i} \dot{\mathbf{Q}}_{j,i}^T \end{aligned} \tag{2.102}$$

where $\mathbf{Q}_{j,i} = [\theta_1 \ \mathbf{Q}_{1,t}^T \ \theta_2 \ \mathbf{Q}_{2,t}^T \ \cdots \ \theta_j \ q_{j,2i-1} \ q_{j,2i} \ q_{j,2i+1} \ q_{j,2i+2}]^T$ is the generalized coordinates, with $\mathbf{Q}_{j,t} = [q_{j,2n-1} \ q_{j,2n} \ q_{j,2n+1} \ q_{j,2n+2}]^T$, and $\mathbf{M}_{j,i}$ is obtained by collecting together all the terms corresponding to the degree of freedom of $Q_{j,i}$.

Similarly, for $E_{k,j,p}$, we have

$$\begin{aligned} E_{kp} &= \frac{1}{2} M_t \{\dot{\mathbf{s}}_j\}^T \{\dot{\mathbf{s}}_j\} \\ &= \frac{1}{2} \dot{\mathbf{Q}}_N^T \mathbf{M}_p \dot{\mathbf{Q}}_N \end{aligned}$$

The potential energy of the i-th element $E_{p,j,i}$ is given by

$$\begin{aligned} E_{pi} &= \frac{1}{2} EI \int_0^l \left[\frac{\partial^2 s_{j,i}}{\partial x_{j,i}^2}\right]^T \left[\frac{\partial^2 s_{j,i}}{\partial x_{j,i}^2}\right] dx_{j,i} \\ &= \frac{1}{2} \mathbf{Q}_{j,i}^T \mathbf{K}_{j,i} \mathbf{Q}_{j,i} \end{aligned} \tag{2.103}$$

where $\mathbf{K}_{j,i}$ is the stiffness matrix. Similarly, the base displacement and rotation are zero, i.e. $q_{j,1} = q_{j,2} = 0$, $j = 1, 2 \ldots N$. Now, we need to transform the result of the kinetic energy and the potential energy to a global generalized coordinate system. Introduce a vector $\mathbf{Q} \in R^{N(2n+3)}$ as

$$\begin{aligned} \mathbf{Q} &= [\theta_1 \; q_{1,3} \; q_{1,4} \; \cdots \; q_{1,2n+2} \; \cdots \; \theta_N \; q_{N,3} \; \cdots \; q_{N,2n+2}]^T \\ &= \left[\eta_1 \; \eta_2 \; \cdots \; \eta_{N(2n+1)}\right]^T \end{aligned} \tag{2.104}$$

and $\mathbf{H}_{j,i} \in R^{5N \times N(2n+1)} (j = 1, 2, \cdots, N \text{ and } i = 1, 2, \cdots, n)$ is defined as

$$\mathbf{H}_{j,i} = \begin{bmatrix} \mathbf{H}_t^{vec} \\ \mathbf{H}_i \\ \mathbf{H}_o^{vec} \end{bmatrix}$$

where

$$\mathbf{H}_t^{vec} = \begin{bmatrix} \mathbf{H}_t \\ \cdots \\ \mathbf{H}_t \end{bmatrix} \in R^{5j \times N(2n+1)}$$

and

$$\mathbf{H}_o^{vec} = \begin{bmatrix} \mathbf{H}_o \\ \cdots \\ \mathbf{H}_o \end{bmatrix} \in R^{5(N-j) \times N(2n+1)}$$

with

$$\mathbf{H}_t = \begin{bmatrix} 1 & 0 & \cdots 0 & 0 & 0 & 0 \\ 0 & 0 & \cdots 1 & 0 & 0 & 0 \\ 0 & 0 & \cdots 0 & 1 & 0 & 0 \\ 0 & 0 & \cdots 0 & 0 & 1 & 0 \\ 0 & 0 & \cdots 0 & 0 & 0 & 1 \end{bmatrix} \in R^{5\times N(2n+1)},$$

and

$$\mathbf{H}_o = [\mathbf{0}] \in R^{5\times N(2n+1)}$$

and $\mathbf{H}_1$ is define as

$$\mathbf{H}_1 = \begin{bmatrix} 1 & 0 & 0 & \cdots & 0 \\ 0 & 1 & 0 & \cdots & 0 \\ 0 & 0 & 1 & \cdots & 0 \end{bmatrix} \in R^{3\times N(2n+1)}$$

and $\mathbf{H}_i \in R^{5N\times(2N+1)}$, with all the elements are zeros except for $h_{1,1} = h_{2,2i-2} = h_{3,2i-1} = h_{4,2i} = h_{5,2i+1} = 1$. Thus, it is easy to see that

$$\mathbf{Q}_{j,i} = \mathbf{H}_{j,i}\mathbf{Q} \tag{2.105}$$

Defining two matrices

$$\tilde{\mathbf{M}}_{j,i} = \mathbf{H}_{j,i}^T \mathbf{M}_{j,i}\mathbf{H}_{j,i} \tag{2.106}$$

$$\tilde{\mathbf{K}}_{j,i} = \mathbf{H}_{j,i}^T \mathbf{K}_{j,i}\mathbf{H}_{j,i} \tag{2.107}$$

and we have

$$E_{k,j,i} = \frac{1}{2}\mathbf{Q}_{j,i}^T \tilde{\mathbf{M}}_{j,i}\mathbf{Q}_{j,i} \tag{2.108}$$

$$E_{p,j,i} = \frac{1}{2}\mathbf{Q}_{j,i}^T \tilde{\mathbf{K}}_{j,i}\mathbf{Q}_{j,i} \tag{2.109}$$

and the same procedure are carried out for E_{kp} and E_{kmj}, with

$$\tilde{\mathbf{M}}_p = \mathbf{H}_{N,n}^T \mathbf{M}_p \mathbf{H}_{N,n} \tag{2.110}$$

$$\tilde{\mathbf{M}}_m = \begin{bmatrix} \mathbf{M}_{m1} & 0 & \cdots & 0 \\ 0 & \mathbf{M}_{m2} & & \\ \vdots & & \ddots & \\ 0 & & & \mathbf{M}_{mN} \end{bmatrix} \in R^{(2N+1)\times(2N+1)} \tag{2.111}$$

where

$$\mathbf{M}_{mj} = \begin{bmatrix} I_h & 0 & \cdots & 0 \\ 0 & & & \\ \vdots & & 0 & \\ 0 & & & \end{bmatrix}, \quad j = 1, 2, \ldots, N,$$

E_{kp} and E_{kmj} are given by

$$E_{kp} = \frac{1}{2}\mathbf{Q}_{j,i}^T \tilde{\mathbf{M}}_p \mathbf{Q}_{j,i} \tag{2.112}$$

$$E_{km} = \frac{1}{2}\mathbf{Q}_{j,i}^T \tilde{\mathbf{M}}_m \mathbf{Q}_{j,i} \tag{2.113}$$

Then, the total kinetic energy E_k and potential energy E_p are given by

$$\begin{aligned} E_k &= \sum_{i=1}^{N}\sum_{i=1}^{n} E_{k,j,i} + E_{kp} + E_{km} \\ &= \frac{1}{2}\dot{\mathbf{Q}}^T \left[\sum_{i=1}^{N}\sum_{i=1}^{n} \tilde{\mathbf{M}}_{j,i} + \tilde{\mathbf{M}}_p + \tilde{\mathbf{M}}_m\right] \dot{\mathbf{Q}} \\ &= \frac{1}{2}\dot{\mathbf{Q}}^T \mathbf{M} \dot{\mathbf{Q}} \end{aligned} \tag{2.114}$$

$$\begin{aligned} E_p &= \sum_{j=1}^{N}\sum_{i=1}^{n} E_{p,j,i} \\ &= \frac{1}{2}\mathbf{Q}^T \left[\sum_{j=1}^{N}\sum_{i=1}^{n} \mathbf{K}_{j,i}\right] \mathbf{Q} \end{aligned} \tag{2.115}$$

where the symmetric positive definite mass matrix $\mathbf{M}$ and the stiffness matrix $\mathbf{K}$ are defined by

$$\mathbf{M} = \sum_{i=1}^{N}\sum_{i=1}^{n}\tilde{\mathbf{M}}_{j,i} + \tilde{\mathbf{M}}_p + \tilde{\mathbf{M}}_m \tag{2.116}$$

$$\mathbf{K} = \sum_{j=1}^{N}\sum_{i=1}^{n}\mathbf{K}_{j,i} \tag{2.117}$$

Substituting (2.114) and (2.115) into the Euler-Lafrange's Equations, we have the dynamic model

$$\mathbf{M}(\mathbf{Q})\ddot{\mathbf{Q}} + \mathbf{C}(\mathbf{Q},\dot{\mathbf{Q}})\dot{\mathbf{Q}} + \mathbf{K}\mathbf{Q} = \mathbf{T} \tag{2.118}$$

where the matrix $\mathbf{C} = [c_{kj}]$, $k, j = 1, 2, \ldots, N * (2n + 1)$ is calculated by

$$c_{kj} = \sum_{i=1}^{2N+1}\frac{1}{2}\left(\frac{\partial m_{kj}}{\partial \eta_i} + \frac{\partial m_{ki}}{\partial \eta_j} - \frac{\partial m_{ij}}{\partial \eta_k}\right)\dot{\eta}_i \tag{2.119}$$

in which m_{ij} denote the ijth element of $\mathbf{M}$ and η_i's are the system generalized coordinates (2.104), and the force vector $\mathbf{T} = [\tau_1\ \mathbf{0}\ \tau_2\ \mathbf{0}\ldots\ \tau_N\ \mathbf{0}]$. Further defining the state vector $\mathbf{X} = [\mathbf{Q}^T\ \dot{\mathbf{Q}}^T]^T$, we can obtain the state-space model of the system,

$$\dot{X} = \begin{bmatrix} 0 & \mathbf{I} \\ -\mathbf{M}^{-1}\mathbf{K} & -\mathbf{M}^{-1}\mathbf{C} \end{bmatrix}\mathbf{X} + \begin{bmatrix} 0 \\ \mathbf{M}^{-1} \end{bmatrix}\mathbf{T} \tag{2.120}$$

2.4 Summary

In this chapter the foundation is developed for subsequent flexible robot control system design and analysis. A new property that is essential to controller design is discovered. Fundamental concepts for modeling flexible links and several methods

are presented for obtaining approximate mode shapes for beams and beam-like structures. A detail explanation is given for the extension of the existing methods to multilink applications. Both AMM and FEM develop dynamic models that are incorporated into the controller design and simulations in the proceeding chapter.

Chapter 3

Control Design Based on Singular Perturbation

3.1 Introduction

Light weight manipulators offer many challenges in comparison with rigid robot manipulators. Energy consumption is smaller than other types of manipulators, so that the payload-to-arm weight ratio can be increased as well as faster movements can be achieved. Because of their characteristics, this class of manipulators are especially suitable for a number of nonconventional robotic applications. Various approaches such as linear control [29], optimal control [30], sliding mode control [31], direct strain feedback control [3], inverse dynamics methods, and energy-based control [32] have been studied based on a truncated model obtained form either

the FEM or AMM [1].

Singular perturbation theory has been a convenient tool for reduced order modeling [59,60]. The two-time scale model of the flexible link robot has been derived in [35]. According to singular perturbation theory [61], the whole system can be modeled as two reduced order subsystems by decoupling the fast variables and slow variables. In order to achieve the tracking control of flexible robots, the problem is often converted into composite control problem: (i) tracking control of the joint motion, and (ii) suppression of the elastic vibrations of the flexible links. The attractive feature of this strategy is that the slow control can be designed based on the well-established control schemes for rigid body manipulators, [25, 62, 63]. However, all of these work are based on the exact knowledge about the nonlinear functions or the bounds of uncertainties. If fact, such a priori knowledge may be difficult to obtain in practice. To overcome the limitation, the approximation capabilities of neural networks have been utilized to approximate the nonlinear characteristics of the systems. The introduction of neural networks can remove the need for tedious dynamic modeling of the system and the possibility of errors when obtaining the regression matrix. In recent literature, there are many neural network controls proposed for robot arm [43–45]. On the other hand, in a series of work [46–48], the control of the slow subsystem is designed and analyzed based on fuzzy logic algorithm to treat uncertainty.

However, for fast subsystem the adaptive control problem is open to question. Due

to the unknown parameters, the design difficulties mainly come from the fact that the fast state $\eta_1 = \mathbf{z}_1 - \bar{\zeta}$ are unmeasurable, and only η_2 is available for the control design. In order to avoid this problem, the tracking control for smart material robot is proposed in [64]. The active vibration control is achieved using smart material voltage, which turns out to be independent of the unknown dynamics. In this paper, we shall show a rigorous approach to position tracking control of a flexible link robot. By investigating the dynamic model, some critical properties of inertia matrix $\mathbf{M}$ are found. Using this properties, a fast subcontrol is designed based on $\boldsymbol{\eta}_2$. In addition, $\bar{\zeta}$ can be considered as a constant in the boundary layer [53]. Neural network based adaptive subcontrollers are proposed for the fast unknown dynamics by updating the estimation of $\bar{\zeta}$ in the fast feedback loop. The controllers ensure that the system asymptotically converge to a bounded invariant set. Furthermore, due to the existence of internal structural damping in a flexible link in practice, the flexible robot must tend to stop vibrating and finally be static at the undeformed position. Consequently, the controller approaches cannot hold at a nonzero constant, which implies the tip regulation is achieved.

The paper is organized as follows. In Section 2, the problems of NN approximation is briefly introduced. The singular perturbed model of flexible link robot is presented in Section 3. In Section 4, adaptive NN composite controller design is presented for the slow unknown dynamics, and an adaptive controllers are designed for the fast unknown dynamics. Numerical simulations are given in Section 5 to

show the effectiveness of the proposed methods.

3.2 Singular Perturbed Flexible Link Robot

Following from Chapter 2, the dynamic equation of the motion for an n DOF manipulator with up to n flexible links can be written in the following form:

$$\mathbf{M}(\mathbf{q}) \begin{bmatrix} \ddot{\mathbf{q}}_r \\ \\ \ddot{\mathbf{q}}_f \end{bmatrix} + \mathbf{C}(\mathbf{q}) \begin{bmatrix} \dot{\mathbf{q}}_r \\ \\ \dot{\mathbf{q}}_r \end{bmatrix} + \mathbf{K} \begin{bmatrix} \mathbf{q}_r \\ \\ \mathbf{q}_f \end{bmatrix} = \mathbf{T} \tag{3.1}$$

where

1. $\mathbf{q} = [\mathbf{q}_r^T \quad \mathbf{q}_f^T] \in \mathcal{R}^n$, $n = n_f + n_r$, with $\mathbf{q}_r \in \mathcal{R}^{n_r}$ the vector of the rigid variables and $\mathbf{q}_f \in \mathcal{R}^{n_f}$ the vector of the flexible variables;

2. $\mathbf{M}(q) \in \mathcal{R}^{n \times n}$ is the symmetric positive definite inertia matrix;

3. $\mathbf{C}(q, \dot{\mathbf{q}})\dot{\mathbf{q}} \in \mathcal{R}^n$ represents the Coriolis and Centrifugal forces;

4. $\mathbf{K} = diag[\mathbf{0}\ k_1\ k_2 \cdots k_{n_f}]^T$ is the constant matrix of the flexible link materials robot, with $k_i = \omega_i \rho$, $i = 1, n_f$;

5. $\mathbf{T}$ the vector of joint control torques.

Exploiting the natural time-scale separation between the faster flexible mode dynamics and the slower desired rigid mode dynamics, we use singular perturbation theory to formulate a boundary layer correction that stabilizes non-minimum phase

internal dynamics. Dynamic equation (3.1) can be partitioned as

$$\begin{bmatrix} \mathbf{M}_{rr} & \mathbf{M}_{rf} \\ \mathbf{M}_{fr} & \mathbf{M}_{ff} \end{bmatrix} \begin{bmatrix} \ddot{\mathbf{q}}_r \\ \ddot{\mathbf{q}}_f \end{bmatrix} + \begin{bmatrix} \mathbf{H}_r \\ \mathbf{H}_f \end{bmatrix} + \begin{bmatrix} \mathbf{0} \\ \mathbf{K}_{ff}\mathbf{q}_f \end{bmatrix} = \begin{bmatrix} \tau \\ \mathbf{0} \end{bmatrix} \tag{3.2}$$

where

$$\begin{aligned} \mathbf{H}_r &= \mathbf{C}_{rr}\dot{\mathbf{q}}_r + \mathbf{C}_{rf}\dot{\mathbf{q}}_f \\ \mathbf{H}_f &= \mathbf{C}_{fr}\dot{\mathbf{q}}_r + \mathbf{C}_{ff}\dot{\mathbf{q}}_f \end{aligned}$$

It should be noted that $\dot{\mathbf{M}} - 2\mathbf{C}$ is skew-symmetric as in the rigid robot case. Correspondingly, $\dot{\mathbf{M}}_{rr} - 2\mathbf{C}_{rr}$ is also skew-symmetric. Since inertia matrix $\mathbf{M}$ is positive definite, its inverse exists and is denoted by D as

$$\mathbf{M}^{-1} = \mathbf{D} = \begin{bmatrix} \mathbf{D}_{rr} & \mathbf{D}_{rf} \\ \mathbf{D}_{fr} & \mathbf{D}_{ff} \end{bmatrix} \tag{3.3}$$

where

$$\mathbf{D}_{rr} = (\mathbf{M}_{rr} - \mathbf{M}_{rf}\mathbf{M}_{ff}^{-1}\mathbf{M}_{fr})^{-1} \tag{3.4}$$

$$\mathbf{D}_{rf} = -\mathbf{M}_{rr}^{-1}\mathbf{M}_{rf}(\mathbf{M}_{ff} - \mathbf{M}_{fr}\mathbf{M}_{rr}^{-1}\mathbf{M}_{rf})^{-1} \tag{3.5}$$

$$\mathbf{D}_{fr} = -\mathbf{M}_{ff}^{-1}\mathbf{M}_{fr}(\mathbf{M}_{rr} - \mathbf{M}_{rf}\mathbf{M}_{ff}^{-1}\mathbf{M}_{fr})^{-1} \tag{3.6}$$

$$\mathbf{D}_{ff} = (\mathbf{M}_{ff} - \mathbf{M}_{fr}\mathbf{M}_{rr}^{-1}\mathbf{M}_{rf})^{-1} \tag{3.7}$$

Equation (3.1) then becomes

$$\ddot{\mathbf{q}}_r = -\mathbf{D}_{rr}\mathbf{H}_r - \mathbf{D}_{rf}\mathbf{H}_f - \mathbf{D}_{rf}\mathbf{K}\mathbf{q}_f + \mathbf{D}_{rr}\mathbf{u} \tag{3.8}$$

$$\ddot{\mathbf{q}}_f = -\mathbf{D}_{fr}\mathbf{H}_r - \mathbf{D}_{ff}\mathbf{H}_f - \mathbf{D}_{ff}\mathbf{K}\mathbf{q}_f + \mathbf{D}_{fr}\mathbf{u} \tag{3.9}$$

Assume that the orders of magnitude of the k_i are comparable. Introducing an appropriate scale factor k such that

$$\mathbf{K} = k\tilde{\mathbf{K}} \tag{3.10}$$

The following new variables can be defined as

$$\zeta := k\tilde{\mathbf{K}}\mathbf{q}_f \tag{3.11}$$

Define $\epsilon^2 := 1/k$, equation (3.8) can be modified as

$$\ddot{\mathbf{q}}_r = -\mathbf{D}_{rr}(\mathbf{q}_r, \epsilon^2\zeta)\mathbf{H}_r(\mathbf{q}_r, \dot{\mathbf{q}}_r, \epsilon^2\zeta, \epsilon^2\dot{\zeta}) - \mathbf{D}_{rf}(\mathbf{q}_r, \epsilon^2\zeta)\mathbf{H}_f(\mathbf{q}_r, \dot{\mathbf{q}}_r, \epsilon^2\zeta, \epsilon^2\dot{\zeta}) - \mathbf{D}_{rf}(\mathbf{q}_r, \epsilon^2\zeta)\zeta + \mathbf{D}_{rr}(\mathbf{q}_r, \epsilon^2\zeta)\tau \tag{3.12}$$

$$\epsilon^2\ddot{\zeta} = -\mathbf{D}_{fr}(\mathbf{q}_r, \epsilon^2\zeta)\mathbf{H}_r(\mathbf{q}_r, \dot{\mathbf{q}}_r, \epsilon^2\zeta, \epsilon^2\dot{\zeta}) - \mathbf{D}_{ff}(\mathbf{q}_r, \epsilon^2\zeta)\mathbf{H}_f(\mathbf{q}_r, \dot{\mathbf{q}}_r, \epsilon^2\zeta, \epsilon^2\dot{\zeta}) - \mathbf{D}_{ff}(\mathbf{q}_r, \epsilon^2\zeta)\zeta + \mathbf{D}_{fr}(\mathbf{q}_r, \epsilon^2\zeta)\tau \tag{3.13}$$

which is a singularly perturbed model of the flexible arm. Notice that all the quantities on the right side of (3.12) have been conveniently scaled by $\tilde{\mathbf{K}}$. The slow subsystem is formally obtained by setting $\epsilon = 0$, and solving for ζ. Then, we have

$$\bar{\zeta} = \mathbf{D}_{ff}^{-1}(\bar{\mathbf{q}}_r, 0)[-\mathbf{D}_{fr}(\bar{\mathbf{q}}_r, 0)\mathbf{H}_r(\bar{\mathbf{q}}_r, \dot{\bar{q}}_r, 0, 0) + \mathbf{D}_{fr}(\bar{\mathbf{q}}_r, 0)\bar{\tau}] - \mathbf{H}_f(\bar{\mathbf{q}}_r, 0) \tag{3.14}$$

where the upbar is used to indicate that the system is considered with $\epsilon = 0$. Substitute (3.14) into (3.12) with $\epsilon = 0$, we obtain

$$\ddot{\bar{\mathbf{q}}}_r = [\mathbf{D}_{rr}(\bar{\mathbf{q}}_r, \mathbf{0}) - \mathbf{D}_{rf}(\bar{\mathbf{q}}_r, \mathbf{0})\mathbf{D}_{ff}^{-1}(\bar{\mathbf{q}}_r, \mathbf{0})\mathbf{D}_{fr}(\bar{\mathbf{q}}_r, \mathbf{0})][-\mathbf{H}_r(\bar{\mathbf{q}}_r, \dot{\bar{\mathbf{q}}}_r, \mathbf{0}, \mathbf{0}) + \bar{\tau}] \tag{3.15}$$

Utilizing the definition of matrix $\mathbf{D}$, yields

$$\mathbf{D}_{rr}(\bar{\mathbf{q}}_r, \mathbf{0}) - \mathbf{D}_{rf}(\bar{\mathbf{q}}_r, \mathbf{0})\mathbf{D}_{ff}^{-1}(\bar{\mathbf{q}}_r, \mathbf{0})\mathbf{D}_{fr}(\bar{\mathbf{q}}_r, \mathbf{0}) = \mathbf{M}_{rr}^{-1}(\bar{\mathbf{q}}_r) \tag{3.16}$$

Choosing $\mathbf{x}_1 = \mathbf{q}_r$, $\mathbf{x}_2 = \dot{\mathbf{q}}_r$, and $\mathbf{z}_1 = \zeta$, $\mathbf{z}_2 = \epsilon\dot{\zeta}$ gives the state-space form of the system (3.12)

$$\begin{aligned}
\dot{\mathbf{x}}_1 &= \mathbf{x}_2 \qquad (3.17)\\
\dot{\mathbf{x}}_2 &= -\mathbf{D}_{rr}(\mathbf{x}_1, \epsilon^2\mathbf{z}_1)\mathbf{H}_r(\mathbf{x}_1, \mathbf{x}_2, \epsilon^2\mathbf{z}_1, \epsilon\mathbf{z}_2)\\
&\quad -\mathbf{D}_{rf}(\mathbf{x}_1, \epsilon^2\mathbf{z}_1)\mathbf{H}_f(\mathbf{x}_1, \mathbf{x}_2, \epsilon^2\mathbf{z}_1, \epsilon\mathbf{z}_2)\\
&\quad -\mathbf{D}_{rf}(\mathbf{x}_1, \epsilon^2\mathbf{z}_1)\mathbf{z}_1 + \mathbf{D}_{rr}(\mathbf{x}_1, \epsilon^2\mathbf{z}_1)\tau\\
\epsilon\dot{\mathbf{z}}_1 &= \mathbf{z}_2\\
\epsilon\dot{\mathbf{z}}_2 &= -\mathbf{D}_{fr}(\mathbf{x}_1, \epsilon^2\mathbf{z}_1)\mathbf{H}_r(\mathbf{x}_1, \mathbf{x}_2, \epsilon^2\mathbf{z}_1, \epsilon\mathbf{z}_2)\\
&\quad -\mathbf{D}_{ff}(\mathbf{x}_1, \epsilon^2\mathbf{z}_1)\mathbf{H}_f(\mathbf{x}_1, \mathbf{x}_2, \epsilon^2\mathbf{z}_1, \epsilon\mathbf{z}_2)\\
&\quad -\mathbf{D}_{ff}(\mathbf{x}_1, \epsilon^2\mathbf{z}_1)\mathbf{z}_1 + \mathbf{D}_{fr}(\mathbf{x}_1, \epsilon^2\mathbf{z}_1)\tau
\end{aligned}$$

At this point, singular perturbation theory requires that the slow subsystem and the fast subsystem be identified. The slow subsystem is formally obtained by setting $\epsilon = 0$, i.e., the rigid model of the arm obtained above through use of $\bar{\zeta}$ in (3.14):

$$\begin{aligned}
\dot{\bar{\mathbf{x}}}_1 &= \bar{\mathbf{x}}_2 \qquad (3.18)\\
\dot{\bar{\mathbf{x}}}_2 &= \mathbf{M}_{rr}^{-1}(\bar{\mathbf{x}}_1)[-\mathbf{H}_r(\bar{\mathbf{x}}_1, \bar{\mathbf{x}}_2) + \bar{\tau}]
\end{aligned}$$

To derive the fast subsystem, we introduce the fast time scale $\tau = t/\epsilon$. Then it can be recognized that the system (3.17) in the fast time scale becomes

$$\begin{aligned}
\dot{\mathbf{x}}_1 &= \mathbf{x}_2 \\
\dot{\mathbf{x}}_2 &= -\mathbf{D}_{rr}(\mathbf{x}_1, \epsilon^2(\eta_1 + \bar{\zeta}))\mathbf{H}_r(\mathbf{x}_1, \mathbf{x}_2, \epsilon^2(\eta_1 + \bar{\zeta}), \epsilon\eta_2) \\
&\quad -\mathbf{D}_{rf}(\mathbf{x}_1, \epsilon^2(\eta_1 + \bar{\zeta}))\mathbf{H}_f(\mathbf{x}_1, \mathbf{x}_2, \epsilon^2(\eta_1 + \bar{\zeta}), \epsilon\eta_2) \\
&\quad -\mathbf{D}_{rf}(\mathbf{x}_1, \epsilon^2(\eta_1 + \bar{\zeta}))(\eta_1 + \bar{\zeta}) + \mathbf{D}_{rr}(\mathbf{x}_1, \epsilon^2(\eta_1 + \bar{\zeta}))\tau \\
\dot{\eta}_1 &= \eta_2 \\
\epsilon\dot{\eta}_2 &= -\mathbf{D}_{fr}(\mathbf{x}_1, \epsilon^2(\eta_1 + \bar{\zeta}))\mathbf{H}_r(\mathbf{x}_1, \mathbf{x}_2, \epsilon^2(\eta_1 + \bar{\zeta}), \epsilon\eta_2) \\
&\quad -\mathbf{D}_{ff}(\mathbf{x}_1, \epsilon^2(\eta_1 + \bar{\zeta}))\mathbf{H}_f(\mathbf{x}_1, \mathbf{x}_2, \epsilon^2(\eta_1 + \bar{\zeta}), \epsilon\eta_2) \\
&\quad -\mathbf{D}_{ff}(\mathbf{x}_1, \epsilon^2(\eta_1 + \bar{\zeta}))(\eta_1 + \bar{\zeta}) + \mathbf{D}_{fr}(\mathbf{x}_1, \epsilon^2(\eta_1 + \bar{\zeta}))\tau
\end{aligned} \tag{3.19}$$

where the new fast variables η_1 and η_2 are defined as

$$\boldsymbol{\eta}_1 = \mathbf{z}_1 - \bar{\zeta} = \mathbf{z}_1 - \bar{\mathbf{z}}_1, \qquad \eta_2 = \mathbf{z}_2 \tag{3.20}$$

Setting $\epsilon = 0$ gives $\frac{d\mathbf{x}_1}{d\tau} = \frac{d\mathbf{x}_2}{d\tau} = 0$; i.e., $\mathbf{x}_1$ and $\mathbf{x}_2$ are constant on the boundary layer. Furthermore, it can be recognized that $\mathbf{H}_f(\mathbf{x}_1, \mathbf{x}_2, \mathbf{0}, \mathbf{0}) = 0$ and $\mathbf{H}_r(\mathbf{x}_1, \mathbf{x}_2, \mathbf{0}, \mathbf{0}) = 0$, since, by definition, those terms are representative of products of the components of $\mathbf{x}_1$ and $\mathbf{x}_2$ with the components of $\epsilon^2\mathbf{z}_1$ and $\epsilon\mathbf{z}_2$. Therefore, the fast subsystem can be found to be

$$\begin{aligned}
\frac{d\eta_1}{d\tau} &= \eta_2 \\
\frac{d\eta_2}{d\tau} &= -\mathbf{D}_{ff}(\bar{\mathbf{x}}_1, 0)\eta_1 + \mathbf{D}_{fr}(\bar{\mathbf{x}}_1, 0)\tau_f
\end{aligned} \tag{3.21}$$

which is a linear system parameterized in the slow variable $\bar{\mathbf{x}}_1$ and $\tau_f = \tau - \bar{\tau}$.

3.3 Composite Control for Known System

In this section, we shall investigate the problem of adaptive control for a flexible robot. As shown in the previous section, using the singular perturbation theory, the full system can be modeled as two subsystems: fast dynamics and slow dynamics. Thus, a composite control strategy can be carried out. Singular perturbed model of the system is derived which allows the controller design be split for two reduced-order subsystems. The main control objective is to let the rigid motion $\mathbf{q}_r$ track a desired trajectory $\mathbf{q}_d$ and at the same time provide active damping to the flexible motion of the flexible links. The design of a feedback control of the full system can be split into two separate designs of feedback controls $\bar{\tau}$ and τ_f for the two reduced-order systems

$$\tau = \bar{\tau}(\bar{\mathbf{x}}_1, \bar{\mathbf{x}}_2) + \tau_f(\mathbf{x}_1, \eta_1, \eta_2) \tag{3.22}$$

with the constraint that $\mathbf{u}_f(\bar{\mathbf{x}}_1, \mathbf{0}, \mathbf{0}) = \mathbf{0}$ such that $\mathbf{u}_f$ is inactive along the solution of $\bar{\eta}$, which is an equalibrium trajectory of (3.19).

3.3.1 Slow Subcontroller

As far as the slow control is concerned all the well-established control techniques developed for rigid manipulators can be applied. We generalize the slow subsystem to strict feedback form as

$$\dot{\mathbf{x}}_1 \;=\; \mathbf{x}_2 \tag{3.23}$$

$$\dot{\mathbf{x}}_2 = \mathbf{F}_2(\mathbf{x}_1, \mathbf{x}_2) + \mathbf{G}_2(\mathbf{x}_1, \mathbf{x}_2)\bar{\tau}$$

Choose the virtual control α as

$$\alpha = \dot{\mathbf{x}}_d - k_1(\mathbf{x}_1 - \mathbf{x}_d), \quad k_1 > 0. \tag{3.24}$$

Consider the Lyapunov candidate

$$V = \frac{1}{2}\mathbf{z}_1^T\mathbf{z}_1 + \frac{1}{2}\mathbf{z}_2^T\mathbf{z}_2 \tag{3.25}$$

where $\mathbf{z}_1 = \mathbf{x}_1 - \mathbf{x}_d$, $z_2 = \mathbf{x}_2 - \alpha$. Its derivative is given by

$$\begin{aligned} \dot{V} &= \mathbf{z}_1^T\dot{\mathbf{z}}_1 + \mathbf{z}_2^T\dot{\mathbf{z}}_2 \qquad (3.26)\\ &= \mathbf{z}_1^T(\mathbf{z}_2 - k_1\mathbf{z}_1) + \mathbf{z}_2^T(\mathbf{F}_2(\mathbf{x}_1, \mathbf{x}_2) + \mathbf{G}_2(\mathbf{x}_1, \mathbf{x}_2)\bar{\tau}) \end{aligned}$$

Thus, we can obtain

$$\bar{\tau} = \mathbf{G}_2^{-1}(-\mathbf{F}_2(\mathbf{x}_1, \mathbf{x}_2) - \mathbf{z}_1 - k_2\mathbf{z}_2), \quad k_2 > 0 \tag{3.27}$$

which gives

$$\dot{V} = -k_1\mathbf{z}_1^T\mathbf{z}_1 - k_2\mathbf{z}_2^T\mathbf{z}_2 \leq 0 \tag{3.28}$$

Since $\dot{V} \leq 0$, it follows from LaSalle-Yoshizawa theorem that the equilibrium $\mathbf{z} = [\mathbf{z}_1 \ \mathbf{z}_2]^T = \mathbf{0}$ is globally asymptotically stable [65]. Note that $\bar{\tau}$ and α are both smooth functions and satisfy $\bar{\tau}(0,0) = 0$ and $\alpha(0,0) = 0$. Thus, we can conclude that $\mathbf{z} = \mathbf{0}$ is globally asymptotically stable, i.e., $\mathbf{x}_1 \to \mathbf{x}_d$ as $t \to \infty$.

3.3.2 Fast Subcontroller

It might be observed that the strategy of adaptively controlling the system by just neglecting the flexible dynamics and considering $\mathbf{z}_1$ and $\mathbf{z}_2$ as a disturbance to the system is likely to fail, since no assumption on the boundedness of the disturbance can be made. Singular perturbation theory requires that the boundary layer system be uniformly stable along the equalibrium trajectory $\bar{\zeta}$. This can be accomplished if the pair

$$\mathbf{A} = \begin{bmatrix} \mathbf{0} & \mathbf{I} \\ -\mathbf{D}_{ff} & \mathbf{0} \end{bmatrix}, \quad \mathbf{B} = \begin{bmatrix} \mathbf{0} \\ \mathbf{D}_{fr} \end{bmatrix} \tag{3.29}$$

is uniformly stabilizable for any slow trajectory $\bar{\mathbf{x}}_1(t)$.

The fast state feedback control of the type

$$\tau_f(\bar{\mathbf{x}}_1, \eta_1, \eta_2) = \mathbf{K}_{f1}\eta_1 + \mathbf{K}_{f2}\eta_2 \tag{3.30}$$

stabilize the boundary (3.21) to $\eta_1 = \mathbf{0}$ and $\eta_2 = \mathbf{0}$. The fast subcontroller can be designed as an optimal control for the boundary layer. The performance index will be a function of the slow state variables. Since the main purpose in flexible manipulator control is to damp the deflections at steady state as fast as possible, the feedback gain matrices can be designed also on the basis that the final joint configuration, provided that under that particular choice of η_1 and η_2 will go unstable along the slow trajectory. In this way the solution of a Riccati equation for each joint configuration can be avoided. Under the above conditions, Tikhonov's theorem, a fundamental result in singular perturbation theory, ensures that the

state vectors of the full system can be approximated by

$$\mathbf{x}_1 = \bar{\mathbf{x}}_1 + \mathbf{O}(\epsilon) \tag{3.31}$$

$$\mathbf{x}_2 = \bar{\mathbf{x}}_2 + \mathbf{O}(\epsilon) \tag{3.32}$$

$$\mathbf{z}_1 = \bar{\zeta}_1 + \eta_1 + \mathbf{O}(\epsilon) \tag{3.33}$$

$$\mathbf{z}_2 = \eta_2 + \mathbf{O}(\epsilon) \tag{3.34}$$

Under the slow control (3.27), $\mathbf{x}_1$, $\mathbf{x}_2$. The fast control (3.27) will derive η_1, η_2 to zero. The goal of following a reference model for the joint variable and stabilizing the deflections around the equlibrium trajectory, naturally set up by the rigid system under the slow control, is achieved by an $\mathbf{O}(\epsilon)$ approximation. This is the typical result of a singular perturbation approach.

Remark 3.1 *When the system model is known, then all the states can be used to design the fast subsystem. Then the subsystem can be written as*

$$\frac{d\eta}{d\tau} = \mathbf{A}\eta + \mathbf{B}\tau_f \tag{3.35}$$

where $\mathbf{z} = [\mathbf{z}_1^T \ \mathbf{z}_2^T]^T$ *and*

$$\mathbf{A} = \begin{bmatrix} \mathbf{0} & \mathbf{I} \\ -\mathbf{D}_{ff}(\bar{\mathbf{q}}_r, \mathbf{0}) & \mathbf{0} \end{bmatrix}, \quad \mathbf{B} = \begin{bmatrix} \mathbf{0} \\ \mathbf{D}_{fr}(\bar{\mathbf{q}}_r, 0) \end{bmatrix} \tag{3.36}$$

and $\tau_f = \tau - \bar{\tau}$*, some control strategies such as LQR can be carried out to design the fast control law* τ_f*.*

However, in case of an unknown system model, i.e., the matrix $\mathbf{M}$ *in (3.1) is unknown. It is clear from both (3.14) and (3.20), the unknown equalibrium* $\bar{\zeta}$ *will*

lead to the unmeasurement of state η_1. It is also important to note that $\eta_2 = \frac{d\eta_1}{d\tau} = \frac{d\mathbf{z}_1}{d\tau}$, in which the unknown $\bar{\zeta}$ does not appear. Thus, only state $\mathbf{z}_2$ (η_2) is expected to be employed in the design of fast control τ_f.

3.3.3 Simulation Studies

To illustrate the proposed strategy, a planar single-link flexible manipulator is considered. The following parameters are set up for the link and a payload is assumed to be placed at the manipulator tip:

$$\begin{aligned}
\rho &= 0.1kg/m && \text{(link uniform density)} \\
l &= 1.0m && \text{(link length)} \\
m &= 0.1kg && \text{(link mass)} \\
I_h &= 3.0kgm^2 && \text{(hub inertia)} \\
I_b &= 0.033kgm^2 && \text{(rigid inertia)} \\
EI &= 5.0Nm^2 && \text{(flexural link rigidity)}
\end{aligned}$$

The desired trajectory for rigid joint angle is expressed as a Hermite polynomial of the fifth degree in t with continuous bounded position, velocity and bounded acceleration. The general expression for the desired position trajectory is:

$$q_d(t, t_d) = q_0 + (6.0\frac{t^5}{t_d^5} - 15\frac{t^4}{t_d^4} + 10.0\frac{t^3}{t_d^3})(q_f - q_0) \tag{3.37}$$

t_d represents the time that the desired arm trajectory reaches the desired final position q_f starting from the desired initial position q_0. In this paper, $q_0 = 0.0$, $q_f = 1.0$ and $t_d = 2.0$ seconds.

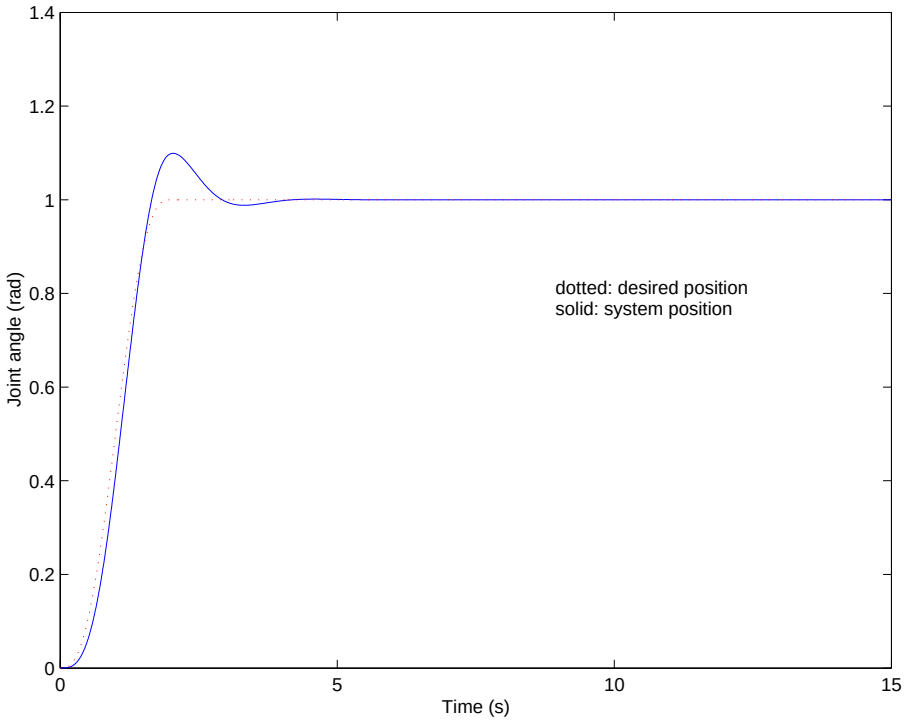

Figure 3.1: Joint angle trajectory.

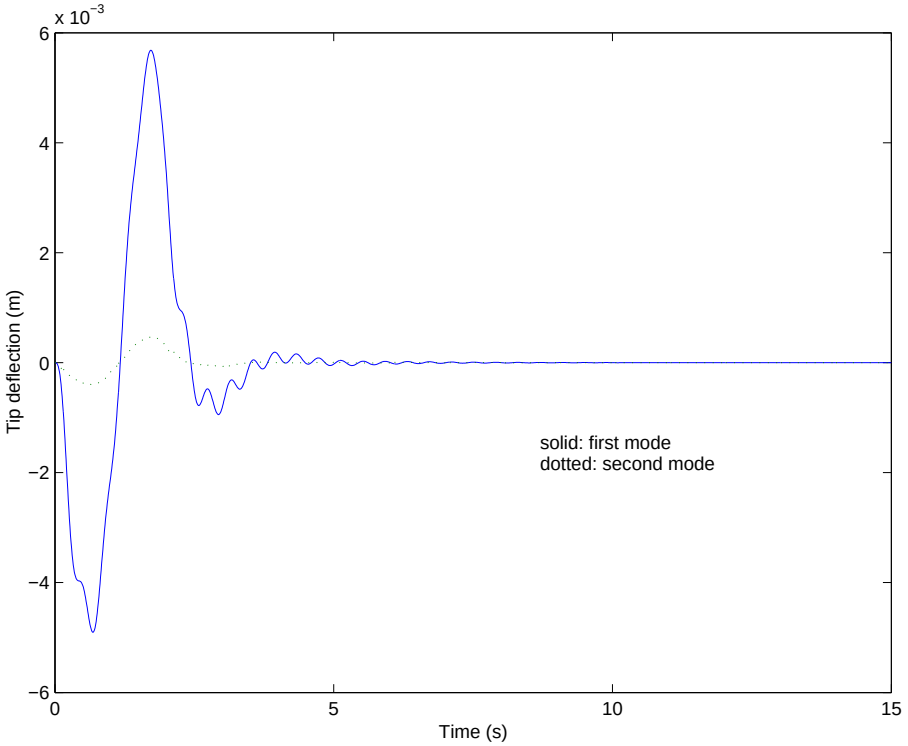

Figure 3.2: Tip deflections.

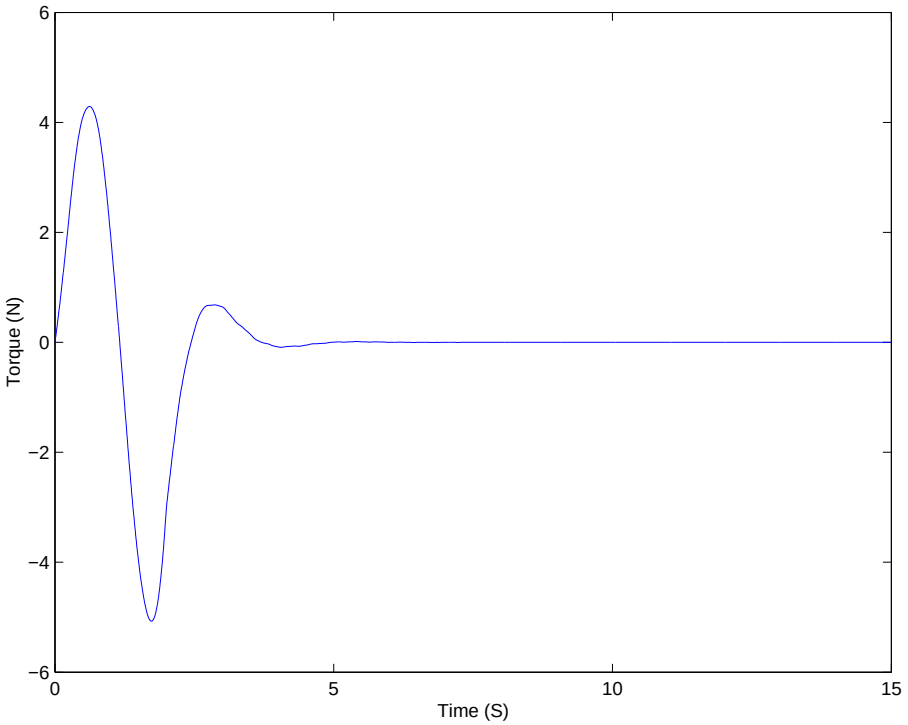

Figure 3.3: Torque control.

The slow system can be chosen as the linear model following control

$$\bar{\tau} = \mathbf{M}_{11}[\ddot{\mathbf{q}}_d + k_v(\dot{\mathbf{q}}_d - \dot{\mathbf{q}}_r) + k_p(\mathbf{q}_d - \mathbf{q}_r)] \tag{3.38}$$

where k_p and k_v are to be selected so as to maintain the time scale separation between the slow and the fast subsystem. This corresponds to $k_p = 11.0$ and $k_v = 10.0$. On the other hand, the fast control can be chosen according to the pole placement technique for linear systems. Consider $k_{pf} = (5\ 3)$ and $k_{vf} = (3\ 5)$. The simulation results are shown in Figures 3.1 through 3.3.

3.4 Control Design for Unknown Single Link System

In this section, we shall investigate the problem of adaptive control for a flexible robot. As shown in the previous section, using the singular perturbation theory, the full system can be modeled as two subsystems: fast dynamics and slow dynamics. Thus, a composite control strategy can be carried out. Singular perturbed model of the system is derived which allow the controller design be split into two separated controller design for the two reduced-order subsystems. The main control objective is to let the rigid motion $\mathbf{q}_r$ track a desired trajectory $\mathbf{q}_d$ and at the same time provide active damping to the flexible motion of the flexible links. The design of a feedback control for the full system can be split into two separate designs of feedback controls $\bar{\tau}$ and τ_f for the two reduced-order systems

$$\tau = \bar{\tau}(\bar{\mathbf{x}}_1, \bar{\mathbf{x}}_2) + \tau_f(\mathbf{x}_1, \eta_1, \eta_2) \tag{3.39}$$

with the constraint that $\tau_f(\bar{\mathbf{x}}_1, \mathbf{0}, \mathbf{0}) = \mathbf{0}$ such that τ_f is inactive along the solution of $\bar{\eta}$, which is an equalibrium trajectory of (3.19).

3.4.1 Neural Network Structure

Neural networks (NN) have been widely used in modeling and control of nonlinear systems because of their proficiency in nonlinear function approximation, learning and fault tolerance. The feasibility of applying NNs to dynamic system control has been demonstrated in many studies [66–69]. In control engineering, a NN

is usually used to generate input/output maps using the property that a multi-layer NN can approximate any function, under mild assumptions, with any desired accuracy. There are two distinct problems in function approximation, namely, the *representation problem* of choosing the best approximating function $\hat{f}(\psi, x)$ and the *learning problem* of finding the training method to obtain the optimal parameters ψ^*.

The adaptive NN portion of the proposed controller utilizes controller parameterization techniques coupled with methods of direct adaptive control. Thus, the architecture of the NNs has to be chosen such that it can be linearly parameterized (*representation problem*) and direct adaptive laws can be used to update the parameters of the networks on-line (*learning problem*).

It has been demonstrated in [70] that a linear superposition of Gaussian RBFs results in an optimal mean square approximation to an unknown function which is infinitely differentiable and whose values are specified at a finite set of points in $\mathcal{R}^n$. Furthermore, it has been proven [71] that any continuous function, not necessarily infinitely smooth, can be uniformly approximated by a linear combination of Gaussian RBFs.

The RBF network is most suitable for this application. The Gaussian RBF neural network is a particular network architecture [71] utilizing k numbers of Gaussian radial basis functions (activation functions), $a_i(q)$, with input variables $q \in R^n$, variance $\sigma^2 \in R$ and the centers vector $\mathbf{c} = (c_1, ..., c_n)^T \in R^n$. For any given

function, $\mathbf{y} = f(\mathbf{q})$, it is known that it can be approximated by the Gaussian RBF neural network expressed as

$$\mathbf{y} = \mathbf{W}^T\mathbf{a}(\mathbf{q}) + \epsilon \tag{3.40}$$

$$a_i(\mathbf{q}) = exp(-\frac{\|\mathbf{q}-\mathbf{c}\|^2}{\sigma^2}) = exp(-\frac{(\mathbf{q}-\mathbf{c})^T(\mathbf{q}-\mathbf{c})}{\sigma^2}) \tag{3.41}$$

where $\mathbf{W}^T = [w_{ij}]$, $\mathbf{a} = [a_1\ a_2\ ...\ a_k]^T$ and $\mathbf{y} \in R^n$ and ϵ is the NN reconstruction error.

Let I_0 be the set of integers, and $\mathbf{W}_{ij}, \mathbf{X}_{ij}(\mathbf{q}) \in R^{n_{ij}}$, $n_{ij} \in I_0$, $i = 1, ..., n$, $j = 1, ..., k$. The product $\mathbf{W}_{ij}^T\mathbf{X}_{ij}$ can be taken as a network emulator for the $ijth$ element, $d_{ij}(\mathbf{q})$, of matrix $\mathbf{D}(\mathbf{q}) \in R^{n\times k}$, with $\mathbf{W}_{ij}$ and $\mathbf{X}_{ij}(\mathbf{q})$ the weight and basis function vectors respectively. Define $\mathbf{W}_i$ and $\mathbf{W}_i^T$ as

$$\mathbf{W}_i = \begin{bmatrix} \mathbf{W}_{i1} \\ \mathbf{W}_{i2} \\ ... \\ \mathbf{W}_{ik} \end{bmatrix} \in R^{m_i}, \quad \mathbf{W}_i^T = [\mathbf{W}_{i1}^T\ \mathbf{W}_{i2}^T\ ...\ \mathbf{W}_{ik}^T]$$

in the conventional way for comparison, where $m_i = \sum_{j=1}^{k} n_{ij}$. Now, let us introduce the definition of GL vectors and matrices, denoted by $\{*\}$ [68]. A GL row vector $\{\mathbf{W}_i\}$ and its transpose $\{\mathbf{W}_i\}^T$ are defined as:

$$\{\mathbf{W}_i\} = \{\mathbf{W}_{i1}\ \mathbf{W}_{i2}\ ...\ \mathbf{W}_{ik}\}, \quad \{\mathbf{W}_i\}^T = \{\mathbf{W}_{i1}^T\ \mathbf{W}_{i2}^T\ ...\ \mathbf{W}_{ik}^T\}$$

The definition for GL matrices is accordingly defined as below

$$\{\mathbf{W}\} := \left\{ \begin{array}{c} \{\mathbf{W}_1\} \\ ... \\ \{\mathbf{W}_n\} \end{array} \right\} = \left\{ \begin{array}{ccc} \mathbf{W}_{11} & ... & \mathbf{W}_{1k} \\ ... & ... & ... \\ \mathbf{W}_{n1} & ... & \mathbf{W}_{nk} \end{array} \right\}$$

The transpose of a GL matrix is defined as

$$\{\mathbf{W}\}^T := \left\{ \begin{array}{ccc} \mathbf{W}_{11}^T & ... & \mathbf{W}_{1k}^T \\ ... & ... & ... \\ \mathbf{W}_{n1}^T & ... & \mathbf{W}_{nk}^T \end{array} \right\} \tag{3.42}$$

It can be seen that the transpose of a GL matrix also transposes its elementary vectors locally. Should any confusion arise in the text, $[*]$ is used to denote an ordinary matrix, and $\{*\}$ for a GL matrix explicitly.

The corresponding GL operator, denoted by "$\bullet$" is defined as below:

$$\mathbf{D}_0(\mathbf{q}) = \left[\{\mathbf{W}\}^T \bullet \{\mathbf{X}(\mathbf{q})\}\right] := \left[\begin{array}{cccc} \mathbf{W}_{11}^T\mathbf{X}_{11} & \mathbf{W}_{12}^T\mathbf{X}_{12} & ... & \mathbf{W}_{1k}^T\mathbf{X}_{1k} \\ ... & ... & ... & ... \\ \mathbf{W}_{n1}^T\mathbf{X}_{n1} & \mathbf{W}_{n2}^T\mathbf{X}_{n2} & ... & \mathbf{W}_{nk}^T\mathbf{X}_{nk} \end{array} \right] \in R^{n\times k}$$

Therefore, a matrix network emulator can be conveniently expressed as a GL product of two GL matrices as shown above.

3.4.2 Neural Network Control of Slow Subsystem

Given a desired trajectory $q_d(t) \in \mathrm{R}^1$ which is twice differentiable for the slow part of the flexible link dynamics, the tracking error is

$$e = q_d - \bar{q}_r \tag{3.43}$$

$$\dot{q}_v = \dot{q}_d + \Lambda e \tag{3.44}$$

$$r = \dot{q}_v - \dot{\bar{q}}_r = \dot{e} + \lambda e \tag{3.45}$$

where Λ is a symmetric positive definite matrix. The asymptotic behavior of e and $\dot{e}$ can be established from that of the new tracking measure r based on the following lemma.

Lemma 3.1: *Let $e(t) = h * r$, where $h = L^{-1}(H(s))$ and $H(s)$ is an $n \times n$ strictly proper, exponentially stable transfer function. Then $r \in L_n^2 \Longrightarrow e \in L_n^2 \cap L_n^\infty$, $\dot{e} \in L_n^2$, e is continuous and $e \to 0$ as $t \to \infty$. If, in addition, $r \to 0$ as $t \to \infty$, then $\dot{e} \to 0$ [72].*

The slow subsystem (3.15) can be modified into a standard form as

$$\mathbf{D}_{rr}(\bar{q}_r)\ddot{\bar{q}}_r + \mathbf{C}_{rr}(\bar{q}_r, \dot{\bar{q}}_r)\dot{\bar{q}}_r = \bar{\tau} \tag{3.46}$$

It can be seen that $d_{ij}(\bar{q}_r)$ and $g_i(\bar{q}_r)$ are functions of $\bar{q}_r$ only and infinite differentiable, thus static NNs are sufficient to emulate the $\mathbf{D}_{rr}(\bar{q}_r)$ matrix. On the other hand, $c_{ij}(\bar{q}_r, \dot{\bar{q}}_r)$ are function of $\bar{q}_r$ and $\dot{\bar{q}}_r$, and infinitely differentiable, thus dynamic NNs are needed to emulate the $\mathbf{C}_{rr}(\bar{q}_r, \dot{\bar{q}}_r)$ matrix. Suppose $d_{ij}(\bar{q}_r)$ and $c_{ij}(\bar{q}_r, \dot{\bar{q}}_r)$

can be approximated as

$$d_{ij}(\bar{q}_r) = \psi_{ij}^T \xi_{ij}(\bar{q}_r) + \epsilon \mathbf{D}_{ij} \tag{3.47}$$

$$c_{ij}(\bar{q}_r, \dot{\bar{q}}_r) = \alpha_{ij}^T \omega_{ij}(\bar{q}_r, \dot{\bar{q}}_r) + \epsilon \mathbf{C}_{ij} \tag{3.48}$$

where ψ_{ij}, α_{ij} are the weight vectors; $\xi_{ij}(\bar{q}_r)$, $\omega_{ij}(\bar{q}_r, \dot{\bar{q}}_r)$ are Gaussian RBFs; and $\epsilon \mathbf{D}_{ij}$, $\epsilon \mathbf{C}_{ij}$ are the NN reconstruction errors respectively.

Using the notation for"Gl" matrix and operator, the function emulators (3.47)-(3.48) can be collectively expressed as

$$\mathbf{D}_{rr}(\bar{q}_r) = [\{\mathbf{\Psi}\}^T \bullet \{\mathbf{\Xi}\}] + \mathbf{E}_D \tag{3.49}$$

$$\mathbf{C}_{rr}(\bar{q}_r, \dot{\bar{q}}_r) = [\{\mathbf{A}\}^T \bullet \{\mathbf{\Omega}\}] + \mathbf{E}_C \tag{3.50}$$

where $([\{\mathbf{\Psi}\}, \{\mathbf{\Xi}\})$ and $([\{\mathbf{A}\}, \{\mathbf{\Omega}\})$ are the desired parameters and basis function pairs of the NN emulation of $\mathbf{D}_{rr}(\bar{q}_r)$ and $\mathbf{C}_{rr}(\bar{q}_r, \dot{\bar{q}}_r)$ respectively; and $\mathbf{E}_D$ and $\mathbf{E}_C$ are the collective NN reconstruction errors.

Let $(\hat{*})$ be the estimate of $(*)$ and the estimation error given as $(\tilde{*}) = (*) - (\hat{*})$. Suppose $\hat{\mathbf{D}}_{rr}(\bar{q}_r)$ and $\hat{\mathbf{C}}_{rr}(\bar{q}_r, \dot{\bar{q}}_r)$ are estimates of $\mathbf{D}_{rr}(\bar{q}_r)$ and $\mathbf{C}_{rr}(\bar{q}_r, \dot{\bar{q}}_r)$ respectively, defined by

$$\hat{\mathbf{D}}_{rr}(\bar{q}_r) = [\{\hat{\mathbf{\Psi}}\}^T \bullet \{\mathbf{\Xi}\}] + \mathbf{E}_D \tag{3.51}$$

$$\hat{\mathbf{C}}_{rr}(\bar{q}_r, \dot{\bar{q}}_r) = [\{\hat{\mathbf{A}}\}^T \bullet \{\mathbf{\Omega}\}] + \mathbf{E}_C \tag{3.52}$$

From Equation (3.45), $\dot{\tilde{q}}_r = \dot{q}_v - r$ and $\ddot{q}_v - \dot{r}$, thus

$$\mathbf{D}_{rr}(\bar{q}_r)\ddot{q}_r + \mathbf{C}_{rr}(\bar{q}_r, \dot{\bar{q}}_r)\dot{\tilde{q}}_r = [\{\mathbf{\Psi}\}^T \bullet \{\mathbf{\Xi}\}]\ddot{q}_v + [\{\mathbf{A}\}^T \bullet \{\mathbf{\Omega}\}]\dot{q}_v \tag{3.53}$$

$$+\mathbf{E} - \mathbf{D}_{rr}(\bar{q}_r) - \mathbf{C}_{rr}(\bar{q}_r, \dot{\bar{q}}_r)r$$

where $\mathbf{E} = \mathbf{E}_D\ddot{q}_v + \mathbf{E}_C\dot{q}_v$. To control the slow subsystem, consider the general controller of the form

$$\begin{aligned} \bar{\tau} &= \hat{\mathbf{D}}_{rr}(\bar{q}_r)\ddot{\bar{q}}_r + \hat{\mathbf{C}}_{rr}(\bar{q}_r, \dot{\bar{q}}_r)\dot{q}_v + \mathbf{K}_p r + \mathbf{K}_s \text{sgn}(r) \\ &= [\{\hat{\mathbf{\Psi}}\}^T \bullet \{\mathbf{\Xi}\}]\ddot{\bar{q}}_r + [\{\hat{\mathbf{A}}\}^T \bullet \{\mathbf{\Omega}\}]\dot{q}_v + \mathbf{K}_p r + \mathbf{K}_s \text{sgn}(r) \end{aligned} \tag{3.54}$$

where $\mathbf{K}_p$ and $\mathbf{K}_s \geq ||\mathbf{E}||$ for robust closed-loop stability. Substituting (3.53) into (3.54) yields the error equation

$$\begin{aligned} &\mathbf{D}_{rr}(\bar{q}_r)\dot{r} + \mathbf{C}_{rr}(\bar{q}_r, \dot{\bar{q}}_r)r + \mathbf{K}_p r + \mathbf{K}_s \text{sgn}(r) \\ &= [\{\tilde{\mathbf{\Psi}}\}^T \bullet \{\mathbf{\Xi}\}]\ddot{\bar{q}}_r + [\{\tilde{\mathbf{A}}\}^T \bullet \{\mathbf{\Omega}\}]\dot{q}_v + E \end{aligned} \tag{3.55}$$

The stability properties of the closed loop system (3.55) are stated in the following proposition.

Proposition 3.1: *For a closed-loop system given in (3.55), asymptotic stability, i.e., $r \to 0$ as $t \to \infty$, is achieved if $\mathbf{K}_p > 0$, $\mathbf{K}_s \geq ||E||$ and the parameter adaptation laws are given by*

$$\begin{aligned} \dot{\hat{\psi}}_i &= \Gamma_i \bullet \{\xi_i\}\ddot{q}_v r_i \\ \dot{\hat{\alpha}}_i &= W_i \bullet \{\omega_i\}\dot{q}_v r_i \end{aligned} \tag{3.56}$$

where Γ_i and W_i are dimensional compatible symmetric positive definite matrices, then $\hat{\psi}_i$ and $\hat{\alpha}_i \in L^\infty$; and $e \in L_n^2 \cap L_n^\infty$; $\dot{e} \in L_n^2$, e is continuous and e, $\dot{e} \to 0$ as $t \to \infty$. **Proof:** Omitting the arguments again for brevity, choose the non-negative

function V as

$$2V = r^T \bar{\mathbf{D}}_{rr} r + \sum_{i=1}^{n_r} \tilde{\psi}_i^T \Gamma_i \tilde{\psi}_i + \sum_{i=1}^{n_r} \tilde{\alpha}_i^T W_i \tilde{\alpha}_i \tag{3.57}$$

Its time derivative along (3.55) is

$$\dot{V} = r^T [\bar{\mathbf{D}}_{rr} \dot{r} + \bar{\mathbf{C}}_{rr} r] + \sum_{i=1}^{n_r} \tilde{\psi}_i^T \Gamma_i \dot{\tilde{\psi}}_i + \sum_{i=1}^{n_r} \tilde{\alpha}_i^T W_i \dot{\tilde{\alpha}}_i \tag{3.58}$$

which exploits the slow-symmetric property of $\dot{\bar{D}}_{rr} - 2\bar{\mathbf{C}}_{rr}$. Substituting the error equation (3.55) into (3.58), we obtain

$$\begin{aligned} \dot{V} &= -r^T \mathbf{K}_p r + r^T \mathbf{E} - r^T \mathbf{K}_s \text{sgn}(r) \\ &\quad r^T [\{\tilde{\psi}\}^T \bullet \{\Xi\}] \ddot{q}_v + r^T [\{\tilde{A}\}^T \bullet \{\Omega\}] \dot{q}_v \\ &\quad + \sum_{i=1}^{n_r} \tilde{\psi}_i^T \Gamma_i \dot{\tilde{\psi}}_i + \sum_{i=1}^{n_r} \tilde{\alpha}_i^T W_i \dot{\tilde{\alpha}}_i \end{aligned} \tag{3.59}$$

By noting that

$$\begin{aligned} r^T [\{\tilde{\psi}\}^T \bullet \{\Xi\}] \ddot{q}_v &= \sum_{i=1}^{n_r} \{\tilde{\psi}_i\}^T \bullet \{\xi_i\} \ddot{q}_v r_i \\ r^T [\{\tilde{A}\}^T \bullet \{\Omega\}] \dot{q}_v &= \sum_{i=1}^{n_r} \{\tilde{\alpha}_i\}^T \bullet \{\omega_i\} \dot{q}_v r_i \end{aligned} \tag{3.60}$$

Equation (3.58) becomes

$$\begin{aligned} \dot{V} &= -r^T \mathbf{K}_p r + r^T \mathbf{E} - r^T \mathbf{K}_s \text{sgn}(r) \\ &\quad + \sum_{i=1}^{n_r} \{\tilde{\psi}_i\}^T \bullet \{\xi_i\} \ddot{q}_v r_i + \sum_{i=1}^{n_r} \{\tilde{\alpha}_i\}^T \bullet \{\omega_i\} \dot{q}_v r_i \\ &\quad + \sum_{i=1}^{n_r} \tilde{\psi}_i^T \Gamma_i \dot{\tilde{\psi}}_i + \sum_{i=1}^{n_r} \tilde{\alpha}_i^T W_i \dot{\tilde{\alpha}}_i \end{aligned} \tag{3.61}$$

Since ψ_i and α_i are bounded constants which implies that $\dot{\tilde{\psi}}_i = -\dot{\hat{\psi}}_i$, $\dot{\tilde{\alpha}}_i = -\dot{\hat{\alpha}}_i$; and substituting the adaptation laws into (3.61) yields

$$\dot{V} = -r^T \mathbf{K}_p r + r^T E - r^T \mathbf{K}_s \text{sgn}(r) \leq -r^T \mathbf{K}_p r \tag{3.62}$$

when $\mathbf{K}_s \geq ||E||$. Hence, V is a Lyapunov function and

$$\lambda_{min}(\mathbf{K}_p) \int =_0^t r^T r d\tau \leq \int_0^t r^T \mathbf{K}_p r d\tau \leq V(0) \tag{3.63}$$

Since $V(0)$ and $\lambda_{min}(\mathbf{K}_p)$ are positive constants, it follows that $r \in L^2_{n_r}$. Consequently from Lemma 3.4.2, $e \in L^2_{n_r} \cap L^\infty_{n_r}$; e is continuous and $e \to 0$ as $t \to \infty$; and $\dot{e} \in L^2_{n_r}$. Since $\dot{V} \leq -r^T \mathbf{K}_p r \leq 0$, it follows that $0 \leq V \leq V(0)$, $\forall t \geq 0$. Hence, $V(t) \in L^\infty$ implies that $\int_0^t r d\tau$, $\tilde{\psi}_i$ and $\tilde{\alpha}_i \in L^\infty_{n_r}$, i.e., $\hat{\psi}_i$ and $\hat{\alpha}_i \in L^\infty_{n_r}$. By noting that $r \in L^2_{n_r}$; q_{rd}, $\dot{q}_{rd}$, $\ddot{q}_{rd} \in L^\infty_n$; and $\{\Xi\}$, $\{\Omega\}$ are bounded basis functions, it can be concluded from (3.55) that $\dot{e} \in L^\infty_n$, which implies that r is uniformly continuous. Finally, the proof is complete using the implication: r is uniformly continuous and $r \in L^2_{n_r}$

$$\Rightarrow r \to 0 \; as \; t \to \infty \Rightarrow \dot{e} \to 0 \quad \square$$

3.4.3 Stabilizing the Fast Subsystem

The fast subsystem must be uniformly stable along the equilibrium trajectory $\bar{\zeta}$. Following from Section 3.2, the subsystem can be written as

$$\frac{d\eta}{d\tau} = \mathbf{A}\eta + \mathbf{B}\tau_f \tag{3.64}$$

where $\eta = [\eta_1^T \; \eta_2^T]^T$ and

$$\mathbf{A} = \begin{bmatrix} \mathbf{0} & \mathbf{I} \\ -\mathbf{D}_{ff}(\bar{\mathbf{q}}_r, \mathbf{0}) & \mathbf{0} \end{bmatrix}, \quad \mathbf{B} = \begin{bmatrix} \mathbf{0} \\ \mathbf{D}_{fr}(\bar{\mathbf{q}}_r, 0) \end{bmatrix}$$

with $\mathbf{D}_{fr}$ and $\mathbf{D}_{ff}$ defined in equations (3.6) and (3.7), respectively. It is easy to verify that $\mathbf{D}_{ff}$ is a positive definite matrix according to its definition. As for $\mathbf{D}_{fr}$, let us rewrite it here

$$\begin{aligned} \mathbf{D}_{fr} &= -\mathbf{M}_{ff}^{-1}\mathbf{M}_{fr}(\mathbf{M}_{rr} - \mathbf{M}_{rf}\mathbf{M}_{ff}^{-1}\mathbf{M}_{fr})^{-1} \\ &= -\mathbf{M}_{ff}^{-1}\mathbf{M}_{fr}\mathbf{D}_{rr} \end{aligned} \tag{3.65}$$

Property 3.1: *Following Property 2.1, For all positive β_i, m_i will be positive. It should be also noted that $\mathbf{M}_{ff}^{-1} = diag[\frac{1}{\rho}, \cdots, \frac{1}{\rho}] \in R^{n_f \times n_f}$ and $\mathbf{D}_{rr} > 0$, which lead to that the items of $\mathbf{D}_{fr}$, $d_{fr}^i < 0$, $i = 1, 2, \ldots, n_f$.*

As has been stated in Remark 3.1, only η_2 is available for the fast controller design, due to the unmeasurement of $\bar{\zeta}$. In this Subsection, we will present three methods for the fast controller design. In the first part, only η_2 are used for the controller design of the fast subsystem. In the second and third part, a neural network based controls are presented, respectively, by estimating the unknown equilibrium $\bar{\zeta}$.

η_2 Based Design

For the fast subsystem (3.64), consider the general form of controller τ_f

$$\tau_f = [c_1 \ c_2 \ \cdots \ c_n] \begin{bmatrix} \eta_{21} \\ \eta_{22} \\ \vdots \\ \eta_{2n} \end{bmatrix} \tag{3.66}$$

where c_i, $i = 1, 2 \ldots, n$ are controller parameters. The stability of the closed loop system are stated in the following proposition.

Proposition 3.2: *The solution of the system (3.64) with controller (3.66) approaches a bounded invariant set M as t goes to ∞, if $c_i < 0$, $i = 1, 2 \ldots, n$.*

Proof: Consider the non-negative scalar function V as

$$V = \frac{1}{2}\eta_1^T \mathbf{D}_{ff}\eta_1 + \frac{1}{2}\eta_2^T \eta_2 \tag{3.67}$$

Computing the time derivative of the above equation, yields

$$\begin{aligned} \frac{dV}{d\tau} &= \eta_1^T \mathbf{D}_{ff}\eta_2 - \eta_2^T \mathbf{D}_{ff}\eta_1 + \eta_2^T \mathbf{D}_{fr}\tau_f \\ &= \eta_2^T \mathbf{D}_{fr}\tau_f \end{aligned} \tag{3.68}$$

where $\mathbf{D}_{fr} \in R^{n\times 1}$ is a unknown vector, τ_f is a scalar. Substituting the fast controller (3.66) gives

$$\begin{aligned} \frac{dV}{d\tau} &= [\eta_{21}\ \eta_{22}\ \cdots\ \eta_{2n}] \begin{bmatrix} d_{fr}^1 \\ d_{fr}^2 \\ \vdots \\ d_{fr}^n \end{bmatrix} [c_1\ c_2\ \cdots\ c_n] \begin{bmatrix} \eta_{21} \\ \eta_{22} \\ \vdots \\ \eta_{2n} \end{bmatrix} \\ &= \eta_2^T \mathbf{\Delta}\eta_2 \end{aligned} \tag{3.69}$$

where

$$\mathbf{\Delta} = \begin{bmatrix} d_{fr}^1 c_1 & d_{fr}^1 c_2 & \cdots & d_{fr}^1 c_n \\ d_{fr}^2 c_1 & d_{fr}^2 c_2 & \cdots & d_{fr}^2 c_n \\ \vdots & & & \\ d_{fr}^n c_1 & d_{fr}^n c_2 & \cdots & d_{fr}^n c_n \end{bmatrix} \tag{3.70}$$

It is easy to find that $Rank(\mathbf{\Delta}) = 1$ thus $\mathbf{\Delta}$ can be modified as

$$\Delta = \mathbf{P}^T \begin{bmatrix} \lambda & 0 & \cdots & 0 \\ 0 & 0 & \cdots & 0 \\ \vdots & \vdots & \ddots & 0 \\ 0 & 0 & \cdots & 0 \end{bmatrix} \mathbf{P} \tag{3.71}$$

where λ is the only nonzero eigenvalue, $\mathbf{P}$ is a square matrix consisting of eigenvectors. Thus, the characteristic equation of $\mathbf{\Delta}$ is

$$\begin{vmatrix} \lambda - d_{fr}^1 c_1 & -d_{fr}^1 c_2 & \cdots & -d_{fr}^1 c_n \\ -d_{fr}^2 c_1 & \lambda - d_{fr}^2 c_2 & \cdots & -d_{fr}^2 c_n \\ \vdots & & & \\ -d_{fr}^n c_1 & d_{fr}^n c_2 & \cdots & \lambda - d_{fr}^n c_n \end{vmatrix} = \lambda^n + p\lambda^{n-1} = 0 \tag{3.72}$$

where $p = \sum_{i=1}^{n} c_i d_{fr}^i$.

Follow from Property 3.1, we know $d_{fr}^i < 0$, it is clear that for all $c_i > 0$, $i = 1, 2 \ldots, n$, $\lambda = p < 0$, and $\mathbf{\Delta}$ is a negative semi-definite matrix. We can readily obtain that

$$\frac{dV}{d\tau} \leq 0 \tag{3.73}$$

it follows from LaSalle's theorem [73], the solution of the closed loop system will converge to a bounded invariant set M. □

Model Free Adaptive Control Design

In time scale τ, $\bar{\zeta}$ can be a unknown constant. Such that, we are able to design an adaptive controller for the fast subsystem with an update law in fast feedback loop. To control the fast subsystem, consider the general controller of the form

$$\tau_f = -\mathbf{C}_1\hat{\eta}_1 - \mathbf{C}_2\eta_2 \tag{3.74}$$

where $\hat{\eta}_1$ is the estimate of η_1, $c_1^i > 0$, $c_2^i > 0$, $\mathbf{C}_1 \in R^{1\times n}$ and $\mathbf{C}_2 \in R^{1\times n}$.

Property 3.2: *Note that*

$$\eta_1 = z_1 - \bar{\zeta}, \tag{3.75}$$

where z_1 can be measurable, while $\bar{\zeta}$ cannot due to the system uncertainty. Since $\bar{\zeta}$ is slow time-varying variable, in the boundary layer system it can be approximated as a constant parameter. If the estimate of η_1 is denoted by $\hat{\eta}_1$, then

$$\hat{\eta}_1 = z_1 - \hat{\bar{\zeta}}, \tag{3.76}$$

where $\hat{\bar{\zeta}}$ is the estimate of $\bar{\zeta}$. It is also easy to see that

$$\tilde{\eta}_1 = \tilde{\bar{\zeta}}. \tag{3.77}$$

From the proof of Proposition 3.2, we know that it is easy to choose $\mathbf{C}_1$ which provides $\mathbf{D}_{fr}\mathbf{C}_1 \in R^{n_f\times n_f}$ be a negative semi definite matrix. Substituting (3.74)

into (3.55) yields the closed loop system

$$\begin{aligned} \frac{d\eta_1}{d\tau} &= \eta_2 \\ \frac{d\eta_2}{d\tau} &= -\mathbf{D}_{ff}\eta_1 + \mathbf{D}_{fr}(\mathbf{C}_1\hat{\eta}_1 + \mathbf{C}_2\eta_2) \end{aligned} \tag{3.78}$$

The stability of the closed-loop system are stated in the following proposition.

Proposition 3.3: *The closed-loop system given in (3.78) is asymptotically approaches a bounded invariant set M as t goes to ∞, if $K_s \geq ||\mathbf{C}_1\mathbf{E}||$, and the parameter adaptation laws are given by*

$$\frac{d\hat{\eta}_1}{d\tau} = \frac{d(z_1 - \hat{\tilde{\zeta}})}{d\tau} = \Gamma\eta_2 \tag{3.79}$$

Proof: Let us rewrite the fast subsystem as

$$\begin{aligned} \frac{d\eta_1}{d\tau} &= \eta_2 \\ \frac{d\eta_2}{d\tau} &= -\mathbf{D}_{ff}\eta_1 + \mathbf{D}_{fr}\tau_f \end{aligned} \tag{3.80}$$

As has been proved in Proposition 3.2, all the items in $\mathbf{D}_{fr}$ are positive definite. Consider the non-negative scalar function V as

$$V = \frac{1}{2}\eta_1^T(\mathbf{D}_{ff} - \mathbf{D}_{fr}\mathbf{C}_1)\eta_1 + \frac{1}{2}\eta_2^T\eta_2 + \frac{1}{2}\tilde{\tilde{\zeta}}^T(-\mathbf{D}_{fr}\mathbf{C}_1)\Gamma^{-1}\tilde{\tilde{\zeta}} \tag{3.81}$$

Computing the time derivative of V, it becomes

$$\begin{aligned} \frac{dV}{d\tau} &= \eta_1^T(\mathbf{D}_{ff} - \mathbf{D}_{fr}\mathbf{C}_1)\frac{d\eta_1}{d\tau} + \eta_2^T\frac{d\eta_2}{d\tau} + \tilde{\tilde{\zeta}}^T(-\mathbf{D}_{fr}\mathbf{C}_1)\Gamma^{-1}\frac{d\hat{\zeta}}{d\tau} \\ &= \eta_2^T(-\mathbf{D}_{ff}\eta_1 - \mathbf{D}_{fr}\mathbf{C}_1\hat{\eta}_1 - \mathbf{D}_{fr}\mathbf{C}_2\eta_2) \\ &\quad +\eta_1^T(\mathbf{D}_{ff} - \mathbf{D}_{fr}\mathbf{C}_1)\eta_2 + \tilde{\tilde{\zeta}}^T(-\mathbf{D}_{fr}\mathbf{C}_1)\Gamma^{-1}\frac{d\hat{\zeta}}{d\tau} \\ &= \eta_2^T\mathbf{D}_{fr}\mathbf{C}_1\tilde{\eta}_1 - \eta_2^T\mathbf{D}_{fr}\mathbf{C}_2\eta_2 + \tilde{\tilde{\zeta}}^T(-\mathbf{D}_{fr}\mathbf{C}_1)\Gamma^{-1}\dot{\hat{\tilde{\zeta}}} \end{aligned} \tag{3.82}$$

Noting that $\tilde{\eta}_1 = \tilde{\bar{\zeta}}$, (3.82) can be modified as

$$\frac{dV}{d\tau} = \eta_2^T(\mathbf{D}_{fr}\mathbf{C}_1)\tilde{\bar{\zeta}} - \eta_2^T\mathbf{D}_{fr}\mathbf{C}_2\eta_2 + \tilde{\bar{\zeta}}^T(-\mathbf{D}_{fr}\mathbf{C}_1)\Gamma^{-1}\frac{d\hat{\zeta}}{d\tau} \tag{3.83}$$

Substituting (3.79) into (3.83), we have

$$\frac{dV}{d\tau} = -\eta_2^T\mathbf{D}_{fr}\mathbf{C}_2\eta_2. \tag{3.84}$$

Following from proof of Proposition 3.2, we know that $c_2^i > 0$, $i = 1, 2, \ldots n$ guarantee that $\frac{dV}{d\tau} \leq 0$, i.e., the fast system will converge to an invariant set M asymptotically. □

Neural Network Based Adaptive Control Design

As discussed in Section 3.4.2, a dynamic neural network is used to emulate the inertia matrix $\mathbf{D}$ and Coriolis matrix $\mathbf{C}$. In this section, we use a neural network to estimate the unknown constant $\bar{\zeta}$. Following from Remark 3.1, the control design cannot be carried out by using the states η_1. The estimates of $\bar{\zeta}$ is obtained by replacing the true GL weight vectors $\{\mathbf{W}_\zeta\}$ by its estimates $\{\hat{\mathbf{W}}_\zeta\}$, i.e.

$$\hat{\bar{\zeta}} = [\{\hat{\mathbf{W}}_\zeta\}^T \bullet \{\mathbf{\Xi}_\zeta\}] \tag{3.85}$$

then,

$$\bar{\zeta} = [\{\hat{\mathbf{W}}_\zeta\}^T \bullet \{\mathbf{\Xi}_\zeta\}] + E \tag{3.86}$$

where $\mathbf{E} \in R^{n\times 1}$ is the collective NN reconstruction errors. Let $(\tilde{*}) = (\hat{*}) - (*)$. To control the fast subsystem, consider the general controller of the form

$$\tau_f = -\mathbf{C}_1\hat{\eta}_1 - \mathbf{C}_2\eta_2 - K_s\text{sgn}(\eta_2) \tag{3.87}$$

where $c_1^i > 0$, $c_2^i > 0$, $\mathbf{C}_1 \in R^{1\times n}$ and $\mathbf{C}_2 \in R^{1\times n}$, and $K_s \geq ||\mathbf{C}_1\mathbf{E}||$ for robust closed-loop stability. Substituting (3.87) into (3.55) yields the closed loop system

$$\begin{aligned} \frac{d\eta_1}{d\tau} &= \eta_2 \\ \frac{d\eta_1}{d\tau} &= -\mathbf{D}_{ff}\eta_1 - \mathbf{D}_{fr}[\mathbf{C}_1\hat{\eta}_1 + \mathbf{C}_2\eta_2 + K_s\text{sgn}(\eta_2)] \end{aligned} \tag{3.88}$$

The stability of the closed-loop system are stated in the following proposition.

Proposition 3.4: *The closed-loop system given in (3.88) is asymptotically approaches a bounded invariant set M as t goes to ∞, if $K_s \geq ||\mathbf{C}_1\mathbf{E}||$, and the parameter adaptation laws is given by*

$$\frac{d\hat{\mathbf{W}}_\zeta^i}{d\tau} = -\Gamma_{\zeta i} \bullet \{\xi_\zeta^i\} \sum_{j=1}^{n} (\eta_2^j) \tag{3.89}$$

Proof: Let us rewrite the fast subsystem as

$$\begin{aligned} \frac{d\eta_1}{d\tau} &= \eta_2 \\ \frac{d\eta_2}{d\tau} &= -\mathbf{D}_{ff}\eta_1 + \mathbf{D}_{fr}\tau_f \end{aligned} \tag{3.90}$$

As has been proved in Proposition 3.2, all the items in $\mathbf{D}_{fr}$ are positive definite. Consider the non-negative scalar function V as

$$V = \frac{1}{2}\eta_1^T(\mathbf{D}_{ff} - \mathbf{D}_{fr}\mathbf{C}_1)\eta_1 + \frac{1}{2}\eta_2^T\eta_2 + \frac{1}{2}\sum_{i=1}^{n} \tilde{\mathbf{W}}_{\zeta i}^T(-\mathbf{D}_{fr}\mathbf{C}_1)\Gamma_{\zeta i}^{-1}\tilde{\mathbf{W}}_{\zeta i} \tag{3.91}$$

Computing the time derivative of V, it becomes

$$\begin{aligned} \frac{dV}{d\tau} &= \eta_1^T(\mathbf{D}_{ff} - \mathbf{D}_{fr}\mathbf{C}_1)\frac{d\eta_1}{d\tau} + \eta_2^T\frac{d\eta_2}{d\tau} + \sum_{i=1}^{n} \tilde{\mathbf{W}}_{\zeta i}^T(-\mathbf{D}_{fr}\mathbf{C}_1)\Gamma_{\zeta i}^{-1}\frac{d\hat{\mathbf{W}}_{\zeta i}}{d\tau} \\ &= \eta_2^T(-\mathbf{D}_{ff}\eta_1 - \mathbf{D}_{fr}\mathbf{C}_1\hat{\eta}_1 - \mathbf{D}_{fr}\mathbf{C}_2\eta_2 - \mathbf{D}_{fr}K_s\text{sgn}(\eta_2)) \end{aligned} \tag{3.92}$$

$$\eta_1^T(\mathbf{D}_{ff} - \mathbf{D}_{fr}\mathbf{C}_1)\eta_2 + \sum_{i=1}^{n} \tilde{\mathbf{W}}_{\zeta i}^T(-\mathbf{D}_{fr}\mathbf{C}_1)\Gamma_{\zeta i}^{-1}\frac{d\hat{\mathbf{W}}_{\zeta i}}{d\tau}$$

$$= \eta_2^T\mathbf{D}_{fr}\mathbf{C}_1\tilde{\eta}_1 - \eta_2^T\mathbf{D}_{fr}\mathbf{C}_2\eta_2 + \sum_{i=1}^{n} \tilde{\mathbf{W}}_{\zeta i}^T(-\mathbf{D}_{fr}\mathbf{C}_1)\Gamma_{\zeta i}^{-1}\frac{d\hat{\mathbf{W}}_{\zeta i}}{d\tau} - \eta_2^T\mathbf{D}_{fr}K_s\text{sgn}(\eta_2)$$

Noting that $\tilde{\eta}_1 = \tilde{\tilde{\zeta}} = [\{\tilde{\mathbf{W}}_\zeta\}^T \bullet \{\mathbf{\Xi}_\zeta\}] - E$, (3.92) can be modified as

$$\begin{aligned}
\frac{dV}{d\tau} &= \eta_2^T(\mathbf{D}_{fr}\mathbf{C}_1)\{[\{\tilde{\mathbf{W}}_\zeta\}^T \bullet \{\mathbf{\Xi}_\zeta\}] - E\} - \eta_2^T\mathbf{D}_{fr}\mathbf{C}_2\eta_2 \qquad (3.93)\\
&\quad + \sum_{i=1}^{n} \tilde{\mathbf{W}}_{\zeta i}^T(-\mathbf{D}_{fr}\mathbf{C}_1)\Gamma_{\zeta i}^{-1}\frac{d\hat{\mathbf{W}}_{\zeta i}}{d\tau} - \eta_2^T\mathbf{D}_{fr}K_s\text{sgn}(\eta_2)\\
&= \eta_2^T(\mathbf{D}_{fr}\mathbf{C}_1)[\{\tilde{\mathbf{W}}_\zeta\}^T \bullet \{\mathbf{\Xi}_\zeta\}] - \eta_2^T(\mathbf{D}_{fr}\mathbf{C}_1)E - \eta_2^T\mathbf{D}_{fr}\mathbf{C}_2\eta_2\\
&\quad + \sum_{i=1}^{n} \tilde{\mathbf{W}}_{\zeta i}^T(-\mathbf{D}_{fr}\mathbf{C}_1)\Gamma_{\zeta i}^{-1}\frac{d\hat{\mathbf{W}}_{\zeta i}}{d\tau} - \eta_2^T\mathbf{D}_{fr}K_s\text{sgn}(\eta_2)
\end{aligned}$$

Noting that

$$\eta_2^T(\mathbf{D}_{fr}\mathbf{C}_1)[\{\tilde{\mathbf{W}}_\zeta\}^T \bullet \{\mathbf{\Xi}_\zeta\}] = \sum_{i=1}^{n}\{\tilde{\mathbf{W}}_{\zeta i}\}^T \bullet \{\xi_\zeta^i\}\sum_{j=1}^{n}(\eta_2^j d_{fr}^j \sum_{k=1}^{n} c_1^k) \qquad (3.94)$$

and substituting (3.89) into (3.93), we have

$$\frac{dV}{d\tau} = -\eta_2^T\mathbf{D}_{fr}\mathbf{C}_1\mathbf{E} - \eta_2^T\mathbf{D}_{fr}\mathbf{C}_2\eta_2 - \eta_2^T\mathbf{D}_{fr}K_s\text{sgn}(\eta_2) \le -\eta_2^T\mathbf{D}_{fr}\mathbf{C}_2\eta_2, \qquad (3.95)$$

when $K_s \ge ||\mathbf{C}_1\mathbf{E}||$. Following from proof of Proposition 3.2, we know if $c_2^i > 0$, $i = 1, 2, \ldots n$, then $\frac{dV}{d\tau} \le 0$, i.e., the fast system will converge to an invariant set M asymptotically. □

Note that only the closed-loop stability is claimed in Propositions 3.2-3.4. To prove the asymptotic stability is difficult due to the infinite dimensionality of the system. This means the robot may stop before reaching the final position and thus the regulation will fail. However, we shall show in the following that practically the

flexible robot can only possibly stop at the final position $\mathbf{q}_f = 0$ without vibrating. Consider the general form controller (3.66). Assume that it stops at a position $\mathbf{q}_r = \alpha$ (hence $\dot{\mathbf{q}}_r = 0$) with $\alpha \neq 0$, thus there is no energy input to the system since $\dot{\mathbf{q}}_r = 0$. Due to the existence of internal structural damping in a flexible link in practice, the flexible robot must tend to stop vibrating and finally be static at the undeformed position. Consequently, the controller in (3.66) approaches a nonzero constant and thus $\mathbf{q}_r = \alpha$ cannot hold. The only possibility is that the flexible link is at the final position $\mathbf{q}_r \equiv 0$ without vibrating, which implies the tip regulation is achieved.

Although the explanation of the practical asymptotic behaviour of the system above is reasonable, it cannot be taken as a rigorous mathematical proof. Indeed, for any damped traditional truncated-model obtained by either AMM or FEM (the effect of internal structural damping has been modeled as a positive definite damping matrix), the controller can be easily shown to be asymptotically stable using the LaSalle's Theorem, since the system in this case has been reduced to a finite dimensional one.

3.4.4 Simulation Studies

To verify the effectiveness of the proposed method, numerical simulations are carried out for a single-link flexible materials robot operating in the horizontal plane.

The flexible link robot is simulated using a 2 modes dynamic model with the following parameters. A fourth-order Runge-Kutta program with adaptive-step-size is used to numerically solve the ODEs [68]. The sampling interval is set to $0.001s$.

$$\begin{aligned}
\rho &= 0.1kg/m && \text{(link uniform density)} \\
l &= 1.0m && \text{(link length)} \\
m &= 0.1kg && \text{(link mass)} \\
I_h &= 3.0kgm^2 && \text{(hub inertia)} \\
I_b &= 0.033kgm^2 && \text{(rigid inertia)} \\
EI &= 5.0Nm^2 && \text{(flexural link rigidity)}
\end{aligned}$$

The desired trajectory for the rigid joint angle is expressed as a Hermite polynomial of the fifth degree in t with continuous bounded position, velocity and bounded acceleration. The general expression for the desired position trajectory is:

$$q_d(t, t_d) = q_0 + (6.0\frac{t^5}{t_d^5} - 15\frac{t^4}{t_d^4} + 10.0\frac{t^3}{t_d^3})(q_f - q_0) \tag{3.96}$$

t_d represents the time that the desired arm trajectory reaches the desired final position q_f starting from the desired initial position q_0. In this paper, $q_0 = 0.0$, $q_f = 1.0$ and $t_d = 2.0$ seconds.

Figures 3.4-3.6 shows the simulation result without estimating $\bar{\zeta}$, and Figures 3.7-3.10 show the result of the design by estimating $\bar{\zeta}$. Figures 3.4 and 3.7 present the joint angle trajectory under control (3.66) and (3.74), respectively. It can be seen that the controller with estimating $\bar{\zeta}$ gives better performance whereas $\boldsymbol{\eta}_2$

based control made the joint angle oscillate about the desired trajectory. From Figures 3.5 and 3.8, It indicates that tip deflections of flexible robot under control (3.74) converge faster than those under (3.66). For completeness and clarity in presentation, other signals in the closed-loop are included. Figures 3.6 and 3.10 show the bounded joint control torque signals under both controllers, while Figure 3.9 shows the estimation of $\bar{\zeta}$.

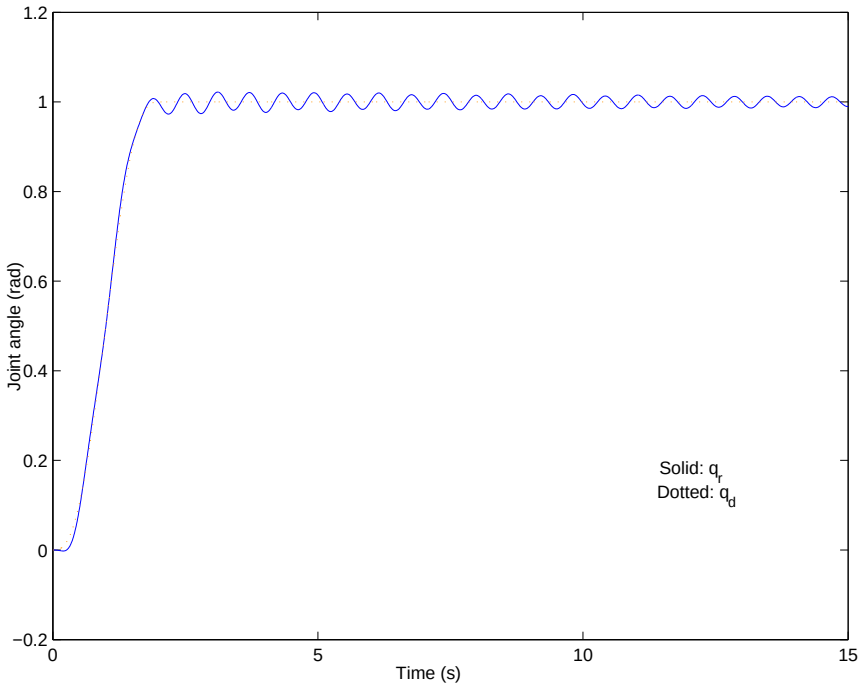

Figure 3.4: Joint angle trajectory.

The most important trajectories are those of tip position. The tip is required to track the desired trajectory fast with small residual vibration to improve the positioning accuracy. Under the assumption of small deflection, the tip position of the robot can be approximated by

$$p_t = L\theta(t) + y(L,t) \tag{3.97}$$

where p_t is the tip position, $y(L,t)$ is the tip deflection of the flexible robot and the angular position should be represented in radians instead of degrees. The tip positions under different controllers are depicted in Figure 3.11.

In fact, different tracking performance can be achieved by adjusting parameter adaptation gains and other factors, such as the size of the networks. Because neural networks are used to approximate system's functions, the requirements on the initial knowledge of the system is greatly reduced.

3.5 Summary

Since η_1 is unmeasurable, the adaptive control for unknown flexible robot remains open. In this chapter, an adaptive neural network control problem for flexible link robot is studied based on the singular perturbation theory. By using the critical properties of $\mathbf{M}$, a controller for fast subsystem is proposed. It is proven that the fast controller can guarantee the boundedness of flexible part, and stabilize the state at the origin by its internal structure damping. Then an adaptive neural network controller is developed to control the slow system. By using the composite controller combining the slow and fast controller, it seems that the fast variables are asymptotically stable, while adaptive trackings are achieved for slow variables. Simulations have been carried out to illustrate the performance of the controller designed by the proposed methods.

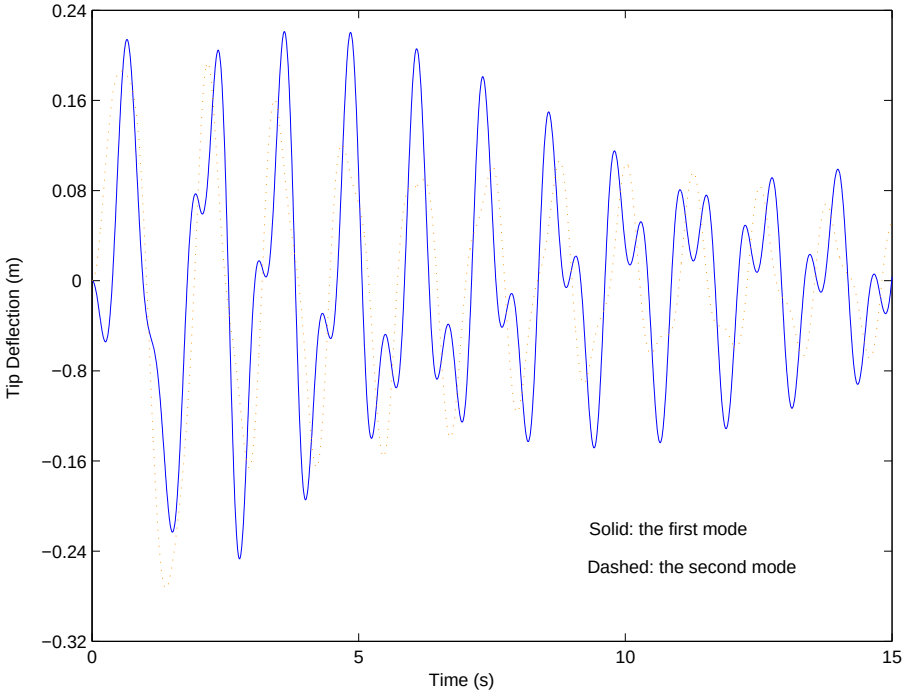

Figure 3.5: Tip deflections.

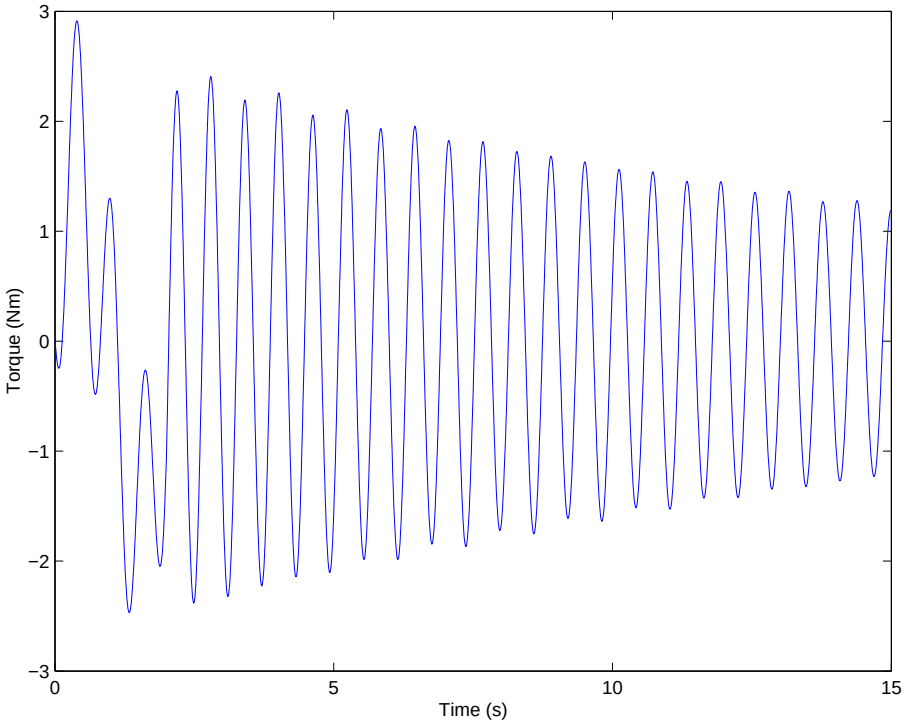

Figure 3.6: Torque control.

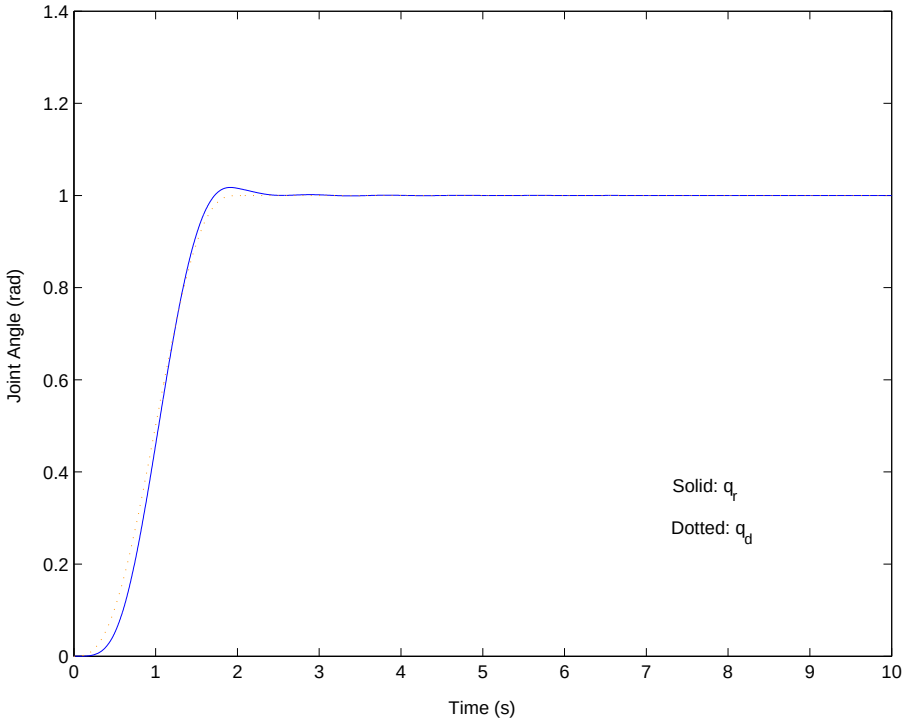

Figure 3.7: Joint angle trajectory.

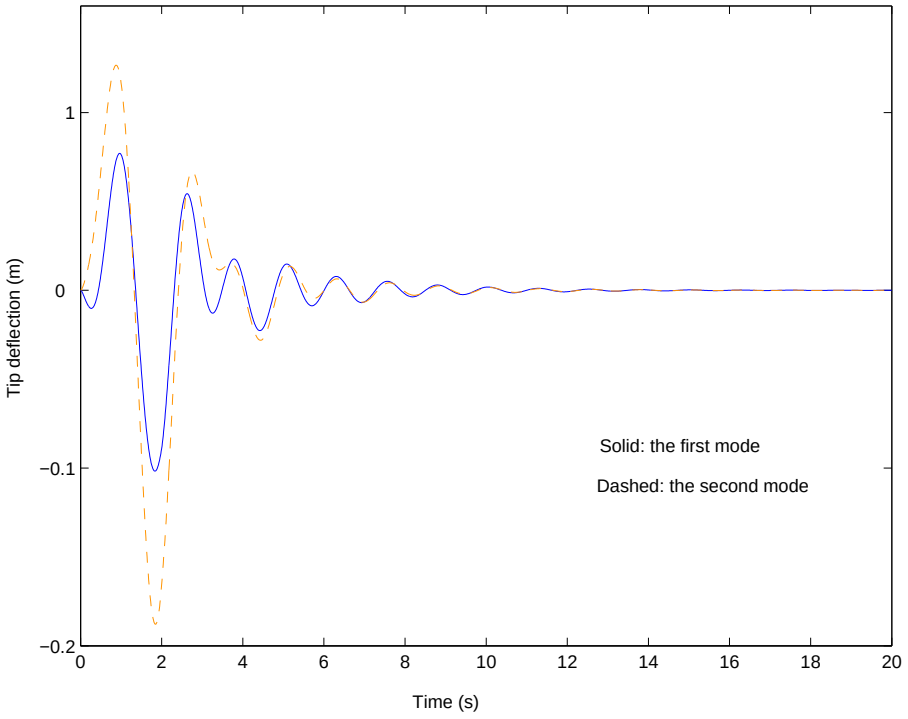

Figure 3.8: Tip deflections.

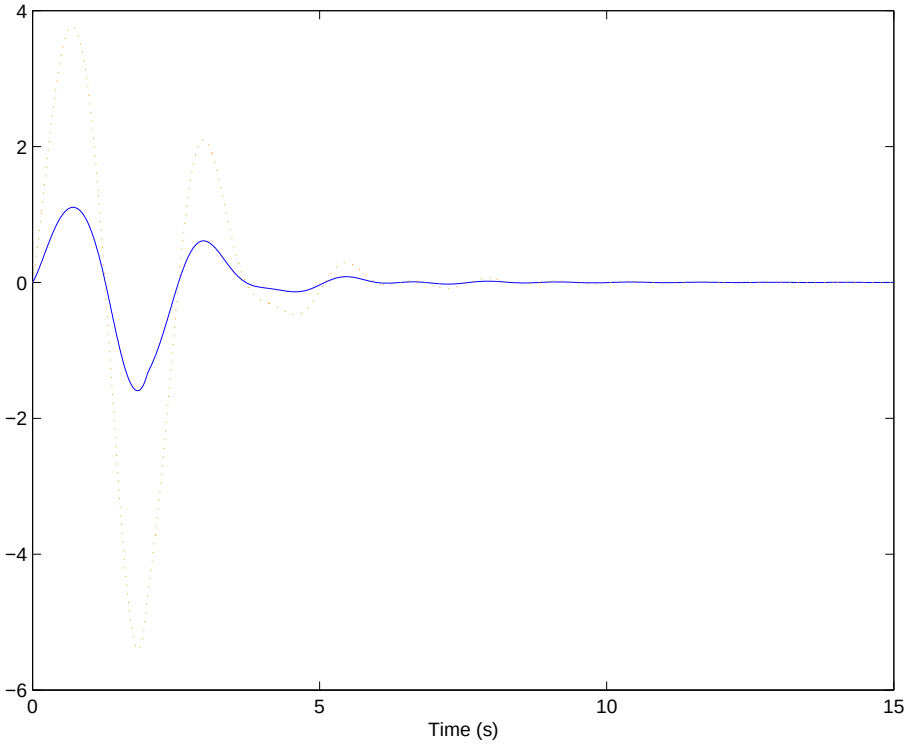

Figure 3.9: Trajectory of $\hat{\tilde{\zeta}}$.

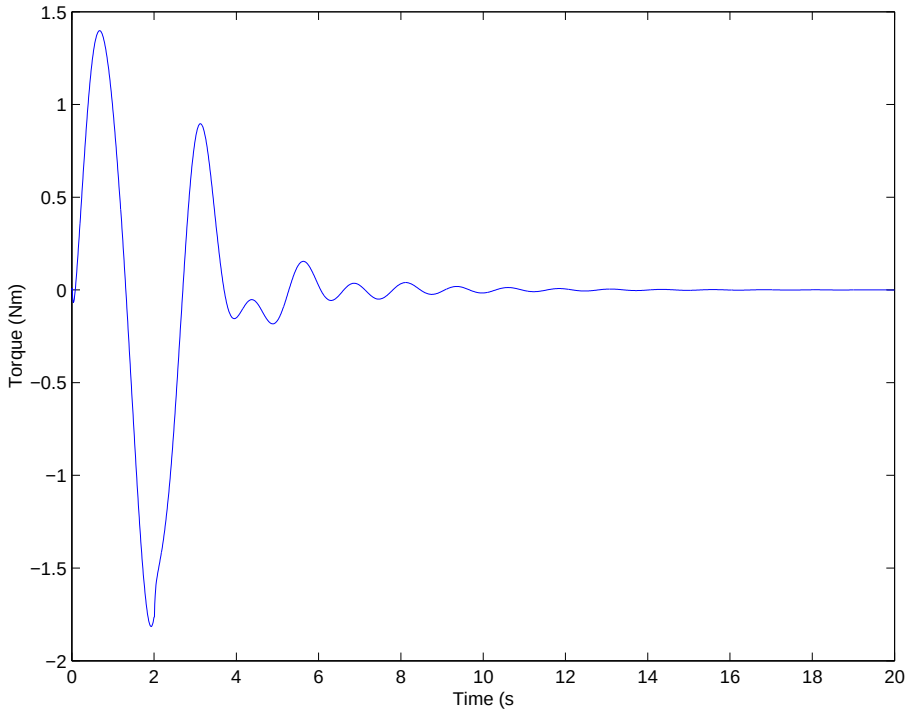

Figure 3.10: Control action.

Chapter 4

Force/Position Control of Flexible Link Robots

The problem of controlling force and position of a multi-link flexible link manipulator with constraint is studied in this chapter. The control for a known parameter multilink system in contact with environment are considered. The model has been developed in Section 2.2. Using singular perturbation theory, a slow subsystem associated with rigid dynamics and a fast subsystem associated with flexible dynamics are identified. Consequently, a composite control strategy is applied. It consists of a force and position control for the slow subsystem and a stabilizing control for the fast subsystem. Simulations are presented for a two-link manipulator to demonstrate the performance of the proposed controller.

4.1 Introduction

The tasks of industrial robots may be divided into two categories. The first is the so-called free motion task, and the second category, however, involves interactions between the robot end-effector and the environment. Many robot applications in manufacturing involve some kind of contact between the end-effector and the environment, as the robot moves along a prescribed trajectory. Therefore, constrained robots have become a useful mathematical method to model the physical and dynamic effects of a robot when it is engaged in one of the contact tasks. Unlike free motion control, where the only control objective is trajectory tracking or set-point regulation, the control of a constrained robot has an additional difficulty in controlling the constrained force.

In the case of interaction with the environment, it is required to consider both force control and position control. While several control methods exist for the rigid robot manipulators, only few works addressed on flexible link robot. A hybrid position and force control approach is proposed in [18, 49, 50]. A nonlinear decoupling method is considered in [51], and the application of computed-torque controller for constrained robots is carried out in [52]. Adaptive control dealing with parameter uncertainties are proposed in [74, 75], while the same problem is solved by using sliding mode control [76, 77]. All the existing methods depend on the exact cancellation of the robot dynamics to achieve.

On the other hand, when the link stiffness is large, the two-time scale model of the flexible manipulator can be derived [35], which consists of a slow subsystem for rigid motion and a fast subsystem for flexible motion. Thus, a composite strategy can be carried out with the slow control designing for the rigid part and fast control stabilizing the flexible part. Several papers considered the free motion task based on singular perturbation theory [18, 35, 42, 64, 78], but the postion/force control of constrained flexible link robot remains open.

In this chapter, a two time scale position and force control for flexible manipulators is proposed. A composite control is designed for known parameter multi-link flexible manipulator system.

The chapter is organized as follows. Section 4.2 reviews the dynamic model of constrained robots and its properties; A two time scale force and position control with known parameters is presented in Section 4.3; Section 4.4 contains simulations to show the effectiveness of the proposed control; and conclusion and summary are given in Section 4.5.

4.2 Dynamical Model and Properties

Consider the multi-link flexible manipulator, as sketched in Figure 4.1. The rigid motion is described by the joint angles θ_i, while $y_i(x_i)$ denotes the transversal deflection of link i at x_i with $0 \leq x_i \leq l_i$, being l_i the link length.

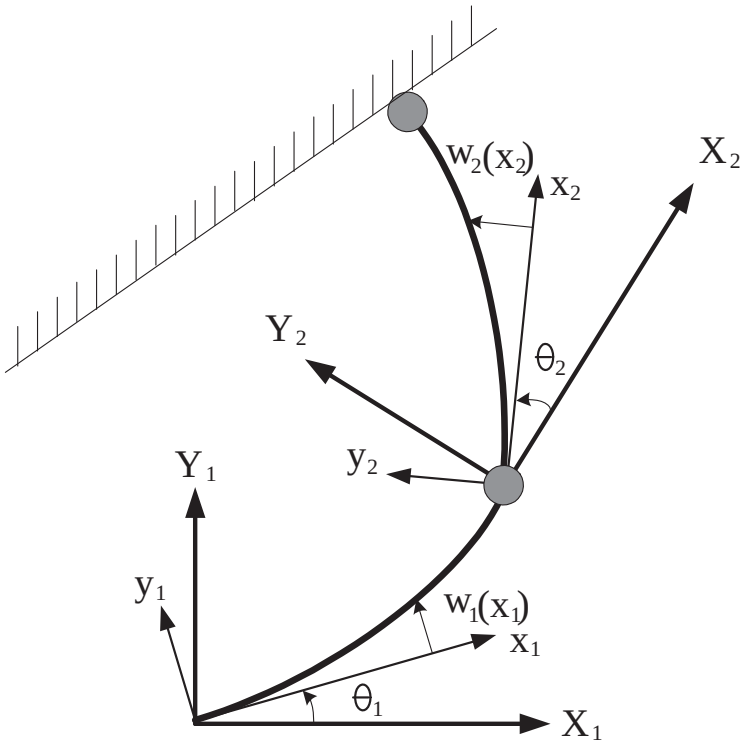

Figure 4.1: Two link flexible manipulator.

The finite dimensional model can be obtained by AMM. From Section 2.2, the direct kinematics equation expressing the position vector $\mathbf{p}$ of the manipulator tip point as a vector $\mathbf{q}_r = [\theta_1, \cdots, \theta_n]^T \in R^{n\times 1}$ of the joint variable and the vector $\mathbf{q}_f = [q_{1,1} \cdots q_{1,N_1} \cdots q_{n,1} \cdots q_{n,N_n}]^T \in R^{N\times 1}$ of the deflection variable can be written in the form [22]

$$\mathbf{p} = k(\mathbf{q}_r, \mathbf{q}_f) \tag{4.1}$$

where $N = \sum_{i=1}^{n} N_i$, with N_i being the number of modes considered to express the deflection of link i, and $\phi(\mathbf{q}_r, \mathbf{q}_f)$ is twice continuously differentiable [52]. From (4.1), the differential kinematics equation expressing the tip velocity $\dot{p}$ as a function

of $\dot{\mathbf{q}}_r$ and $\dot{\mathbf{q}}_f$ is

$$\dot{\mathbf{p}} = J_{\mathbf{q}_r}^{\prime T}(\mathbf{q}_r, \mathbf{q}_f)\dot{\mathbf{q}}_r + J_{\mathbf{q}_f}^{\prime T}(\mathbf{q}_r, \mathbf{q}_f)\dot{\mathbf{q}}_f, \tag{4.2}$$

where $J_{\mathbf{q}_r}^{\prime T} = \frac{\partial \phi(\mathbf{q}_r, \mathbf{q}_f)}{\partial \mathbf{q}_r}$ and $J_{\mathbf{q}_f}^{\prime T} = \frac{\partial \phi(\mathbf{q}_r, \mathbf{q}_f)}{\partial \mathbf{q}_f}$

The above kinematics description is at the basis of the dynamic modeling of the flexible manipulator using the Lagrange approach that requires computation of kinetic and potential energy [20, 22].

Consider now the situation when the manipulator tip is in contact with a holonomic and frictionless infinitely stiff surface the constraint imposed by the surface can be described by the differential scalar function

$$\phi(p) = \phi(k(\mathbf{q}_r, \mathbf{q}_f)) = 0, \tag{4.3}$$

where the direct kinematics equation (4.1) has been used to express the constraint in terms of joint and deflection variable. Also, it is assumed that the manipulator tip is always in contact with the surface. In static situation, the deflection can be shown to satisfy the equation

$$f_{\mathbf{q}_f} = \mathbf{K}_{ff}\mathbf{q}_f = J_{\mathbf{q}_f}^{\prime T}(\mathbf{q}_r, \mathbf{q}_f)J_\phi \lambda \tag{4.4}$$

where $\mathbf{K}_{ff}$ is the link stiffness matrix

$$\mathbf{K}_{ff} = diag(k_{1,1}, \cdots, k_{1,N_1}, \cdots, k_{n,1}, \cdots, k_{n,N_n}) \tag{4.5}$$

with $k_{i,j}$ defining in (2.56). Also in (4.4), $J'_{\mathbf{q}_f}$ is the Jacobian appearing in (4.2), J_ϕ is the gradient of the constraint space with respect to the two coordinates of the

manipulator position, i.e.

$$J_\phi = \left(\frac{\partial \phi}{\partial \mathbf{p}}\right)^T \tag{4.6}$$

and $\lambda \in R^m$ is a generalized Lagrangian multiplier relating to the magnitude of the constraint force [52]. Constraint force, $f_{\mathbf{q}_r}$, can then be expressed by

$$f_{\mathbf{q}_r} = J^T_{\mathbf{q}_r}(\mathbf{q}_r, \mathbf{q}_f)\lambda \in R^{m\times n} \tag{4.7}$$

$$f_{\mathbf{q}_f} = J^T_{\mathbf{q}_f}(\mathbf{q}_r, \mathbf{q}_f)\lambda \in R^{m\times N}, \tag{4.8}$$

where $J_{\mathbf{q}_r} = J'_{\mathbf{q}_r} J_\phi$, $J_{\mathbf{q}_f} = J'_{\mathbf{q}_f} J_\phi$, and m is the dimension of the constraint surface and it is assumed that $m < n$.

By the virtual work principle, the vector f of the force exerted by the manipulator on the environment performing work on $\mathbf{p}$ has to be related to the $(N \times 1)$ vector $J^T_{\mathbf{q}_r}\lambda$ of joint torques performing work on $\mathbf{q}_r$ and the $(n \times 1)$ vector $J^T_{\mathbf{q}_f}\mathbf{q}_f$ of the elastic reaction force performing work on $\mathbf{q}_f$.

A finite-dimensional Lagrangian dynamic model of the planar manipulator in contact with the environment can then be obtained in terms of the $N + n$ generalized coordinates $\mathbf{q}_r$, $\mathbf{q}_f$ in the form [22, 28]:

$$\begin{bmatrix} \mathbf{M}_{rr} & \mathbf{M}_{rf} \\ \mathbf{M}_{fr} & \mathbf{M}_{ff} \end{bmatrix} \begin{bmatrix} \ddot{\mathbf{q}}_r \\ \ddot{\mathbf{q}}_f \end{bmatrix} + \begin{bmatrix} \mathbf{H}_r \\ \mathbf{H}_f \end{bmatrix} + \begin{bmatrix} \mathbf{0} \\ \mathbf{K}_{ff}\mathbf{q}_f \end{bmatrix} = \begin{bmatrix} \tau \\ \mathbf{0} \end{bmatrix} + \begin{bmatrix} J^T_{\mathbf{q}_r}\lambda \\ J^T_{\mathbf{q}_f}\lambda \end{bmatrix} \tag{4.9}$$

where

$$\mathbf{H}_r = \mathbf{C}_{rr}\dot{\mathbf{q}}_r + \mathbf{C}_{rf}\dot{\mathbf{q}}_f$$

$$\mathbf{H}_f = \mathbf{C}_{fr}\dot{\mathbf{q}}_r + \mathbf{C}_{ff}\dot{\mathbf{q}}_f$$

and $\mathbf{M}_{rr}$, $\mathbf{M}_{fr}$, $\mathbf{M}_{rf}$, $\mathbf{M}_{ff}$ are the blocks of the inertia matrix M, which is symmetric and positive definite, $\mathbf{C}_{rr}$, $\mathbf{C}_{fr}$, $\mathbf{C}_{rf}$, $\mathbf{C}_{ff}$ represents the components of the vector of Coriolis and centrifugal forces, $\mathbf{K}_{ff}$ is the diagonal and positive definite link stiffness matrix, and τ is the vector if the input joint torques.

Due to the m-dimension constraint, m degrees of freedom of the robot are lost. Partitioning the link position vector $\mathbf{q}$ to $\mathbf{q}^1 \in R^{n+N-m}$ and $\mathbf{q}^2 \in R^m$, we have

$$\mathbf{q} = [\mathbf{q}^{1T} \quad \mathbf{q}^{2T}]^T \tag{4.10}$$

and accordingly, the Jacobian $J(\mathbf{q})$ is decomposed as

$$J(\mathbf{q}) = [J_1(\mathbf{q}) \quad J_2(\mathbf{q})] \tag{4.11}$$

with

$$\begin{aligned} J_1(\mathbf{q}) &= \frac{\partial \phi(\mathbf{q})}{\partial \mathbf{q}^1} \in R^{m\times(n+N-m)} \\ J_2(\mathbf{q}) &= \frac{\partial \phi(\mathbf{q})}{\partial \mathbf{q}^2} \in R^{m\times m} \end{aligned}$$

As stated in [79], it is possible to have a partition such that $J_2^{-1}(\mathbf{q})$ and

$$\dot{\mathbf{q}} = \mathbf{L}(\mathbf{q})\dot{\mathbf{q}}^1, \qquad \mathbf{L}(\mathbf{q}) = \begin{bmatrix} \mathbf{I}^{n+N-m\times n+N-m} \\ -J_2^{-1}(\mathbf{q})J_1(\mathbf{q}) \end{bmatrix} \tag{4.12}$$

where $\mathbf{I}$ is an identity matrix.

With the partition of the link position vector in equation (4.10), the position of the robot can be uniquely determined by $\mathbf{q}^1$. The original dynamical model in

equations (4.9) is transformed to

$$\mathbf{M}_r^1\ddot{\mathbf{q}}_r^1 + \mathbf{H}_r^1\dot{\mathbf{q}}_r^1 = \tau + J_{\mathbf{q}_r}^T\lambda \tag{4.13}$$

$$\mathbf{M}_f^1\ddot{\mathbf{q}}_f^1 + \mathbf{H}_f^1\dot{\mathbf{q}}_f^1 + \mathbf{K}_{ff}\mathbf{q}_f^1 = \tau + J_{\mathbf{q}_f}^T\lambda \tag{4.14}$$

where

$$\mathbf{M}^1(\mathbf{q}) = \mathbf{M}(\mathbf{q})L(\mathbf{q}) \in R^{n+N\times m}$$

$$\mathbf{C}^1(\mathbf{q},\dot{\mathbf{q}}) = \mathbf{M}(\mathbf{q})\dot{L}(\mathbf{q}) + \mathbf{C}(\mathbf{q},\dot{\mathbf{q}})L(\mathbf{q}) \in R^{n+N\times m}$$

Define $\mathbf{M}_l(\mathbf{q}) = L^T(\mathbf{q})\mathbf{M}^1(\mathbf{q}) \in R^{m\times m}$, $\mathbf{C}_l(\mathbf{q},\dot{\mathbf{q}}) = L^T(\mathbf{q})\mathbf{C}^1(\mathbf{q},\dot{\mathbf{q}}) \in R^{m\times m}$. It can be proven that the dynamic models (4.13) and 4.14 have the following properties.

Property 4.1 $L^T(\mathbf{q})J^T(\mathbf{q}) = 0$.

Property 4.2 $\mathbf{M}$, $\mathbf{C}$, $\mathbf{M}^1$, $\mathbf{C}^1$, $\mathbf{M}_l$, $\mathbf{C}_l$, $L(\mathbf{q})$, $\dot{L}(\mathbf{q})$, and $J(\mathbf{q})$ are uniformly bounded and continuous if $\mathbf{q}$ and $\dot{\mathbf{q}}$ are uniformly bounded and continuous; $\mathbf{M}$ and $\mathbf{M}_l$ are symmetric positive definite (*s.p.d*).

Property 4.3 $\dot{\mathbf{M}}(\mathbf{q}) - 2\mathbf{C}(\mathbf{q},\ \dot{\mathbf{q}})$ and $\dot{\mathbf{M}}_l(\mathbf{q}) - 2\mathbf{C}_l(\mathbf{q},\ \dot{\mathbf{q}})$ are skew-symmetric if $\mathbf{C}(\mathbf{q},\dot{\mathbf{q}})$ is in the Christoffel form, i.e., $\mathbf{x}_1^T(\dot{M}(\mathbf{q}) - 2\mathbf{C}(\mathbf{q},\ \dot{\mathbf{q}}))\mathbf{x}_1 = 0$, $\mathbf{x}_2^T(\dot{M}_l(\mathbf{q}) - 2\mathbf{C}_l(\mathbf{q},\ \dot{\mathbf{q}}))\mathbf{x}_2 = 0$, $\forall\mathbf{x}_1 \in R^n$ and $\mathbf{x}_2 \in R^{n-m}$.

For the controller design, the following assumptions are made for these terms:

Assumption 4.1 $\mathbf{q}_r(t)$, $\dot{\mathbf{q}}_r(t)$, $\mathbf{q}_f(t)$, $\dot{\mathbf{q}}_f(t)$ and $\lambda(t)$ are all measurable.

Assumption 4.2 The desired link position ($\mathbf{q}_{rd}(t)$) and the constraint force ($\lambda_d(t)$) and their derivatives are bounded and continuously differentiable.

4.3 Two-time Scale Control

When the link stiffness is large, it is reasonable to expect that the dynamics related to link flexibility is much faster than the dynamics associated with the rigid motion of the manipulator so that the system naturally exhibits a two-time scale dynamic behaviour in terms of rigid and flexible variables. this feature can be conveniently exploited for control design. For convenience, define $\mathbf{D}$ as

$$\mathbf{D} = \mathbf{M}^{-1} = \begin{bmatrix} \mathbf{D}_{rr} & \mathbf{D}_{rf} \\ \mathbf{D}_{fr} & \mathbf{D}_{ff} \end{bmatrix} \tag{4.15}$$

where

$$\mathbf{D}_{rr} = (\mathbf{M}_{rr} - \mathbf{M}_{rf}\mathbf{M}_{ff}^{-1}\mathbf{M}_{fr})^{-1} \tag{4.16}$$

$$\mathbf{D}_{rf} = -\mathbf{M}_{rr}^{-1}\mathbf{M}_{rf}(\mathbf{M}_{ff} - \mathbf{M}_{fr}\mathbf{M}_{rr}^{-1}\mathbf{M}_{rf})^{-1} \tag{4.17}$$

$$\mathbf{D}_{fr} = -\mathbf{M}_{ff}^{-1}\mathbf{M}_{fr}(\mathbf{M}_{rr} - \mathbf{M}_{rf}\mathbf{M}_{ff}^{-1}\mathbf{M}_{fr})^{-1} \tag{4.18}$$

$$\mathbf{D}_{ff} = (\mathbf{M}_{ff} - \mathbf{M}_{fr}\mathbf{M}_{rr}^{-1}\mathbf{M}_{rf})^{-1} \tag{4.19}$$

If Assumption 4.1 hold, the vector of joint torques can be conveniently chosen as

$$\tau = J_{\mathbf{q}_r}\lambda + \mathbf{u} \tag{4.20}$$

in order to cancel out the effects of the static torques acting on the rigid part of the manipulator dynamics, where the vector u is a new control input.

System (4.9) then becomes

$$\ddot{\mathbf{q}}_r = -\mathbf{D}_{rr}(\mathbf{q}_r, \mathbf{q}_f)\mathbf{H}_r(\mathbf{q}_r, \dot{\mathbf{q}}_r, \mathbf{q}_f, \dot{\mathbf{q}}_f) - \mathbf{D}_{rf}(\mathbf{q}_r, \mathbf{q}_f)\mathbf{H}_f(\mathbf{q}_r, \dot{\mathbf{q}}_r, \mathbf{q}_f, \dot{\mathbf{q}}_f)$$
$$-\mathbf{D}_{rf}(\mathbf{q}_r, \mathbf{q}_f)(\mathbf{K}_{ff}\mathbf{q}_f - J_{\mathbf{q}_f}^T\lambda) + \mathbf{D}_{rr}(\mathbf{q}_r, \mathbf{q}_f)u \quad (4.21)$$

$$\ddot{\mathbf{q}}_f = -\mathbf{D}_{fr}(\mathbf{q}_r, \mathbf{q}_f)\mathbf{H}_r(\mathbf{q}_r, \dot{\mathbf{q}}_r, \mathbf{q}_f, \dot{\mathbf{q}}_f) - \mathbf{D}_{ff}(\mathbf{q}_r, \mathbf{q}_f)\mathbf{H}_f(\mathbf{q}_r, \dot{\mathbf{q}}_r, \mathbf{q}_f, \dot{\mathbf{q}}_f)$$
$$-\mathbf{D}_{ff}(\mathbf{q}_r, \mathbf{q}_f)(\mathbf{K}_{ff}\mathbf{q}_f - J_{\mathbf{q}_f}^T\lambda) + \mathbf{D}_{fr}(\mathbf{q}_r, \mathbf{q}_f)u \quad (4.22)$$

The time scale separation between the slow and fast dynamics can be determined by defining the singular perturbation parameter ϵ. Assume that the orders of magnitude of the $k_{i,j}$ in (4.5) are comparable. Introducing an appropriate scale factor k such that

$$\mathbf{K}_{ff} = k\tilde{\mathbf{K}}_{ff} \quad (4.23)$$

The following new variables can be defined as

$$\zeta := k\tilde{\mathbf{K}}_{ff}\mathbf{q}_f \quad (4.24)$$

Define $\epsilon^2 := 1/k$, equation (4.21) can be modified as

$$\ddot{\mathbf{q}}_r = -\mathbf{D}_{rr}(\mathbf{q}_r, \epsilon^2\zeta)\mathbf{H}_r(\mathbf{q}_r, \dot{\mathbf{q}}_r, \epsilon^2\zeta, \epsilon^2\dot{\zeta}) - \mathbf{D}_{rf}(\mathbf{q}_r, \epsilon^2\zeta)\mathbf{H}_f(\mathbf{q}_r, \dot{\mathbf{q}}_r, \epsilon^2\zeta, \epsilon^2\dot{\zeta})$$
$$-\mathbf{D}_{rf}(\mathbf{q}_r, \epsilon^2\zeta)(\zeta - J_{\mathbf{q}_f}^T\lambda) + \mathbf{D}_{rr}(\mathbf{q}_r, \epsilon^2\zeta)\mathbf{u} \quad (4.25)$$

$$\epsilon^2\ddot{\zeta} = -\mathbf{D}_{fr}(\mathbf{q}_r, \epsilon^2\zeta)\mathbf{H}_r(\mathbf{q}_r, \dot{\mathbf{q}}_r, \epsilon^2\zeta, \epsilon^2\dot{\zeta}) - \mathbf{D}_{ff}(\mathbf{q}_r, \epsilon^2\zeta)\mathbf{H}_f(\mathbf{q}_r, \dot{\mathbf{q}}_r, \epsilon^2\zeta, \epsilon^2\dot{\zeta})$$
$$-\mathbf{D}_{ff}(\mathbf{q}_r, \epsilon^2\zeta)(\zeta - J_{\mathbf{q}_f}^T\lambda) + \mathbf{D}_{fr}(\mathbf{q}_r, \epsilon^2\zeta)\mathbf{u} \quad (4.26)$$

The system is now decomposed in a slow and a fast subsystems by using singular perturbation theory. This leads to a composite control strategy for the null system based on separate control designs for the two reduced order subsystems.

Formally, setting $\epsilon = 0$ and solving for ζ in (4.26), we obtain

$$\begin{aligned} \bar{\zeta} &= -\mathbf{D}_{ff}^{-1}(\bar{\mathbf{q}}_r, 0)[\mathbf{D}_{fr}(\bar{\mathbf{q}}_r, 0)\mathbf{H}_r(\bar{\mathbf{q}}_r, \dot{\bar{\mathbf{q}}}_r, 0) + \mathbf{D}_{ff}(\bar{\mathbf{q}}_r, 0)\mathbf{H}_f(\bar{\mathbf{q}}_r, \dot{\bar{\mathbf{q}}}_r, 0) \\ &\quad + \mathbf{D}_{ff}(\bar{\mathbf{q}}_r, 0)J_{\mathbf{q}_f}^T\lambda + \mathbf{D}_{fr}(\bar{\mathbf{q}}_r, 0)\mathbf{u}_s] \end{aligned} \tag{4.27}$$

where the overbars are used to indicate that the system with $\epsilon = 0$. The state variable $\bar{\zeta}$ corresponds to a static elastic deformation for the slow time scale. Substituting Eq. (4.27) into Eq. (4.25) with $\epsilon = 0$ and using the relations $\mathbf{M}_{rr} = (\mathbf{D}_{rr} - \mathbf{D}_{rf}\mathbf{D}_{ff}^{-1}\mathbf{D}_{fr})^{-1}$, yields the slow subsystem which is equivalent to the dynamic equation of the rigid manipulators [18].

$$\mathbf{M}_{rr}(\bar{\mathbf{q}}_r, 0)\ddot{\bar{\mathbf{q}}}_r + \mathbf{H}_r(\bar{\mathbf{q}}_r, \dot{\bar{\mathbf{q}}}_r, 0) = \mathbf{u}_s \tag{4.28}$$

Let us define

$$\mathbf{x}_1 = \mathbf{q}_r,\ \mathbf{x}_2 = \dot{\mathbf{q}}_r,\ \mathbf{z}_1 = \epsilon\zeta,\ \mathbf{z}_2 = \epsilon^2\dot{\zeta} \tag{4.29}$$

The full system (4.25) and (4.26) can be rewritten as

$$\dot{\mathbf{x}}_1 = \mathbf{x}_2 \tag{4.30}$$

$$\begin{aligned} \dot{\mathbf{x}}_2 &= -\mathbf{D}_{rr}(\mathbf{x}_1, \epsilon^2\mathbf{z}_1)\mathbf{H}_r(\mathbf{x}_1, \mathbf{x}_2, \epsilon^2\mathbf{z}_1, \epsilon\mathbf{z}_2) - \mathbf{D}_{rf}(\mathbf{x}_1, \epsilon^2\mathbf{z}_1)\mathbf{H}_f(\mathbf{x}_1, \mathbf{x}_2, \epsilon^2\mathbf{z}_1, \epsilon\mathbf{z}_2) \\ &\quad -\mathbf{D}_{rf}(\mathbf{x}_1, \epsilon^2\mathbf{z}_1)\mathbf{z}_1 + \mathbf{D}_{rr}(\mathbf{x}_1, \epsilon^2\mathbf{z}_1)\mathbf{u} + \mathbf{D}_{ff}(\bar{\mathbf{q}}_r, 0)J_{\mathbf{q}_f}^T\lambda \end{aligned}$$

$$\begin{aligned}
\dot{\mathbf{z}}_1 &= \mathbf{z}_2 \qquad (4.31)\\
\epsilon\dot{\mathbf{z}}_2 &= -\mathbf{D}_{fr}(\mathbf{x}_1,\epsilon^2\mathbf{z}_1)\mathbf{H}_r(\mathbf{x}_1,\mathbf{x}_2,\epsilon^2\mathbf{z}_1,\epsilon\mathbf{z}_2) - \mathbf{D}_{ff}(\mathbf{x}_1,\epsilon^2\mathbf{z}_1)\mathbf{H}_f(\mathbf{x}_1,\mathbf{x}_2,\epsilon^2\mathbf{z}_1,\epsilon\mathbf{z}_2)\\
&\quad -\mathbf{D}_{ff}(\mathbf{x}_1,\epsilon^2\mathbf{z}_1)\mathbf{z}_1 + \mathbf{D}_{fr}(\mathbf{x}_1,\epsilon^2\mathbf{z}_1)\mathbf{u} + \mathbf{D}_{ff}(\bar{\mathbf{q}}_r,0)J_{\mathbf{q}_f}^T\lambda
\end{aligned}$$

To derive the fast subsystem, we introduce the fast time scale $\tau = t/\epsilon$, and the new variables

$$\eta_1 = \mathbf{z}_1 - \bar{\zeta},\ \eta_2 = \mathbf{z}_2, \mathbf{u}_f = \mathbf{u} - \mathbf{u}_s \qquad (4.32)$$

Using equations (4.32) and (4.30), the joint angles can be represented as

$$\begin{aligned}
\frac{d\mathbf{x}_1}{d\tau} &= \epsilon\mathbf{x}_2 \qquad (4.33)\\
\frac{d\mathbf{x}_2}{d\tau} &= -\epsilon\mathbf{D}_{rr}\mathbf{H}_r - \epsilon\mathbf{D}_{rf}\mathbf{H}_f - \epsilon\mathbf{D}_{rf}(\eta+\bar{\zeta}) + \epsilon\mathbf{D}_{rr}\mathbf{u} + \epsilon\mathbf{D}_{ff}J_{\mathbf{q}_f}^T\lambda
\end{aligned}$$

From equation (4.33) we can find that $\epsilon \to 0 \Rightarrow \frac{d\mathbf{x}_1}{d\tau} = 0$, $\frac{d\mathbf{x}_2}{d\tau} = 0 \Rightarrow \mathbf{x}_1 =$ constant, $\mathbf{x}_2 =$ constant and the slow variable $\mathbf{x}_1$ and $\mathbf{x}_2$ are constant in the fast subsystem. Using (4.27) (4.31) and (4.32)gives the fast subsystem

$$\begin{aligned}
\frac{d\eta_1}{d\tau} &= \eta_2 \qquad (4.34)\\
\frac{d\eta_2}{d\tau} &= -\mathbf{D}_{ff}(\bar{\mathbf{x}}_1)\eta_1 + \mathbf{D}_{fr}(\bar{\mathbf{x}}_1)\mathbf{u}_f.
\end{aligned}$$

4.3.1 Slow Control

In order to design the slow control for the rigid nonlinear system (4.28), we derive the slow dynamics with respect to the tip position. Differentiating Eq. (4.2), which contains the tip velocity, it gives the tip acceleration

$$\ddot{\mathbf{p}} = J_{\mathbf{q}_r}\ddot{\mathbf{q}}_r + J_{\mathbf{q}_f}\ddot{\mathbf{q}}_f + \dot{J}_{\mathbf{q}_r}\dot{\mathbf{q}}_r + \dot{J}_{\mathbf{q}_f}\dot{\mathbf{q}}_f. \qquad (4.35)$$

Thus, the corresponding slow subsystem is

$$\ddot{\mathbf{p}}_s = \bar{J}_{\mathbf{q}_r} M_{rr}^{-1}(\mathbf{u}_s - \bar{\mathbf{H}}_r) + \bar{\dot{J}}_{\mathbf{q}_r}\dot{\mathbf{q}}_r. \tag{4.36}$$

The slow dynamic models (4.28) and (4.35) enjoy the same properties of the rigid dynamic model [23], hence the control strategies developed for rigid link can be adopted here. For the tracking of a time varying position $\mathbf{p}_d$ on the contact plane, an inverse dynamics parallel control scheme can be adopted for the slow system [24]. Then, we have the following theorem.

Theorem 4.1: *The quasi-steady-state dynamic system (4.30) is exponentially stable given the following slow-time scale control law:*

$$\mathbf{u}_s = \bar{\mathbf{M}}_{rr}\bar{J}_{\mathbf{q}_r}(\ddot{\mathbf{a}}_s - \bar{h}) + \bar{\mathbf{H}}_r \tag{4.37}$$

where

$$\mathbf{a}_s = \ddot{\mathbf{p}}_r + k_d(\dot{\mathbf{p}}_r - \mathbf{p}_s) + k_p(\mathbf{p}_r - \mathbf{p}_s) \tag{4.38}$$

with $\mathbf{p}_r = \mathbf{p}_d + \mathbf{p}_c$ *is the desired position, and* $\mathbf{p}_c$ *is the solution of the differential equation*

$$k_a\ddot{\mathbf{p}}_c + k_v\dot{\mathbf{p}}_c = \lambda_d - \lambda_s \tag{4.39}$$

being k_p*,* k_d*,* k_v*, and* $k_a > 0$ *suitable feedback gains.*

Proof: Substituting (4.37) with (4.38) into (4.36), it gives

$$\ddot{\mathbf{p}}_s = \ddot{\mathbf{p}}_r + k_d(\dot{\mathbf{p}}_r - \mathbf{p}_s) + k_p(\mathbf{p}_r - \mathbf{p}_s) \tag{4.40}$$

Define $\mathbf{e} = \mathbf{p}_r - \mathbf{p}_s$, we have

$$\ddot{e} + k_d\dot{e} + k_p e = 0 \tag{4.41}$$

Since $\mathbf{p}_{d,t} = \mathbf{p}_{r,t}$, where $*_t$ is the projection of $*$ on vector t (Figure 4.2), it can be found that

$$\ddot{\mathbf{e}}_t + k_d\dot{\mathbf{e}}_t + k_p\mathbf{e}_t = 0 \tag{4.42}$$

which implies that the tracking of the tip position to desired value $\mathbf{p}_d$ at the projection along the surface is achieved, for any choice of k_d and $k_p > 0$.

On the other hand, a better insight into the behavior of the system during the interaction can be achieve by considering a model of the compliant environment. To this purpose, a planar surface of regular, which is locally a good approximation to surfaces of regular curvature (Figure 4.2), and the model of the contact force is given by

$$\lambda = k_e\mathbf{n}\mathbf{n}^T(\mathbf{p} - \mathbf{p}_o) \tag{4.43}$$

where $\mathbf{p}_o$ represents the position of any point on the underformed plane and $k_e > 0$ is the contact stiffness coefficient. For the purpose of this work, it is assumed that the same equation can be established in terms of the slow variables. Such a model shows that the contact force is normal to the plane, and thus a null force error can be obtained only if the desired force λ_d is aligned with n. In addition, null position errors can be obtained only on the contact plane while the component of the position along n has to accommodate the force requirement specified by λ_d [27].

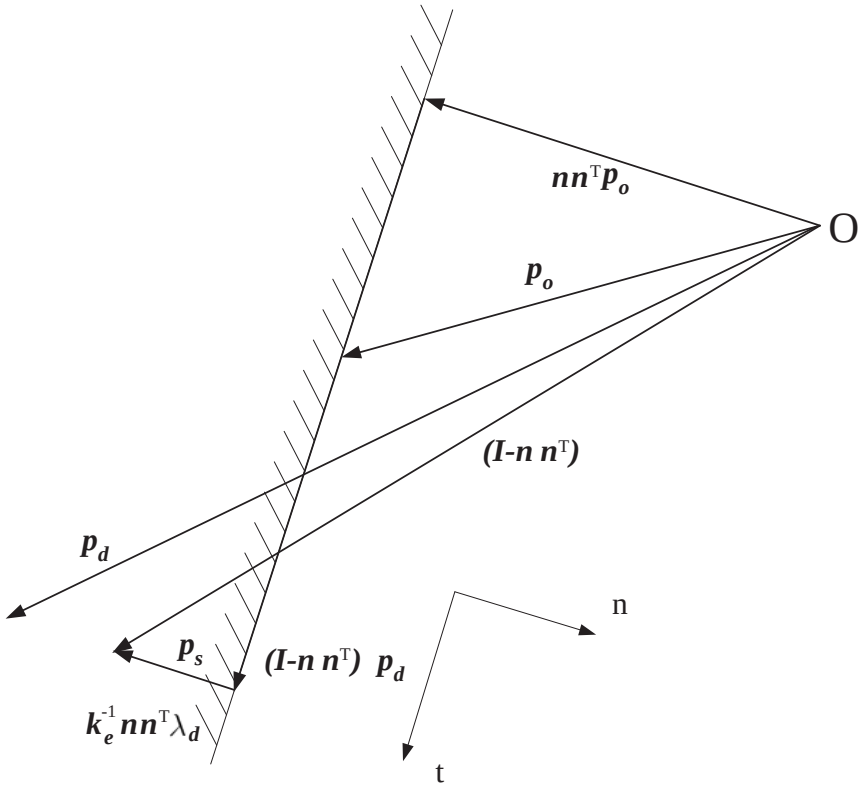

Figure 4.2: Scheme of contact plane and equilibrium position.

Projecting (4.39) along n gives

$$k_a\ddot{\mathbf{p}}_{c,n} + k_v\dot{\mathbf{p}}_{c,n} = \delta\lambda_n \tag{4.44}$$

assuming that the component of $\mathbf{p}_d$ is along vector n is constant, we project $\mathbf{p}_s$ and $\dot{\mathbf{p}}_s$ on the normal to the contact plane gives

$$\dot{\mathbf{p}}_{e,n} = \dot{\mathbf{p}}_{c,n} \tag{4.45}$$

$$\ddot{\mathbf{p}}_{e,n} = \ddot{\mathbf{p}}_{c,n} \tag{4.46}$$

where $*_n$ is the projection of $*$ on vector n.

In view of the model (4.43), we have

$$\mathbf{p}_s - \mathbf{p}_d + \mathbf{p}_d - \mathbf{p}_o = (k_e \mathbf{n}\mathbf{n}^T)^{-1}\lambda \tag{4.47}$$

Projecting (4.47) on n, we have

$$\mathbf{e}_{p,n} = k_n^{-1}(\mathbf{e}_{\lambda,n} - \lambda_{d,n} - \mathbf{p}_{d,n} + \mathbf{p}_{o,n}) \tag{4.48}$$

where $\mathbf{e}_p = \mathbf{p}_s - \mathbf{p}_d$ and $\mathbf{e}_\lambda = \lambda - \lambda_d$. Then, substituting (4.45) and (4.46) into (4.39) and using (4.48) with constant $\mathbf{p}_{d,n}$, $\lambda_{d,n}$ and $\mathbf{p}_{o,n}$ yields

$$k_a k_n^{-1}\ddot{\mathbf{e}}_\lambda + k_v k_n^{-1}\dot{\mathbf{e}}_\lambda = \mathbf{e}_\lambda \tag{4.49}$$

which implies that regulation of the contact force to the desired value along the constrained task direction is achieved, for any choice of k_a and $k_v > 0$. □

By using the similar arguments developed in [24] for rigid manipulators, it can be easily shown that the control law (4.37), (4.38), (4.39) ensures regulation of the contact force to the desired set-point λ_d and tracking the time-varying component of the desired position on the contact plane $(I - \mathbf{n}\mathbf{n}^T)\mathbf{p}_d$, where n is the unit vector along the normal to the plane.

4.3.2 Fast Controller

The fast subsystem can be rewritten as

$$\frac{d\eta}{d\tau} = \mathbf{A}(\bar{x})\eta + \mathbf{B}(\bar{x})\mathbf{u}_f \tag{4.50}$$

where $\eta = [\eta_1 \ \eta_2]^T$, $\mathbf{A} = \begin{bmatrix} \mathbf{O} & \mathbf{I} \\ -\mathbf{D}_{ff}(\bar{x}) & \mathbf{O} \end{bmatrix}$, $\mathbf{B} = \begin{bmatrix} \mathbf{O} \\ \mathbf{D}_{fr}(\bar{x}) \end{bmatrix}$

System (4.50) is a marginally stable linear slowly time varying system that can be stabilized to the equilibrium manifold by a proper choice of the control input $\mathbf{u}_f$, A reasonable way to achieve this goal is to design a state space control law of the form

$$\mathbf{u}_f = \mathbf{K}_1\eta_1 + \mathbf{K}_2\eta_2 \tag{4.51}$$

where matrices $\mathbf{K}_1$ and $\mathbf{K}_2$ can be determined based on classical pole placement.

4.3.3 Composite Controller

Combining the slow control law (4.37) and the fast control law (4.51), it gives the input torque

$$\mathbf{u} = \mathbf{u}_s + \mathbf{u}_f, \tag{4.52}$$

which achieves the dynamics hybrid position/froce control of the flexible manipulator. A scheme of the composite controller is shown in Figure 4.3.3. Following from Tikhonov's theorem, a fundamental result in the singular perturbation theory, the state vectors of the full system can be approximated as

$$\begin{aligned} \mathbf{x}_1 &= \bar{\mathbf{x}}_1 + O(\epsilon) & \mathbf{x}_2 &= \bar{\mathbf{x}}_2 + O(\epsilon) \\ \mathbf{z}_1 &= \bar{\zeta} + \eta_1 + O(\epsilon) & \mathbf{x}_1 &= \eta_2 + O(\epsilon) \end{aligned}$$

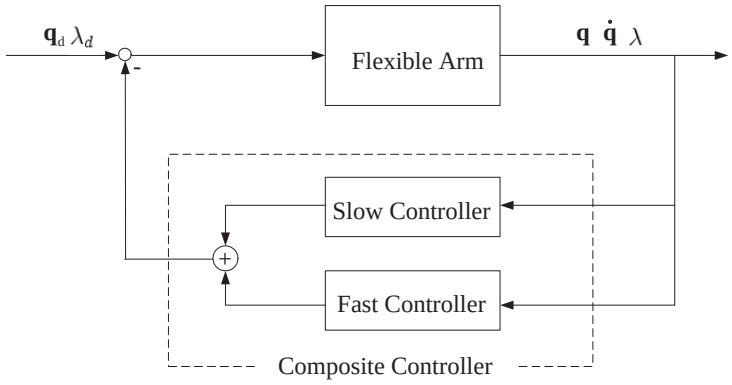

Figure 4.3: Block diagram of composite controller

4.4 Simulation

To test the proposed method, a two link (n=2) flexible arm which is rotate by two motors in a horizontal plane (Figure 4.4) with two assumed mode ($N_1 = N_2 = 2$) for each link is considered. For completeness, the components of **M**, **H** and **K** are detailed in Appendix [22]. Assume that the contact surface is

$$\phi = x - 0.5 = 0, \tag{4.53}$$

and the desired tip position $\mathbf{p}_d = [x_d\ y_d]^T$m move along the following trajectory on the constraint surface defined by

$$\begin{aligned} x_d(t) &= 0.5 \\ y_d(t) &= 1.2t^5 - 3t^4 + 2t^3 \end{aligned} \tag{4.54}$$

Apparently, the normal vector in (4.43) is $n = [1\ 0]^T$; a point of the underformed plane is $\mathbf{p}_o = [0.3\ 0]^T$m and the contact stiffness is $k_e = 20$ N/m. The manipulator is initially placed with the tip in contact with the underformed plane in the position

$p(0) = [0.18\ 0]^T$m, and the desired force is taken from zero to the value $\lambda_d = [2\ 0]^T$N. The following parameters are set up for the links and placement of a payload is

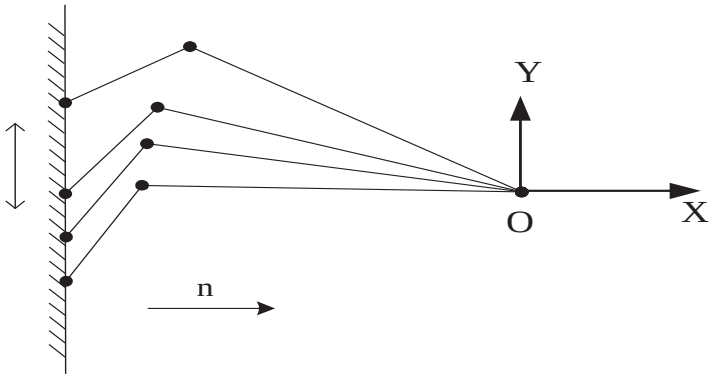

Figure 4.4: Manipulator configurations

assumed to be at the manipulator tip:

$$\begin{aligned}
\rho_1 = \rho_2 &= 1.0kg/m && \text{(link uniform density)} \\
l_1 = l_2 &= 0.5m && \text{(link length)} \\
d_1 = d_2 &= 0.25m && \text{(link center of mass)} \\
m_1 = m_2 &= 0.5kg && \text{(link mass)} \\
I_{h1} = I_{h2} &= 3.0kgm^2 && \text{(hub inertia)} \\
I_{b1} = I_{b2} &= 0.51kgm^2 && \text{(rigid inertia)} \\
EI_1 = EI_2 &= 10Nm^2 && \text{(flexural link rigidity)} \\
m_t &= 0.1kg && \text{(payload mass)}
\end{aligned}$$

In the simulation study, the slow controller (4.37) has been used in the composite control law (4.52). The actual force f and position p are used in the controller in lieu of the corresponding slow variables. The slow control gains have been set to $k_p = 25$ and $k_d = 10$, $k_a = 1.73$, $k_v = 3.19$, and the fast control gains have been set

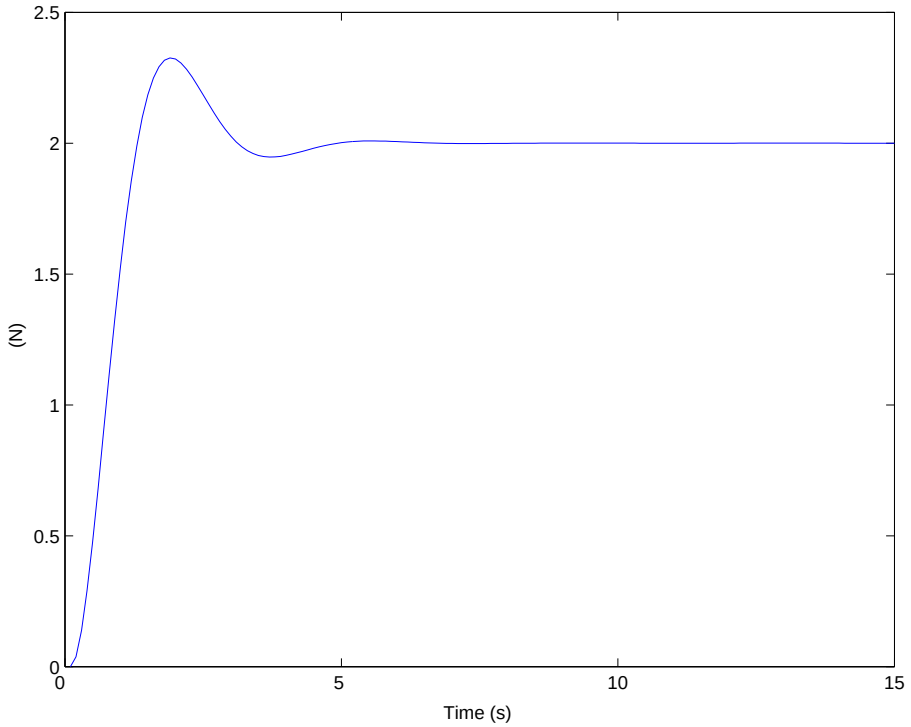

Figure 4.5: Contact force

to $K_1 = [2.198\ 0.281\ 10.231\ -7.121]^T$ and $K_2 = [6.112\ -12.930\ 3.884\ 1.582]^T$. The simulation result are shown in Figures 4.5-4.11.

Figures 4.5 and 4.6 indicate the trajectories of the contact force and the position errors of respectively. The joint angles q_{r1}, q_{r2} and link deflections q_{f11}, q_{f12}, q_{f21}, q_{f22} are shown in Figures 4.7-4.10. The joint torque u is reported in Figure 4.11.

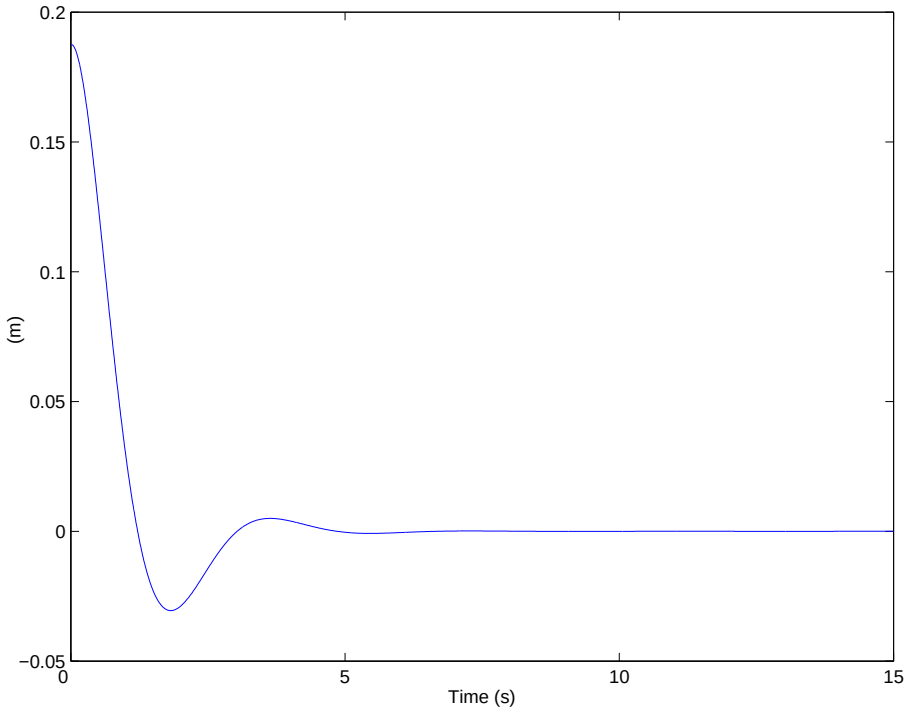

Figure 4.6: Position error along the surface, $||\mathbf{e}_t||$

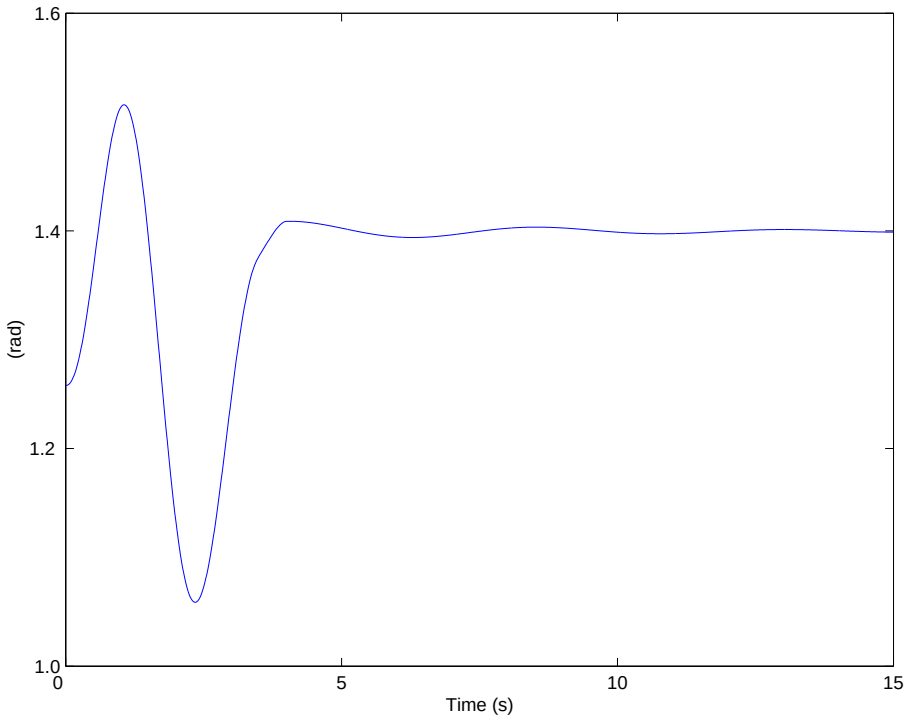

Figure 4.7: 1st joint angle

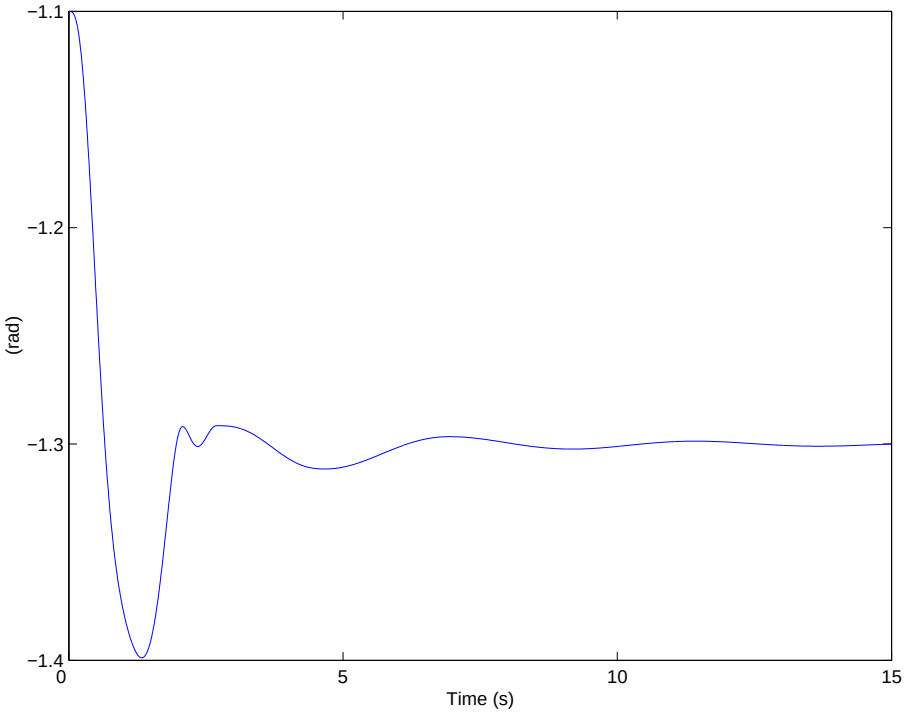

Figure 4.8: 2nd joint angle

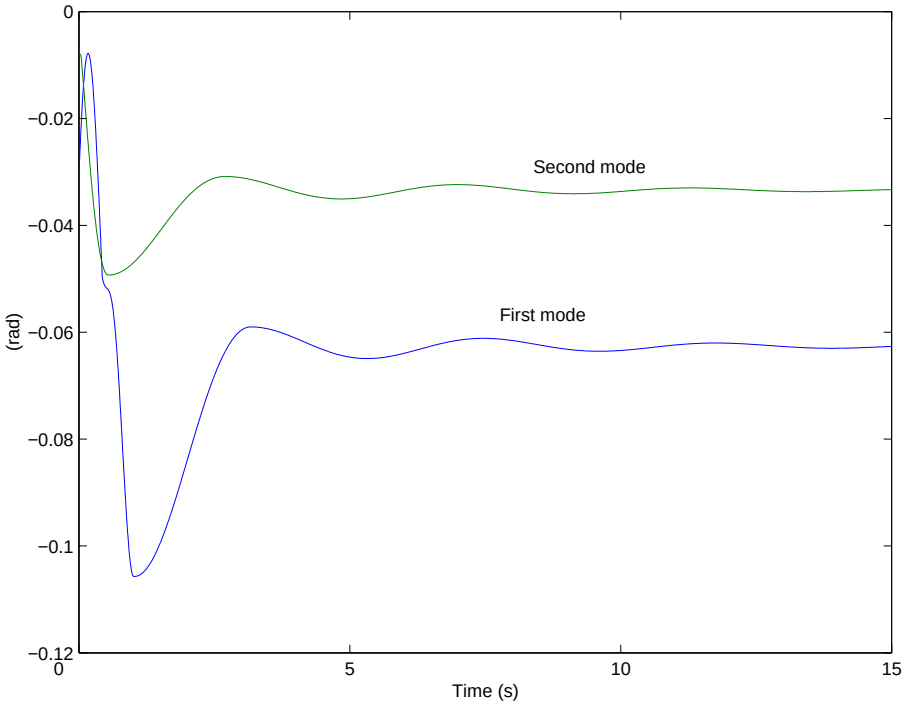

Figure 4.9: 1st link deflections

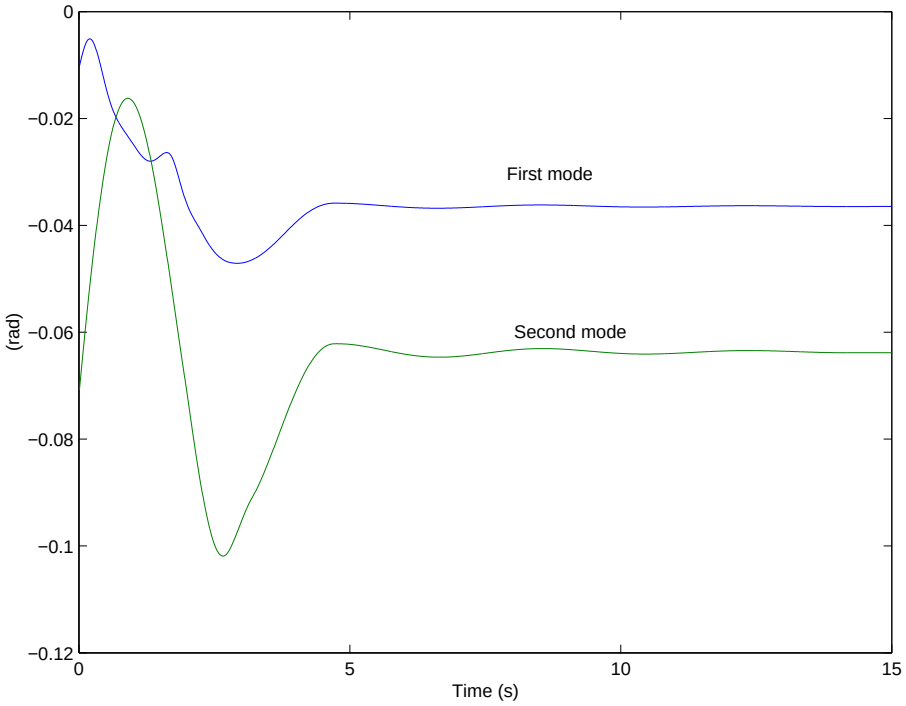

Figure 4.10: 2nd link deflections

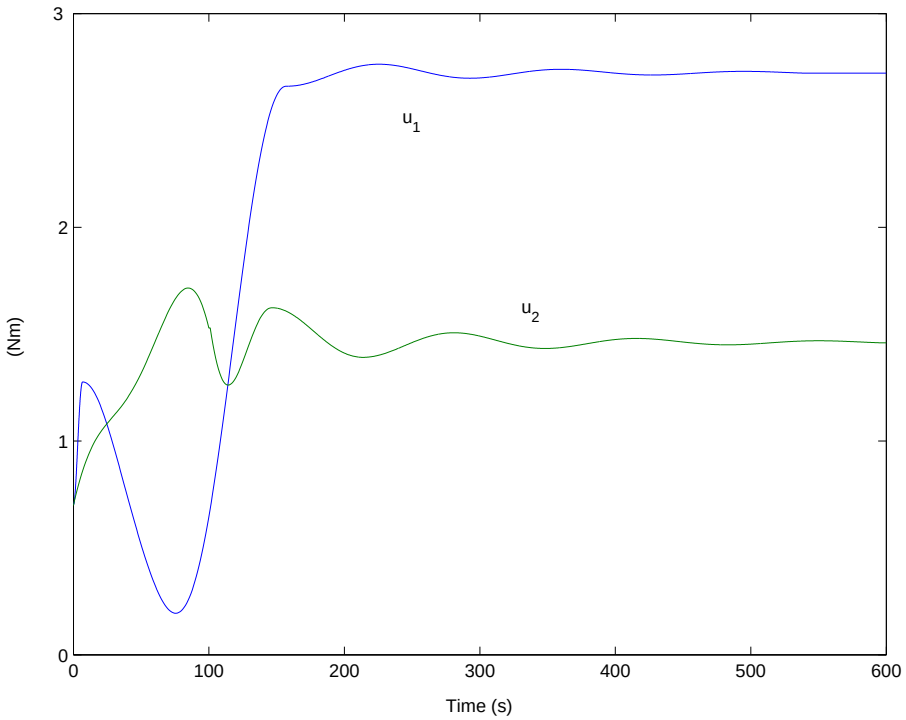

Figure 4.11: Joints torques

4.5 Summary

The problem of force and position control for the flexible robots has been investigated. By using singular perturbation theory, the original system is regrouped into two subsystems, based on the assumption of large link stiffness. A slow subsystem represents the dynamics of rigid part and a fast subsystem describes the dynamics of flexible part. A force and position parallel control, which is developed for rigid link manipulators, has been applied for the control of the slow rigid dynamics. The fast control is designed by the classical pole placement. Simulations show the effectiveness of the proposed method.

Chapter 5

Conclusions and Further Research

5.1 Conclusions

The work presented in this thesis basically consists of two parts: the dynamic modeling part (Chapter 2) and the controller design part (Chapter 3-4).

In Chapter 2, the modeling of flexible robot manipulators is studied. First, by using Lagrange's equations of motion, a closed-form dynamics model, where link deflection is described in terms of assumed modes, is obtained. Subsequently, by using FEM, the flexible beam is divided into a finite number of elements, and the link's elastic deformation is represented in the form of a linear combination of admissible functions and generalized coordinates. Although the model obtained from AMM and FEM can both be used in the design of the controller, the generalized coordinates in the FEM model are more physically meaningful than those in the

AMM model. Therefore, a multi-link model is developed using the results from FEM. All of the models described in Chapter 2 are used throughout the controller design part.

In Chapter 3, the FEM model is separated into two subsystems based on singular perturbation theory, under the assumption of large link stiffness. Then, an adaptive neural network controller is developed for the unknown systems. The unknown equilibrium $\bar{\zeta}$ is considered as a constant in the boundary layer, so that an adaptive law can be designed for the fast subsystem. It is noted that the fast variables are asymptotically stable, while adaptive trackings are achieved for slow variables. It is found that the proposed controller can achieve better tracking performance compared with the existing PID methods.

Chapter 4 is dedicated to the position/force control for a constrained flexible multi-link robot. The constrained robot model and its properties are briefly reviewed. By cancelling out the effects of the static torques acting on the rigid part of the manipulator dynamics, a new control input is introduced. By using singular perturbation theory, under the assumption of large link stiffness, the system is split into two subsystems. Assuming that all the states measurement are available, a composite control is proposed. It has been proven that the controller guarantees the regulation of the contact force and the tracking of the tip position to the desired trajectories. A simulation study has confirmed the effectiveness of the proposed approach.

5.2 Further Research

There are still many investigations that can be carried out to extend the work in this thesis. For example,

- *Design of the observer to measure the unknown $\bar{\zeta}$ for fast control design.*

  As discussed in Chapter 3, the equilibrium cannot be measured directly for a unknown system, although full states measurement are available. In Chapter 3, some critical properties of the single link model have been found, and by using this, the fast stabilizer is developed without a priori knowledge. However, for multi-link robots, this property may not hold. One possible method to solve the problem is to design an adaptive observer. By cementing enough strain gauge foils on flexible link, it may be possible to measure the movements.

- *Adaptive control of position/force control constrained robots with unknown parameters.*

  All the existing methods are dependent on the exact cancellation of the robot dynamics to achieve the desired result. However, in real application, the exact robot model may not be available to control, i.e., the exact cancellation of the dynamics may not be feasible. The system uncertainty affects the dynamics parameters. The tracking control performance and the accuracy of constrained force are therefore subject to the variance of the systems.

Further research should be dedicated into the adaptive control problem for the unknown or partially unknown multi-link flexible robots. The effects of the force signals on the stability of the overall closed loop system should be further investigated.

Bibliography

[1] G. Zhu, *Modelling and Control of Flexible Robots*. Ph.D Thesis, National University of Singapore, 1997.

[2] V. A. Spector and H. Flashner, "Modeling and design implications of non-collocated control in flexible systems," *ASME Journal of Dynamic Systems, Measurement and Control*, vol. 112, pp. 186–193, 1990.

[3] Z. H. Luo, "Direct strain feedback control of flexible robot arms: new theoretical and experimental results," *IEEE Transactions on Automatic Control*, vol. 38, no. 11, pp. 1610–1622, 1993.

[4] J. J. Shifman, "Lyapunov functions and the control of euler-bernoulli beam," *International Journal of Control*, vol. 57, pp. 971–992, 1993.

[5] W. Book, "Modelling, design, and control of flexible manipulator arms: a tutorial review," in *Proc. 29th Conf. Decision & Control*, (Honolulu, Hawaii), pp. 500–506, Dec., 1990 1990.

[6] H. Kanoh, S. Tzafestas, H. G. Lee, and J. Kalat, "Modelling and control of flexible robot arms," in *Proc. 25th Conf. Decision & Control*, (Athens, Greece), pp. 1866–1870, Dec 1986.

[7] V. V. Korolov and Y. H. Chen, "Robust control of a flexible manipulator arm," in *Proc. 1988 IEEE Int. Conf. Robotics and Auto.*, (Philadelphia, PA, USA), pp. 159–164, Apr 1988.

[8] Y. Sakawa, F. Matsuno, and S. Fukushima, "Modeling and feedback control of a flexible arm," *J. of Robotic Systems*, vol. 2, no. 4, pp. 453–472, 1985.

[9] H. Krishnan, *Bounded Input Discrete-Time Control of a Single-Link Flexible Beam*. University of Waterloo: Master Thesis, Department of Electrical Engineering, 1988.

[10] F. Bellezza, L. Lanari, and G. Ulivi, "Exact modeling of the flexible slewing link," in *Proc. 1990 IEEE Int. Conf. Robotics and Automation*, (Cincinnati, OH, USA), pp. 734–739, May 1990.

[11] E. Bayo, "A finite element approach to control the end-point motion of a single-link flexible robot," *J. of Robotics Systems*, vol. 4, no. 1, pp. 63–75, 1987.

[12] P. B. Usoro, R. Nadira, and S. S. Mahil, "A finite element/lagrange approach to modeling lightweight flexible manipulators," *Trans. ASME, J. Dyn. Syst., Meas., Contr.*, vol. 108, no. 3, pp. 198–205, 1986.

[13] C. Menq and J. Chen, "Dynamic modeling and payload-adaptive control of a flexible manipulator," in *Proc. 1988 IEEE Int. Conf. Rob. and Auto.*, (Philadelphia, PA, USA), pp. 488–493, April 1988.

[14] S. S. Ge, T. H. Lee, and G. Zhu, "A nonlinear feedback controller for a single-link flexible manipulator based on a finite element model," *Journal of Robotic Systems*, vol. 14, no. 3, pp. 165–178, 1997.

[15] S. Ge, T. Lee, and G. Zhu, "Robust nonlinear feedback control of a one-link flexible robot with cone-bounded uncertainties," in *Proc. of* 4*th Int. Conf. on Control, Automation, Robotics and Vision*, (Singapore), pp. 534–538, 1996.

[16] S. Ge, T. Lee, and G. Zhu, "Two-phase regulation of a single-link flexible robot," in *Proc. Asian Control Conference (ASCC'97)*, vol. 3, (Seuol), pp. 355–358, July 22-25 1997.

[17] L. Meirovitch, *Elements of Vibration Analysis*. New York: McGraw-Hill, Inc., 1975.

[18] F. Matsuno and K. Yamamoto, "Dynamic hybrid position/force control of a two degree-of-freedom flexible manipulator," *J. Robotic Systems*, vol. 11, no. 5, pp. 355–366, 1994.

[19] F. Marsuno, "Force control of flexible manipulators," *in Adavanced Studies of Flexible Robotic Manipulators*, no. 1, pp. 129–188, 2003.

[20] W. J. Book, "Recursive lagrangian dynamics of flexible manipulator arms," *Int. J. Robotics Res.*, vol. 3, pp. 87–101, 1984.

[21] R. P. Judd and D. R. Falkenburg, "Dynamics of nonrigid articulated robot linkages," *IEEE Trans. Automatic Contr.*, vol. 30, pp. 499–502, 1985.

[22] A. D. Luca and B. Siciliano, "Closed-form dynamic model of planar multilin lightweight robots," *IEEE Trans. Systems, Man, and Cybernetics*, vol. 21, pp. 826–839, 1991.

[23] C. C. de Wit, B. Siciliano, and G. Bastin, *Theory of Robot Control*. London, New York: Springer, 1996.

[24] B. S. L. Villani, *Robot force control*. Boston, MA: Kluwer Academics Publishers, 1999.

[25] L. Sciavicco and B. Siciliano, *Modeling and Control of Robot Manipulators*. New York: McGraw-Hill, Inc., 1996.

[26] B. Siciliano, "A closed-loop inverse kinematics scheme for on-line joint based robot control," *Robotica*, vol. 8, pp. 231–243, 1990.

[27] B. Siciliano, "Closed-loop inverse kinematics algorithm for constrained flexible manipulators under gravity," *IEEE Trans. on Automatic Control*, vol. 39, pp. 647–652, 1994.

[28] B. Siciliano, "Closed-loop inverse kinematics algorithm for constrained flexible manipulators under gravity," *Journal of Robotic Systems*, vol. 16, no. 6, pp. 353–362, 1999.

[29] R. H. J. Cannon and E. Schmitz, "Initial experiments on the end-point control of a flexible robot," *Int. J. Robotics Res.*, vol. 3, no. 3, pp. 62–75, 1984.

[30] A. Arakawa, T. Fukuda, and F. Hara, "H_∞ control of a flexible robotics arm (effec of parameter uncertainties on stability)," in *IEEE/RSJ Int. Workshop on Intelligent Robots and Systems IROS'91*, (Osaka, Japan), pp. 959–964, 3-5, Nov. 1991.

[31] Y. P. Chen and K. S. Yeung, "Regulation of a one-link flexible robot arm using sliding -mode technique," *Int. J. Control*, vol. 49, pp. 1965–1978, 1989.

[32] S. S. Ge, T. H. Lee, and G. Zhu, "Energy-based robust controller design for multi-link flexible robots," *Mechatronics*, vol. 6, no. 7, pp. 779–798, 1996.

[33] S. S. Ge, "Energy based control of flexible link robots," *in Adavanced Studies of Flexible Robotic Manipulators*, pp. 71–104, 2003.

[34] F. Khorrami and Ümit Özgüner, "Perturbation methods in control of flexible link manipulators," in *Proc. 1988 IEEE Int. Conf. Robotics and Auto.*, (Philadelphia, PA, USA), pp. 310–315, Apr 1988.

[35] B. Siciliano and W. J. Book, "A singular perturbation approach to control of lightweight flexible manipulators," *Int. J. Robotics Research*, vol. 7, no. 4, pp. 79–90, 1988.

[36] Y. Aoustin, C. Chevallereau, A. Glumineau, and C. Moog, "Experimental results for the end-effector control of a single flexible robotic arm," *IEEE Trans. Control Systems Technology*, vol. 2, no. 4, pp. 371–381, 1994.

[37] K. Khorasani and M. W. Spong, "Invariant manifolds and their application to robot manipulators with flexible joints," in *Proc. IEEE Int. Conf. Robotics & Automation*, pp. 978–983, 1985.

[38] Y. Aoustin and C. Chevallereau, "The singular perturbation control of a two-flexible-link robot," in *Proc. 1993 IEEE conf. Rob. Auto.*, (Atlanta, GA), pp. 737–742, 1993.

[39] B. Siciliano, J. V. R. Prasad, and A. J. Calise, "Output feedback two time scale control of multilink flexible arms," *ASME Journal of Dynamic Systems, Measurement, and Control*, vol. 114, pp. 70–77, 1992.

[40] M. W. Spong, K. Khorasani, and R. V. Kokotovic, "An intergral manifold approach to the feedback control of flexible joint robots," *IEEE Journal of Robotics and Automation*, pp. 291–300, 1987.

[41] K. H. Zaad and K. Khorasani, "Control of nonminimum phase sigularly perturbed systems with applications to flexible link manipulators," in *Proc. Workshop on Advances in Control and its Applications*, (Lecture Notes in Control and Information Science 208), pp. 234–265, Springer-Verlag 1995.

[42] M. Moallem, K. Khorasani, and R. V. Patel, "An integral manifold approach for tip-position tracking of flexible multilink manipulators," *IEEE Trans. on Robotics and Automation*, vol. 13, pp. 823–837, 1997.

[43] K. S. Narendra, "Adaptive control using neural networks," *in Neural Networks for Control*, vol. W.T.Miller,R.S.Sutton,andP.J.Werbos Eds. Cambridge,MA:MIT, pp. 115–142, 1991.

[44] G. A. Rovithakis and M. A. Christodoulou, "Adaptive control of unknown plants using dynamical neural networks," *IEEE Trans. Syst., Man, Cybern.*, vol. 24, pp. 400–412, 1994.

[45] H. A. Talebi, K. Khorasani, and R. V. Patel, "Neural network based control schemes for flexible-link manipulators: simulations and experiments," *Neural Networks*, vol. 11, pp. 1357–1377, 1998.

[46] K. Y. Kuo and J. Lin, "Fuzzy logic control for flexible link robot arm by singular perturbation approach," *Applied Soft Computing*, vol. 2, pp. 24–38, 2002.

[47] J. Lin and F. L. Lewis, "Fuzzy controller for flexible link robot arm by reduced order techniques," *IEE Proc.-Control Theory Appl.*, vol. 147, no. 3, pp. 177–187, 2002.

[48] J. Lin, "Hierarchical fuzzy logic controller for a flexible link robot arm performing constrained motion tasks," *IEE Proc.-Control Theory Appl.*, vol. 150, no. 4, pp. 355–364, 2003.

[49] M. H. Raibert and J. J. Craig, "Hybrid position/force control of manipulators," *ASME J. Dynam. Syst., Meas. Contr.*, vol. 102, pp. 126–133, 1981.

[50] T. Yoshikawa, "Dynamic hybrid position/force control of manipulators - description of hand constraints and calculation of joint driving forces," in *Proc. 1981 IEEE International Conference on Robotics and Automation*, (San Francisco, CA), pp. 1393–1398, 1981.

[51] X. Yun, "Dynamic state feedback control of constrained robot manipulator," in *Proc. 27th IEEE International Conference on Decision and Control*, (Austin, Dexas, USA), pp. 622–626, Dec. 1988.

[52] N. H. McClamroch and D. Wang, "Feedback stabilization and tracking of constrained robots," *IEEE Trans. Automat. Contr.*, vol. 33, pp. 419–426, 1988.

[53] M. w. Spong, "Adaptive control of flexible joint manipulators: comments on two papers," *Automatica*, vol. 31, no. 4, pp. 595–590, 1995.

[54] H. Goldstein, *Classical Mechanics*. Cambridge, Mass.: Addison-Wesley Press, INC., 1950.

[55] E. Kreyszig, *Advanced Engineering Mathematics*. New York: John Wiley & Sons, Inc., 1993.

[56] R. D. Blevins, *Formulas for natural frequency and mode shape*. New York: Van Nostrand Reinhold Co., 1979.

[57] G. G. Hastings and W. J. Book, "A linear dynamic model for flexible robotic manipulators," *IEEE Control System Magazine*, vol. 7, pp. 61–64, 1987.

[58] N. Chalhoub and A. Ulsoy, "Control of a flexible robot arm: Experimental and theoretical results," *J. Dynamic Systems, Measurement and Control*, vol. 109, pp. 299–309, 1987.

[59] P. Kokotovic, H. Khalil, and J. O'Reilly, *Singular perturbation methods in control: analysis and design*. New York: Academic Press, 1986.

[60] G. Hastings and W. Book, "Reconstruction and robust reduced-order observation of flexible variables, in: Robotics: Theory and application," *ASME Publications*, vol. 2, pp. 11–16, 1987.

[61] P. V. Kokotovic, "Applications of singular perturbation techniques to control problems," *SIAM review*, vol. 26, no. 4, pp. 501–550, 1984.

[62] Y. Tang, M. Tomizuka, and G. Guerrero, "Robust control of rigid robots," in *Proc. 36th IEEE conference on Decision and Control*, (Kobe, Japan), pp. 791–796, 11-13, Dec. 1996.

[63] M. W. Spong and R. Ortega, "On adaptive inverse dynamics control of rigid robots," *IEEE Trans. on Automatic Control*, vol. 35, no. 1, pp. 92–95, 1990.

[64] S. S. Ge, T. H. Lee, and Z. P. Wang, "Adaptive neural network control for smart materials robots using singular perturbation technique," *Asian Journal of Control*, vol. 3, no. 2, pp. 143–155, 2001.

[65] H. K. Khalil, *Nonlinear Systems, 2nd ed.* Upper Saddle River, NJ: Prentice Hall, 1996.

[66] S. S. Ge and T. H. Lee, "Parallel adaptive neural network control of robots," *Proc. Inst. Mech. Eng., J. Syst. Contr. Eng.*, vol. 208, pp. 231–237, 1994.

[67] S. S. Ge and I. Postlethwaite, "Adaptive neural network controller design for flexible joint robots using singular perturbation technique," *Tran. The Inst. Meas. Contr.*, vol. 17, no. 2, pp. 120–131, 1995.

[68] S. S. Ge, , T. H. Lee, and C. J. Harris, *Adaptive Neural Network Control of Robot Manipulators*. River Edge, NJ: World Scientific, 1998.

[69] F. L. Lewis, S. Jagannathan, and A. Yesildirek, *Neural Network Control of Robot Manipulators and Nonlinear Systems*. London: Taylor and Francis, 1999.

[70] T. Poggio and F. Girosi, "A theory of networks for approximation and learning." no. 1140, MIT, Cambridge, MA, July 1989.

[71] T. Poggio and F. Girosi, "Networks for approximation and learning," *Proceeding of IEEE*, vol. 78, pp. 1481–1497, 1990.

[72] C. A. Desoer and M. Vidyasagar, *Feedback Systems: Input-Output Properties*. New York: Academic Press, 1975.

[73] H. Khalil, *Nonlinear Systems*. Macmillan Publishing Company, 1992.

[74] R. Carelli and R. Kelly, "An adaptive impedence/force controller for robot manipulators," *IEEE Trans. Automat. Contr.*, vol. 36, pp. 967–971, 1991.

[75] L. Lui, Y. Han, R. Lingarkar, N. A. Sinha, and M. A. Elbestawi, "On adaptive force/motion control of constrained robtos," in *Proc. IECON'89, 15th Annual Conference of IEEE Industrial Electronics Society*, pp. 433–437, 1989.

[76] K. D. Young, "Applications of sliding mode to constrained robot motion control," in *Proc. Amer. Contr. Conf.*, (Atlanta, GA, USA), pp. 912–916, June 1988.

[77] C. Y. Su, T. P. Leung, and Q. J. Zhou, "Force/motion control of constrained robots using sliding mode," *IEEE Trans. Automat. Contr.*, vol. 37, pp. 668–672, 1992.

[78] M. W. Vandegrift, F. L. Lewis, and S. Q. Zhu, "Flexible-link robot arm control by a feedback linearization/singular perturbation approach," *J. of Rob. Syst.*, vol. 11, no. 7, pp. 591–603, 1994.

[79] J. Yuan, "Adaptive control of a constrained robot-ensuring zero tracking and zero force errors," *IEEE Trans. Auto. Contr.*, vol. 42, no. 12, pp. 1709–1714, 1997.

Appendix A

Entries of Matrices M, C and K Used in Chapter 4

Since two link with two assumed mode for each link model is investigated in Section 4.4, thus the inertia matrix $\mathbf{M}$ and the Coriolis vector can be assumed as

$$\mathbf{M} = \begin{bmatrix} M_{11} & M_{12} & M_{13} & M_{14} & M_{15} & M_{16} \\ M_{21} & M_{22} & M_{23} & M_{24} & M_{25} & M_{26} \\ M_{31} & M_{32} & M_{33} & M_{34} & M_{35} & M_{36} \\ M_{41} & M_{42} & M_{43} & M_{44} & M_{45} & M_{46} \\ M_{51} & M_{52} & M_{53} & M_{54} & M_{55} & M_{56} \\ M_{61} & M_{62} & M_{63} & M_{64} & M_{65} & M_{66} \end{bmatrix} \quad \mathbf{H} = \begin{bmatrix} H_1 \\ H_2 \\ H_3 \\ H_4 \\ H_5 \\ H_6 \end{bmatrix} \tag{A.1}$$

and the stiffness matrix $\mathbf{K}$ is of form

$$\mathbf{K} = diag\{0, 0, \omega_{11}^2 m_1, \omega_{12}^2 m_1, \omega_{21}^2 m_2, \omega_{22}^2 m_2\} \tag{A.2}$$

The components of $\mathbf{M}$ and $\mathbf{H}$ can be expressed as

$$\begin{aligned}
M_{11} &= m_{111} + m_{112}\cos q_{r2} + (m_{113}(t_{11}q_{f11} + t_{12}q_{f12}) + m_{114}(t_{21}q_{f21} + t_{22}q_{f22}))\sin q_{r2} \\
M_{12} &= (m_{123}(t_{11}q_{f11} + t_{12}q_{f12}) + m_{124}(t_{21}q_{f21} + t_{22}q_{f22}))\sin q_{r2} \\
&\quad + m_{121} + m_{122}\cos q_{r2} \\
M_{13} &= m_{131} + m_{132}\cos q_{r2} + (m_{133}(t_{21}q_{f21} + t_{22}q_{f22}) + m_{134}q_{f12})\sin q_{r2} \\
M_{14} &= m_{141} + m_{142}\cos q_{r2} + (m_{143}(t_{21}q_{f21} + t_{22}q_{f22}) + m_{144}q_{f11})\sin q_{r2} \\
M_{15} &= m_{151} + m_{152}\cos q_{r2} + m_{153}(t_{11}q_{f11} + t_{12}q_{f12})\sin q_{r2} \\
M_{16} &= m_{161} + m_{162}\cos q_{r2} + m_{163}(t_{11}q_{f11} + t_{12}q_{f12})\sin q_{r2} \\
M_{21} &= 0 \\
M_{22} &= m_{221} \\
M_{23} &= (m_{233}(t_{21}q_{f21} + t_{22}q_{f22}) + m_{234}(t_{31}q_{f11} + t_{32}q_{f12}))\sin q_{r2} \\
&\quad + m_{231} + m_{232}\cos q_{r2} \\
M_{24} &= (m_{243}(t_{21}q_{f21} + t_{22}q_{f22}) + m_{244}(t_{31}q_{f11} + t_{32}q_{f12}))\sin q_{r2} \\
&\quad + m_{241} + m_{242}\cos q_{r2} \\
M_{25} &= m_{251} \\
M_{26} &= m_{261} \\
M_{31} &= M_{32} = 0 \\
M_{33} &= m_{331} + m_{332}\cos q_{r2} + m_{333}(t_{21}q_{f21} + t_{22}q_{f22})\sin q_{r2} \\
M_{34} &= m_{341} + m_{342}\cos q_{r2} + m_{343}(t_{21}q_{f21} + t_{22}q_{f22})\sin q_{r2}
\end{aligned}$$

$$
\begin{aligned}
M_{35} &= m_{351} + m_{352}\cos q_{r2} + m_{353}(t_{31}q_{f11} + t_{32}q_{f12})\sin q_{r2} \\
M_{36} &= m_{361} + m_{362}\cos q_{r2} + m_{363}(t_{31}q_{f11} + t_{32}q_{f12})\sin q_{r2} \\
M_{41} &= M_{42} = M_{43} = 0 \\
M_{44} &= m_{441} + m_{442}\cos q_{r2} + m_{443}(t_{21}q_{f21} + t_{22}q_{f22})\sin q_{r2} \\
M_{45} &= m_{451} + m_{452}\cos q_{r2} + m_{453}(t_{31}q_{f11} + t_{32}q_{f12})\sin q_{r2} \\
M_{46} &= m_{461} + m_{462}\cos q_{r2} + m_{463}(t_{31}q_{f11} + t_{32}q_{f12})\sin q_{r2} \\
M_{51} &= M_{52} = M_{53} = M_{54} = 0 \\
M_{55} &= m_{551} \\
M_{56} &= m_{561} \\
M_{61} &= M_{62} = M_{63} = M_{64} = M_{65} = 0 \\
M_{66} &= m_{661} \\
H_1 &= [(h_{101}\dot{q}_{r2} + h_{102}\dot{q}_{f11} + h_{103}\dot{q}_{f12} + h_{104}\dot{q}_{f21} + h_{105}\dot{q}_{f22})\dot{q}_{r1} \\
&\quad +(h_{106}\dot{q}_{r2} + h_{107}\dot{q}_{f11} + h_{108}\dot{q}_{f12} + h_{109}\dot{q}_{f21} + h_{110}\dot{q}_{f22})\dot{q}_{r2} \\
&\quad +(h_{111}\dot{q}_{f21} + h_{112}\dot{q}_{f22})\dot{q}_{f11} + (h_{113}\dot{q}_{f21} + h_{114}\dot{q}_{f22})\dot{q}_{f12}]\sin q_{r2} \\
&\quad +[(h_{115}\dot{q}_{r1} + h_{116}\dot{q}_{r2} + h_{117}\dot{q}_{f21} + h_{118}\dot{q}_{f22})(t_{11}q_{f11} + t_{12}q_{f12}) \\
&\quad +(h_{119}\dot{q}_{r1} + h_{120}\dot{q}_{r2} + h_{121}\dot{q}_{f11} + h_{122}\dot{q}_{f12})(t_{21}q_{f21} + t_{22}q_{f22}) \\
&\quad +h_{123}q_{f12}\dot{q}_{f11} + h_{124}q_{f11}\dot{q}_{f12}]\dot{q}_{r2}\cos q_{r2}
\end{aligned}
$$

$$
\begin{aligned}
H_2 &= (h_{201}\dot{q}_{r1} + h_{202}\dot{q}_{f11} + h_{203}\dot{q}_{f12})\dot{q}_{r1}\sin q_{r2} \\
&\quad +\{[(h_{204}\dot{q}_{r1} + h_{205}\dot{q}_{f21} + h_{206}\dot{q}_{f22}(t_{11}q_{f11} + t_{12}q_{f12}) \\
&\quad +(h_{207}\dot{q}_{r1} + h_{208}\dot{q}_{f21} + h_{209}\dot{q}_{f22}(t_{21}q_{f21} + t_{22}q_{f22}) + h_{210}q_{f12}\dot{q}_{f11} \\
&\quad +h_{211}q_{f11}\dot{q}_{f12}]\dot{q}_{r1} + [(h_{212}\dot{q}_{f11} + h_{213}\dot{q}_{f12})(t_{21}q_{f21} + t_{22}q_{f22}) \\
&\quad +(h_{214}\dot{q}_{f21} + h_{215}\dot{q}_{f22})(t_{31}q_{f11} + t_{32}q_{f12})]\dot{q}_{f11} + [h_{216}\dot{q}_{f12}(t_{21}q_{f21} + t_{22}q_{f22}) \\
&\quad +(h_{217}\dot{q}_{f21} + h_{218}\dot{q}_{f22})(t_{31}q_{f11} + t_{32}q_{f12})]\dot{q}_{f12}\}\cos q_{r2} \\
H_3 &= [(h_{301}\dot{q}_{r1} + h_{302}\dot{q}_{r2} + h_{303}\dot{q}_{f12} + h_{304}\dot{q}_{f21} + h_{305}\dot{q}_{f22})\dot{q}_{r1} \\
&\quad +[(h_{306}\dot{q}_{r2} + h_{307}\dot{q}_{f11} + h_{308}\dot{q}_{f12} + h_{309}\dot{q}_{f21} + h_{310}\dot{q}_{f22})\dot{q}_{r2} \\
&\quad +(h_{311}\dot{q}_{f21} + h_{312}\dot{q}_{f22})\dot{q}_{f11} + (h_{313}\dot{q}_{f21} + h_{314}\dot{q}_{f22})\dot{q}_{f12}]\sin q_{r2} \\
&\quad +[(h_{315}\dot{q}_{r1} + h_{316}\dot{q}_{r2} + h_{317}\dot{q}_{f11} + h_{318}\dot{q}_{f12})(t_{21}q_{f21} + t_{22}q_{f22}) \\
&\quad +(h_{319}\dot{q}_{r2} + h_{320}\dot{q}_{f21} + h_{321}\dot{q}_{f22})(t_{31}q_{f31} + t_{32}q_{f12}) + h_{322}q_{f12}\dot{q}_{r1}]\dot{q}_{r2}\cos q_{r2} \\
H_4 &= [(h_{401}\dot{q}_{r1} + h_{402}\dot{q}_{r2} + h_{403}\dot{q}_{f12} + h_{404}\dot{q}_{f21} + h_{405}\dot{q}_{f22})\dot{q}_{r1} \\
&\quad +[(h_{406}\dot{q}_{r2} + h_{407}\dot{q}_{f11} + h_{408}\dot{q}_{f12} + h_{409}\dot{q}_{f21} + h_{410}\dot{q}_{f22})\dot{q}_{r2} \\
&\quad +(h_{411}\dot{q}_{f21} + h_{412}\dot{q}_{f22})\dot{q}_{f11} + (h_{413}\dot{q}_{f21} + h_{414}\dot{q}_{f22})\dot{q}_{f12}]\sin q_{r2} \\
&\quad +[(h_{415}\dot{q}_{r1} + h_{416}\dot{q}_{r2} + h_{417}\dot{q}_{f11} + h_{418}\dot{q}_{f12})(t_{21}q_{f21} + t_{22}q_{f22}) \\
&\quad +(h_{419}\dot{q}_{r2} + h_{420}\dot{q}_{f21} + h_{421}\dot{q}_{f22})(t_{31}q_{f11} + t_{32}q_{f12}) + h_{422}q_{f12}\dot{q}_{r1}]\dot{q}_{r2}\cos q_{r2} \\
H_5 &= (h_{501}\dot{q}_{r1} + h_{502}\dot{q}_{f11} + h_{503}\dot{q}_{f12})\dot{q}_{r1}\sin q_{r2} + [h_{504}(t_{11}q_{f11} + t_{12}q_{f12})\dot{q}_{r1} \\
&\quad +(h_{505}\dot{q}_{f11} + h_{506}\dot{q}_{f12})(t_{31}q_{f11} + t_{32}q_{f12})]\dot{q}_{r2}\cos q_{r2} \\
H_6 &= (h_{601}\dot{q}_{r1} + h_{602}\dot{q}_{f11} + h_{603}\dot{q}_{f12})\dot{q}_{r1}\sin q_{r2} + [h_{604}(t_{11}q_{f11} + t_{12}q_{f12})\dot{q}_{r1} \\
&\quad +(h_{605}\dot{q}_{f11} + h_{606}\dot{q}_{f12})(t_{31}q_{f11} + t_{32}q_{f12})]\dot{q}_{r2}\cos q_{r2}
\end{aligned}
$$

where

$$
\begin{aligned}
m_{111} &= I_{h1} + I_{b1} + I_{h2} + I_{b2} + I_p + m_2 l_2^2 + m_t(l_1^2 + l_2^2) \\
m_{112} &= 2(m_2 d_2 + m_t l_2) l_1 \\
m_{113} &= 2(m_2 d_2 + m_t l_2) \\
m_{114} &= -2 l_1 \\
m_{121} &= I_{h2} + I_{b2} + I_p + m_t l_2^2 \\
m_{122} &= (m_2 d_2 + m_t l_2) l_1 \\
m_{123} &= (m_2 d_2 + m_t l_2) \\
m_{124} &= -l_1 \\
m_{131} &= \omega_{11} + (I_{h2} + I_{b2} + I_p + m_t l_2^2)\phi'_{11,e} + (m_2 + m_t) l_1 \phi_{11,e} \\
m_{132} &= (m_2 d_2 + m_t l_2)(\phi_{11,e} + \phi'_{11,e} l_1) \\
m_{133} &= -(\phi_{11,e} + \phi'_{11,e} l_1) \\
m_{134} &= -(m_2 d_2 + m_t l_2)\psi_2 \\
m_{141} &= \omega_{12} + (I_{h2} + I_{b2} + I_p + m_t l_2^2)\phi'_{12,e} + (m_2 + m_t) l_1 \phi_{12,e} \\
m_{142} &= (m_2 d_2 + m_t l_2)(\phi_{12,e} + \phi'_{12,e} l_1) \\
m_{143} &= -(\phi_{12,e} + \phi'_{12,e} l_1) \\
m_{144} &= -(m_2 d_2 + m_t l_2)\psi_1 \\
m_{151} &= \omega_{21} + I_p \phi'_{21,e} + m_t l_2 \phi_{21,e} \\
m_{152} &= (v_{21} + m_t \phi_{21,e}) l_1 \\
m_{153} &= v_{21} + m_t \phi_{21,e} \\
m_{161} &= \omega_{22} + I_p \phi'_{22,e} + m_t l_2 \phi_{22,e}
\end{aligned}
$$

$$m_{221} = I_{h2} + I_{b2} + I_p + m_t l_2^2 \qquad m_{231} = (I_{h2} + I_{b2} + I_p + m_t l_2^2)\phi'_{11,e}$$

$$m_{232} = (m_2 d_2 + m_t l_2)\phi_{22,e} \qquad m_{233} = -\phi_{11,e}$$

$$m_{234} = -(m_2 d_2 + m_t l_2)\phi_{11,e} \qquad m_{241} = (I_{h2} + I_{b2} + I_p + m_t l_2^2)\phi_{12,e}$$

$$m_{242} = (m_2 d_2 + m_t l_2)\phi_{12,e} \qquad m_{243} = -\phi_{12,e}$$

$$m_{244} = -(m_2 d_2 + m_t l_2)\phi_{12,e} \qquad m_{251} = \omega_{21} + I_p \phi'_{21,e} + m_t l_2 \phi_{21,e}$$

$$m_{261} = \omega_{22} + I_p \phi'_{22,e} + m_t l_2 \phi_{22,e} \qquad m_{331} = m_1$$

$$m_{332} = 2(m_2 d_2 + m_t l_2)\phi_{11,e}\phi'_{11,e} \qquad m_{333} = -2\phi_{11,e} + \phi'_{11,e}$$

$$m_{341} = 0 \qquad m_{342} = (m_2 d_2 + m_t l_2)(\phi_{11,e}\phi'_{12,e} + \phi_{12,e}\phi'_{11,e})$$

$$m_{343} = -(\phi_{11,e}\phi'_{12,e} + \phi_{12,e}\phi'_{11,e}) \qquad m_{351} = (\omega_{21} + I_p \phi'_{21,e} + m_t l_2 \phi_{21,e})\phi'_{11,e}$$

$$m_{352} = (v_{21} + m_t \phi_{21,e})\phi_{11,e} \qquad m_{353} = -(v_{21} + m_t \phi_{21,e})\phi_{11,e}$$

$$m_{361} = (\omega_{22} + I_p \phi'_{22,e} + m_t l_2 \phi_{22,e})\phi'_{11,e} \qquad m_{362} = (v_{22} + m_t \phi_{22,e})\phi_{11,e}$$

$$m_{363} = -(v_{22} + m_t \phi_{22,e})\phi_{11,e} \qquad m_{441} = m_1$$

$$m_{442} = 2(m_2 d_2 + m_t l_2)\phi_{12,e}\phi'_{12,e} \qquad m_{443} = -2\phi_{12,e}\phi'_{12,e}$$

$$m_{451} = (\omega_{21} + I_p \phi'_{21,e} + m_t l_2 \phi_{21,e})\phi'_{12,e} \qquad m_{452} = (v_{21} + m_t \phi_{21,e})\phi_{12,e}$$

$$m_{453} = -(v_{21} + m_t \phi_{21,e})\phi_{12,e} \qquad m_{461} = (\omega_{22} + I_p \phi'_{22,e} + m_t l_2 \phi_{22,e})\phi'_{12,e}$$

$$m_{462} = (v_{22} + m_t \phi_{22,e})\phi_{12,e} \qquad m_{463} = -(v_{22} + m_t \phi_{22,e})\phi_{12,e}$$

$$m_{551} = m_2 \qquad m_{562} = 0$$

$$m_{661} = m_2$$

$$h_{101} = -2(m_2 d_2 + m_t l_2) l_1 \qquad h_{102} = 2(m_2 d_2 + m_t l_2)(\phi_{11,e} - l_1 \phi'_{11,e})$$

$$h_{103} = 2(m_2 d_2 + m_t l_2)(\phi_{12,e} - l_1 \phi'_{12,e}) \qquad h_{104} = -2(v_{21} + m_t \phi_{21,e}) l_1$$

$$h_{105} = -2(v_{22} + m_t \phi_{22,e}) l_1 \qquad h_{106} = -2(m_2 d_2 + m_t l_2) l_1$$

$$h_{107} = -(m_2 d_2 + m_t l_2) l_1 \phi'_{11,e} \qquad h_{108} = -(m_2 d_2 + m_t l_2) l_1 \phi'_{12,e}$$

$$h_{109} = -2(v_{21} + m_t \phi_{21,e}) l_1 \qquad h_{110} = -2(v_{22} + m_t \phi_{22,e}) l_1$$

$$h_{111} = -2(v_{21} + m_t \phi_{21,e}) l_1 \phi'_{11,e} \qquad h_{112} = -2(v_{22} + m_t \phi_{22,e}) l_1 \phi'_{11,e}$$

$$h_{113} = -2(v_{21} + m_t \phi_{21,e}) l_1 \phi'_{12,e} \qquad h_{114} = -2(v_{22} + m_t \phi_{22,e}) l_1 \phi'_{12,e}$$

$$h_{115} = 2(m_2 d_2 + m_t l_2) \qquad h_{116} = m_2 d_2 + m_t l_2$$

$$h_{117} = -(v_{21} + m_t \phi_{21,e}) \qquad h_{118} = -(v_{22} + m_t \phi_{22,e})$$

$$h_{119} = -2 l_1 \qquad h_{120} = -l_1$$

$$h_{121} = -(\phi_{11,e} + l_1 \phi'_{11,e}) \qquad h_{122} = -(\phi_{12,e} + l_1 \phi'_{12,e})$$

$$h_{123} = -(m_2 d_2 + m_t l_2) \psi_2 \qquad h_{124} = -(m_2 d_2 + m_t l_2) \psi_1$$

$$h_{201} = (m_2 d_2 + m_t l_2) l_1 \qquad h_{202} = 2(m_2 d_2 + m_t l_2) \phi_{11,e}$$

$$h_{203} = 2(m_2 d_2 + m_t l_2) \phi_{12,e} \qquad h_{204} = -(m_2 d_2 + m_t l_2)$$

$$h_{205} = -(v_{21} + m_t \phi_{21,e}) \qquad h_{206} = -(v_{22} + m_t \phi_{22,e})$$

$$h_{207} = l_1 \qquad h_{208} = \phi_{11,e} + l_1 \phi'_{11,e}$$

$$h_{209} = \phi_{12,e} + l_1 \phi'_{12,e} \qquad h_{210} = (m_2 d_2 + m_t l_2) \psi_2$$

$$h_{211} = (m_2 d_2 + m_t l_2) \psi_1 \qquad h_{212} = \phi_{11,e} \phi'_{11,e}$$

$$h_{213} = \phi_{11,e} \phi'_{12,e} + \phi_{12,e} \phi'_{11,e} \qquad h_{214} = (v_{21} + m_t \phi_{21,e}) \phi_{11,e}$$

$$h_{215} = (v_{22} + m_t \phi_{22,e}) \phi_{11,e} \qquad h_{216} = \phi_{12,e} \phi'_{12,e}$$

$$h_{217} = (v_{21} + m_t \phi_{21,e}) \phi_{12,e} \qquad h_{218} = (v_{22} + m_t \phi_{22,e}) \phi_{12,e}$$

$$h_{301} = 2(m_2 d_2 + m_t l_2)(\phi_{11,e} - l_1 \phi'_{11,e}) \qquad h_{302} = -2(m_2 d_2 + m_t l_2) \phi_{11,e}$$

$$h_{303} = 2(m_2 d_2 + m_t l_2) \psi_1 \qquad h_{304} = -2(v_{21} + m_t \phi_{21,e}) \phi_{11,e}$$

$$h_{305} = -2(v_{22} + m_t \phi_{22,e}) \phi_{11,e} \qquad h_{306} = (m_2 d_2 + m_t l_2) \phi_{11,e}$$

$$h_{307} = -2(m_2 d_2 + m_t l_2) \phi_{11,e} \phi'_{11,e} \qquad h_{308} = -2(m_2 d_2 + m_t l_2) \phi_{11,e} \phi'_{12,e}$$

$$h_{309} = -2(v_{21} + m_t\phi_{21,e})\phi_{11,e} \qquad h_{310} = -2(v_{22} + m_t\phi_{22,e})\phi_{11,e}$$

$$h_{311} = -2(v_{21} + m_t\phi_{21,e})\phi_{11,e}\phi'_{11,e} \qquad h_{312} = -2(v_{22} + m_t\phi_{22,e})\phi_{11,e}\phi'_{11,e}$$

$$h_{313} = -2(v_{21} + m_t\phi_{21,e})\phi_{11,e}\phi'_{12,e} \qquad h_{314} = -2(v_{22} + m_t\phi_{22,e})\phi_{11,e}\phi'_{12,e}$$

$$h_{315} = -(\phi_{11,e} + l_1\phi'_{11,e}) \qquad h_{316} = -\phi_{11,e}$$

$$h_{317} = -2\phi_{11,e}\phi'_{12,e} \qquad h_{318} = -(\phi_{11,e}\phi'_{12,e} + \phi_{12,e}\phi'_{11,e})$$

$$h_{319} = -(m_2d_2 + m_tl_2)\phi_{11,e} \qquad h_{320} = -(v_{21} + m_t\phi_{21,e})\phi_{11,e}$$

$$h_{321} = -(v_{22} + m_t\phi_{22,e})\phi_{11,e} \qquad h_{322} = -(m_2d_2 + m_tl_2)\psi_2$$

$$h_{401} = -(m_2d_2 + m_tl_2)(\phi_{12,e} - l_1\phi'_{12,e}) \qquad h_{402} = -2(m_2d_2 + m_tl_2)\phi_{12,e}$$

$$h_{403} = 2(m_2d_2 + m_tl_2)\psi_2 \qquad h_{404} = -2(v_{21} + m_t\phi_{21,e})\phi_{12,e}$$

$$h_{405} = -2(v_{22} + m_t\phi_{22,e})\phi_{12,e} \qquad h_{406} = -(m_2d_2 + m_tl_2)\phi_{12,e}$$

$$h_{407} = -2(m_2d_2 + m_tl_2)\phi_{12,e}\phi'_{11,e} \qquad h_{408} = -2(m_2d_2 + m_tl_2)\phi_{12,e}\phi'_{12,e}$$

$$h_{409} = -2(v_{21} + m_t\phi_{21,e})\phi_{12,e} \qquad h_{410} = -2(v_{22} + m_t\phi_{22,e})\phi_{12,e}$$

$$h_{411} = -2(v_{21} + m_t\phi_{21,e})\phi_{12,e}\phi'_{11,e} \qquad h_{412} = -2(v_{22} + m_t\phi_{22,e})\phi_{12,e}\phi'_{12,e}$$

$$h_{413} = -2(v_{21} + m_t\phi_{21,e})\phi_{12,e}\phi'_{11,e} \qquad h_{414} = -2(v_{22} + m_t\phi_{22,e})\phi_{12,e}\phi'_{12,e}$$

$$h_{415} = -(\phi_{12,e} + l_1\phi'_{12,e}) \qquad h_{416} = -\phi_{12,e}$$

$$h_{417} = -(\phi_{11,e}\phi'_{12,e} + \phi_{12,e}\phi'_{11,e}) \qquad h_{418} = -2\phi_{12,e}\phi'_{12,e}$$

$$h_{419} = -(m_2d_2 + m_tl_2)\phi_{12,e} \qquad h_{420} = -(v_{21} + m_t\phi_{21,e})\phi_{12,e}$$

$$h_{421} = -(v_{22} + m_t\phi_{22,e})\phi_{12,e} \qquad h_{422} = -(m_2d_2 + m_tl_2)\psi_1$$

$$h_{501} = (v_{21} + m_t\phi_{21,e})l_1 \qquad h_{502} = 2(v_{21} + m_t\phi_{21,e})\phi_{11,e}$$

$$h_{503} = 2(v_{21} + m_t\phi_{21,e})\phi_{12,e} \qquad h_{504} = v_{21} + m_t\phi_{21,e}$$

$$h_{505} = -(v_{21} + m_t\phi_{21,e})\phi_{11,e} \qquad h_{506} = -(v_{21} + m_t\phi_{21,e})\phi_{12,e}$$

$$h_{601} = (v_{22} + m_t\phi_{22,e})l_1 \qquad h_{602} = 2(v_{22} + m_t\phi_{22,e})\phi_{11,e}$$

with

$$
\begin{aligned}
h_{603} &= 2(v_{22} + m_t\phi_{22,e})\phi_{12,e} & h_{604} &= v_{22} + m_t\phi_{22,e} \\
h_{605} &= -(v_{22} + m_t\phi_{22,e})\phi_{11,e} & h_{606} &= -(v_{22} + m_t\phi_{22,e})\phi_{12,e} \\
t_{11} &= \phi_{11,e} - l_1\phi'_{11,e} & t_{12} &= \phi_{12,e} - l_1\phi'_{12,e} \\
t_{21} &= v_{21} + m_t\phi_{21,e} & t_{22} &= v_{22} + m_t\phi_{22,e} \\
t_{31} &= \phi'_{11,e} & t_{32} &= \phi'_{12,e} \\
\phi_{ij,e} &= \phi_{ij}(x_i)|_{x_i=l_i} & \phi'_{ij,e} &= \phi'_{ij}(x_i)|_{x_i=l_i} \\
\psi_1 &= \phi_{12,e}\phi'_{11,e} - \phi_{11,e}\phi'_{12,e} & \psi_2 &= \phi_{11,e}\phi'_{12,e} - \phi_{12,e}\phi'_{11,e}.
\end{aligned}
$$

Appendix B

Author's Publications

S. S. Ge, Z. Tian, and T. H. Lee, "Nonlinear Control of a dynamical model of HIV-1", *IEEE Trans. Biomedical Engineering*, Volume 52, Issue 3, pp. 353-361, Mar 2005.

Z. Tian, S. S. Ge, and T. H. Lee, "Globally stable nonlinear control of HIV-1 systems", In *Proc. American Control Conference*, (Boston, MA), pp. 1633-1638, June 30-July 2, 2004.